Electronic Theses and Dissertations

The effects of polychlorinated biphenyls exposure on non-alcoholic fatty liver disease : role of aryl hydrocarbon receptor.

Hongxue Shi
University of Louisville

THE EFFECTS OF POLYCHLORINATED BIPHENYLS EXPOSURE ON NON-ALCOHOLIC FATTY LIVER DISEASE: ROLE OF ARYL HYDROCARBON RECEPTOR

By

Hongxue Shi

M.S. Wenzhou Medical University, 2013

A Dissertation

Submitted to the Faculty of the

School of Medicine of the University of Louisville

for the Degree of

Doctor of Philosophy in Pharmacology and Toxicology

Department of Pharmacology and Toxicology

University of Louisville

Louisville, KY

May 2018

THE EFFECTS OF POLYCHLORINATED BIPHENYLS EXPOSURE ON NON-ALCOHOLIC FATTY LIVER DISEASE: ROLE OF ARYL HYDROCARBON RECEPTOR

By

Hongxue Shi

M.S. Wenzhou Medical University, 2013

Dissertation Approved on

April 19, 2018

By the following Dissertation Committee

_____

Matthew C. Cave, M.D., (Mentor)

_____

Juliane I. Beier, Ph.D.

_____

Wenke Feng, Ph.D.

_____

Russell A. Prough, Ph.D.

_____

J. Christopher States, Ph.D.

ACKNOWLEDGEMENTS

Finally, I would like to thank my wife, Mrs. Xiao, and my daughter, Lola, for their love, support and encouraging in my life. Thanks to my parents and parents-in-law for their selfless love and support.

ABSTRACT

THE EFFECTS OF POLYCHLORINATED BIPHENYLS EXPOSURE ON NON-ALCOHOLIC FATTY LIVER DISEASE: ROLE OF ARYL HYDROCARBON RECEPTOR

Hongxue Shi

April 19, 2018

Polychlorinated biphenyls (PCBs) are detectable in serum of 100% of adults in US, and has been associated with fatty liver disease in epidemiological studies. PCBs are classified as either dioxin-like (DL) or non-dioxin-like (NDL) PCB based on their ability to activate the aryl hydrocarbon receptor (AhR). We used exposures that reflect human bioaccumulation patterns, which resembles Aroclor 1260 with a low level of the DL-PCB, PCB 126. Our aim was to determine if this exposure will activate the human and mouse AhR and examine if receptor activation influences these steatotic responses due to PCB exposures.

DL-PCBs exposure-induced AhR activation in luciferase assays and induction of AhR target gene expression demonstrated that the Mouse AhR was much more sensitive than human AhR to activation by DL-PCBs. Our PCB mixture reflected this by activating the mouse AhR, but not human AhR *in vivo*. The ability of PCBs to activate the AhR would be predicted to be WHO toxicity equivalency = rat >mouse >>human.

Mice were exposed to either PCB 126 (20 µg/kg), Aroclor 1260 (20 mg/kg) or both, for 2 weeks. PCB 126 or Aroclor 1260/PCB 126 significantly activated AhR, but only PCB 126 exposure alone induced mild hepatic steatosis. AhR activation suppressed the induction of CAR and PXR targets. More complex patterns of attenuation were observed with genes involved in lipid metabolism.

PCB exposures require a hypercaloric diet to transition steatosis to steatohepatitis in murine models. Mice were fed high fat diet and received the same treatments as the 2-week study for 12 weeks. Our PCBs mixture exposure did not induce wasting syndrome, and failed to exacerbate steatosis. In addition, PCB 126 exposure activated AhR. Aroclor 1260 exposure drove hepatic steatosis to steatohepatitis. Either PCB 126 or the Aroclor 1260/PCB 126 mixture protected against high fat diet induced liver injury and liver fibrosis. All PCB exposures affected hepatic lipid metabolism.

TABLE OF CONTENTS

LIST OF TABLES

LIST OF FIGURES

CHAPTER I

GENERAL INTRODUCTION

1. Non-alcoholic fatty liver disease

High calorie intake or a Western diet contributes to non-alcoholic fatty liver disease (NAFLD), which is manifested by excessive lipid accumulation in liver, termed hepatic steatosis. NAFLD encompasses a spectrum of fatty liver diseases, ranging from hepatic steatosis to hepatic steatohepatitis (NASH), fibrosis, cirrhosis, and even hepatocellular carcinoma (HCC) (1). Inflammatory cell infiltration drives hepatic steatosis to progress to NASH, which is characterized by hepatic injury, inflammation, oxidative stress and fibrosis. Hepatic steatosis and steatohepatitis can be reversed after timely intervention. If not, steatohepatitis can progress to advanced cirrhosis, which is associated with a high risk of HCC (2).

Liver is one of the important organs in regulation of glucose and lipid metabolism, and the dysfunction of glucose and lipid metabolism are fundamental in development and progression of NAFLD. The homeostasis of lipid metabolism includes lipid input and output in liver (Figure 1.1). On the input side, lipids can be taken up via the blood stream in the form of chylomicrons (CM) from dietary fat ingestion and free fatty acids derived mainly from lipolysis. Lipids may be synthesized (*de novo*) from carbohydrates or other precursors. The key proteins involved in influx of fatty acid in liver include fatty acid transport proteins (FATPs), plasma membrane fatty acid binding protein (FABP) and fatty acid translocase (CD36/FAT), which are associated with hepatic steatosis (3-5). The key

enzymes involved in *de novo* lipogenesis are ATP-citrate lyase (Acly), acetyl-CoA carboxylase (ACC) and fatty acid synthase (Fasn) (6). Moreover, the transcription factors, such as liver X receptor (LXR), sterol regulatory element-binding protein-1c (SREBP-1c), and carbohydrate response element binding protein (ChREBP) also control *de novo* lipogenesis (7, 8). Free fatty acids are mainly used to synthesize triglycerides and are stored in hepatocytes. On the output side, lipids can be secreted into blood in lipoprotein form, such as very-low-density-lipoprotein (VLDL) by interaction with apolipoproteinB-100 (ApoB-100) (8), and be utilized in mitochondria (fatty acid oxidation) as an energy source to produce ATP (9). In the normal physiological status, the liver total lipids input equals the total lipids output. However, once the total lipids input rate exceeds output rate, excessive lipids would be ectopic deposited, resulting in hepatic steatosis. Therefore, the factors that disturb the balance of lipid metabolism will induce NAFLD.
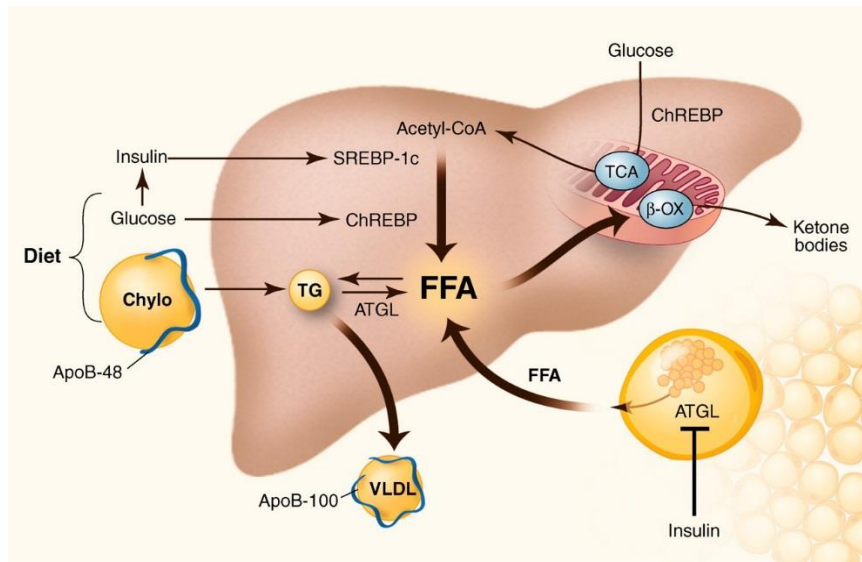
Figure 1.1 The homeostasis of liver lipid metabolism. Figure adapted from Jonathan C. Cohen *et al*., *Science*, 2011; 332:6037

The prevalence of NAFLD parallels the incidence of obesity and type 2 diabetes (T2DM). With the increasing incidence of obesity and T2DM, NAFLD is the most prevalent liver disease with a global prevalence estimate of 24 %, with the highest rates of NAFLD in South America (31 %) and the Middle East (32 %), followed by Asia (27 %), the USA (24%) and Europe (23 %), and lowest in Africa (14 %) (10, 11). The prevalence of NAFLD across geographical locales is shown in Figure 1.2 based on community surveys (11). Not all subjects with obesity develop NAFLD; and not all subjects with steatosis develop progressive liver disease. Seventy to eighty percent of obese and diabetic individuals develop NAFLD, 5-10 % subject with steatosis develop NASH, and 30 % of patients with NASH develop cirrhosis. Among patients diagnosed with cirrhosis, only 1-2 % of patients progress to HCC within 10 years of developing cirrhosis (12). The pathogenesis of NAFLD development, and progression to advanced fatty liver disease is not completely understood. Generally, the interaction of lifestyle (13), nutrients (14) and genetics (15) affect the pathogenesis of NAFLD/NASH. The potential molecular mechanisms include insulin resistance, lipotoxicity, mitochondrial oxidative stress, ER stress, disrupted adipokines, inflammatory cytokines, autophagy, and changes in gut microbiome (16-18). Several susceptibility genes for NAFLD development have been identified, such as patatin-like phospholipase domain-containing-3 (*PNPLA3*). The PNPLA3 (rs738409) polymorphism genotype distribution corelated with worldwide prevalence of NAFLD (Figure 1.2) (11, 19, 20).
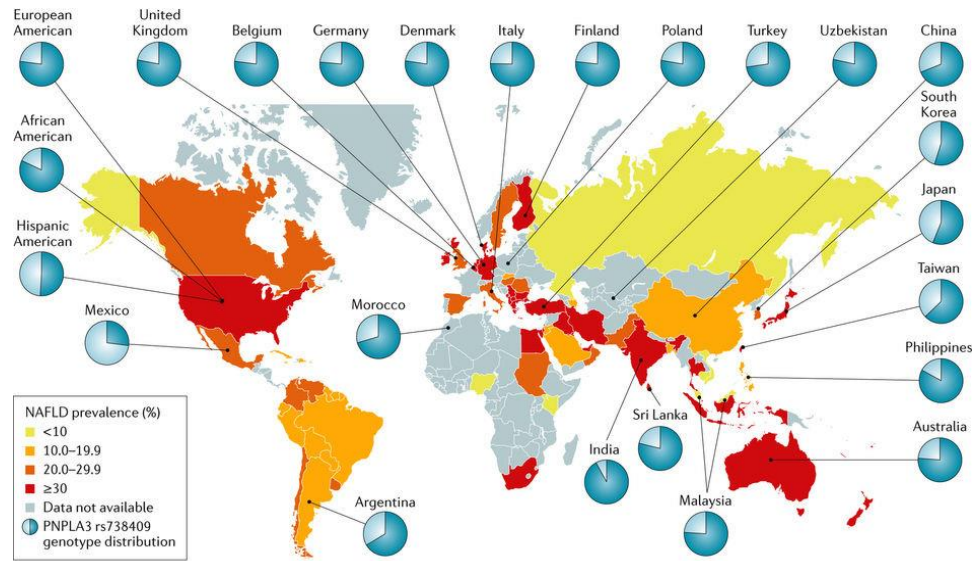
Figure 1.2 The global estimated prevalence of NAFLD and PNPLA3 rs738409 genotype distribution. Figure adapted from Younossi *et al.*, *Nature Reviews Gastroenterology & Hepatology,* 2017;15:11.

NAFLD is associated with abnormal level of blood lipids that increase mortality from liver and cardiovascular disease. Indeed, hypertriglyceridemia is the metabolic comorbidity most frequently associated with NAFLD. For patients with end stage liver disease, and cirrhosis, liver transplantation is the major strategy to rescue them. Thus, NAFLD is a heavy burden on public health globally. In the USA, it is estimated annual direct medical costs for NAFLD are about $103 billion (21). To date, there are no FDA-approved drugs for NAFLD/NASH treatment, and lifestyle improvements, such as body weight loss and physical exercise, are the only ways to improve NAFLD/NASH (22). However, experimental therapies involve targeting hepatic fat accumulation, anti-oxidants, anti-inflammation, anti-apoptosis, gut microbiome and anti-fibrotic (23, 24). Among these

developed chemicals, dual peroxisome proliferator-activator receptor α/δ agonist (elafibranor) (25, 26), farnesoid X receptor agonist (obeticholic acid) (27, 28), apoptosis signaling kinase 1 (ASK1) inhibitor (29, 30), and cysteine–cysteine motif chemokine receptor-2/5 antagonist (cenicriviroc) (31, 32), are being evaluated in phase III trial for NAFLD/NASH .

The "two-hit" hypothesis of NAFLD/NASH has been proposed (33), but this view has been challenged by "multiple parallel hits" hypothesis based on recent new findings (34). In the "two-hit" hypothesis, fat accumulation serves as the first hit, and increases susceptibility to subsequent second hits, which are responsible for liver injury, inflammatory cell infiltration and hepatic fibrosis. Occupational and environmental chemicals are another category of second hit. The terms toxicant-associated fatty liver disease (TAFLD) and/or toxicant-associated steatohepatitis (TASH) have been proposed to describe this condition(35). The TASH was firstly described in non-obese vinyl chloride (VC) workers, which is characterized by the presence of necrotic cell death, as indicated by elevated total cytokeratin 18, elevated proinflammatory cytokines, impaired insulin sensitivity and antioxidant defenses, but with normal serum transaminases levels. Selected pollutants associated with TAFLD/TASH in human and animal studies have been reviewed (36, 37). Since the similar histopathology exists among NAFLD/NASH and TAFLD/TASH, the distinction between them will not be made in the following text.

2. Polychlorinated biphenyls

Polychlorinated biphenyls (PCBs) are thermodynamically stable polyhalogenated aromatic hydrocarbons consisting of up to ten chlorine substituents attached to biphenyl rings (Figure 1.3). There are 209 different congeners, defined by the number and position

of chlorines attached to the biphenyl rings. Due to their thermodynamic stability and excellent electrical insulation and heat transfer properties, PCBs were widely used as insulating fluids in electrical transformers and capacitors. A total of 1.3 million tons of PCB mixtures were produced for a variety of commercial applications before PCBs were banned. PCB production was banned by the United States Congress in the later 1970's and globally by the Stockholm Convention in 2001 (38).

Figure 1.3 Chemical structure of PCBs. PCBs have the basic chemical formula ($C_{12}H_{10-n}Cl_n$), where n means the number of chlorine atoms, and number means the positions where a chlorine atom is attached to biphenyl rings.

Although PCBs production was banned for more than 30 years, PCBs still exist in the environment due to their higher thermostability, and resistant to degradation by the microbes, thus, PCBs belong to a category of "persistent organic pollutants" (POPs), and are widely dispersed in the global ecosystem, including water, soil, air, aquatic wildlife and mammals (39, 40). Highly chlorinated PCBs have bioaccumulated and are detected in human adipose tissues, liver, serum, and milk due to low metabolic degradation rate (41-43). Currently, inadvertent PCB production still occurs (44) and PCBs exposure occur

mainly through inhalation of contaminated indoor air (45) and contaminated food consumption (46).

The chlorination pattern of the PCBs is important for the toxicity of these congeners. PCB congeners have been subclassified into two major categories: coplanar and non-coplanar PCBs. Coplanar PCB congeners have none or only one chlorine atom attach to the ortho-position of biphenyl rings, known as non-ortho and mono-ortho PCBs, respectively. There are total 12 coplanar PCBs. Non-ortho PCBs include PCB 77, PCB 81, PCB 126, and PCB 169, and the rest of them are mono-ortho PCBs, such as PCB 114 and PCB 189, etc (Figure 1.4). Coplanar PCBs exhibit dioxin-like toxicity, and are also known as dioxin-like (DL) PCBs. Non-coplanar PCB congeners have two or more chlorine atoms at the ortho-position of biphenyl rings, and do not resulted in dioxin-like properties, thus, they are known as non-dioxin-like (NDL) PCBs.

The DL-PCB congeners interact with aryl hydrocarbon receptor (AhR), which may mediate their toxic effects. Among 12 DL-PCB congeners, PCB 126 exhibits the highest AhR binding affinity, and is the potent congener of DL-PCBs. Therefore, PCB 126 was selected for the proposed studies. Animal studies have shown that the toxic effects of PCB 126 include developmental toxicity (47), hepatic toxicity (48), reproductive toxicity (49), and neurological toxicity (50). The unfavorable effects of PCB 126 may be also mediated by interaction with other receptors, such as estrogen receptor (ER) (51). On the other hand, the toxicologic mode of action of NDL-PCBs, has been attributed to interactions with a variety of other cellular receptors, including pregnane X receptor (PXR) and constitutive androstane receptor (CAR) (52), as well as, ER, androgen receptor, and thyroid receptor (53). However, the DL-PCBs may also interact with these receptors (52, 53).
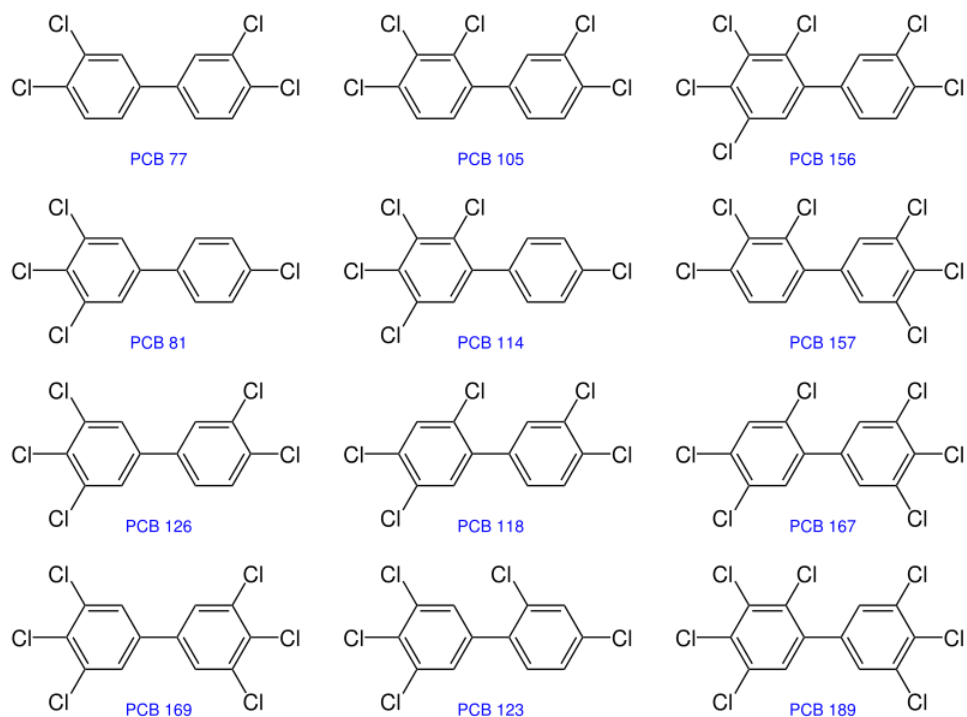
Figure 1.4 Chemical structure of DL-PCB congeners. The DL-PCBs in left column are non-ortho PCBs, and the rest of them are mono-ortho PCBs. Figure adapted from website: https://en.wikipedia.org/wiki/Polychlorinated_biphenyl

The liver is the major organ for PCB metabolism via phase I (cytochrome P450 enzymes) and phase II (conjugation pathways) pathways to convert them to water soluble metabolites, and remove them from body. The detailed metabolic pathways of PCBs bio-transformation are well summarized and reviewed (54). The rate and extent of PCB metabolism depends on the numbers and position of chlorines in the biphenyl rings. Generally, the lower the number of chlorines on the biphenyl rings, the faster the metabolism. Therefore, highly chlorinated PCBs tend to be bio-accumulated and detected

in human fat tissues or in plasma due to their lipophilic properties (55). In fact, the median concentration of the sum of 35 PCB congeners (ΣPCBs) was 528 ng/g lipid in participants of the Anniston Community Health Survey (ACHS) (55), and ACHS participants have serum concentrations of ΣPCBs two to three times higher than those in comparable age and race groups from National Health and Nutrition Examination Survey (NHANES) 2003–2004 sample of the general United States population (56).

Commercial PCBs were made and used in mixtures rather than individual congeners. In the United States, commercial PCB mixtures were produced by the Monsanto Company and marketed under the trade names Aroclor. Manufacturing plants included Anniston, Alabama. There are different types of Aroclor mixtures and each of them has a distinguishing suffix number that indicates the degree of chlorination. The first two numbers usually mean the total number of carbon atoms in biphenyl rings and the last two digits refer to the percentage of chlorines by mass in the mixture. Commercial PCB mixtures were also made globally, and marketed under different trade names. ACHS study demonstrated that higher incidences of hypertension, obesity, diabetes and liver disease was positively correlated to PCBs load in residents (57, 58).

Aroclor 1260, one of the commercial PCB mixtures in North America, contains sixty percent chlorine atoms by mass. The PCB congeners of Aroclor 1260 usually are highly chlorinated congeners with more than 5 chlorine substituents. As lowly chlorinated PCB congeners are easily metabolized and eliminated, only highly chlorinated PCB congeners are resistant to metabolism, and have bio-accumulated in humans. Our previous study demonstrated that the PCB profiles in Aroclor 1260 best mimic the PCBs present in human adipose tissue (52) (Figure 1.5). However, Aroclor 1260 contains lower amounts of DL-

PCB congeners. A 20 mg/kg exposure of Aroclor 1260 did not activate AhR in mice (52, 59). The less chlorinated PCB mixtures were also made by Monsanto Company with tradenames Aroclor 1254, Aroclor 1242, and Aroclor 1248, etc, later.
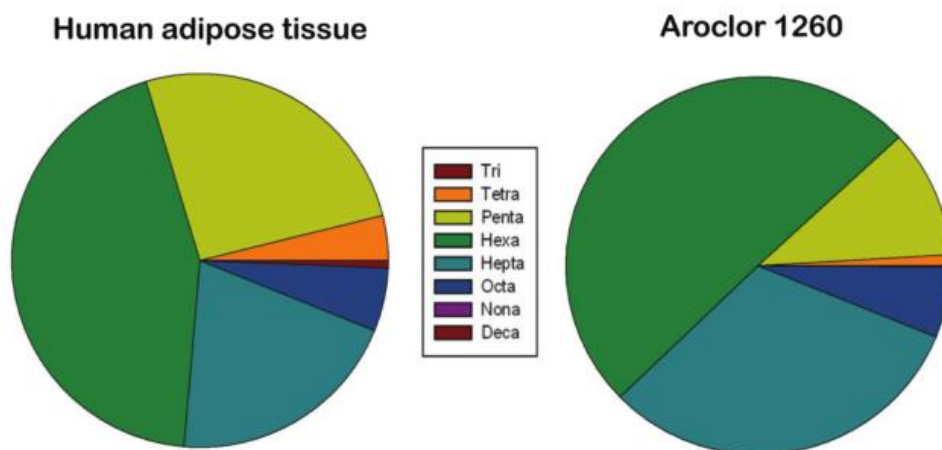
Figure 1.5 Relative PCB composition in human adipose tissue and Aroclor 1260. Figure adapted from Wahlang, *et al*., *Toxicol Sci*, 2014,140 (2): 283-297.

Two major human PCB exposure events occurred in Japan (known as "Yusho") in 1968 (60) and in Taiwan (known as "Yucheng") in 1978 (61), both as results of contaminated rice oil consumption. In Yusho, maternal exposed women tend to give offspring with lower birth weight (62). Follow-up studies of the Yucheng events have demonstrated neurocognitive deficits in elderly women patients (63) and increased mortality from chronic liver disease and cirrhosis in men (64, 65). Moreover, multiple epidemiological studies have reported associations between PCB exposure and suspected steatohepatitis (42) and/or diabetes (57, 66) in NHANES and ACHS studies.

As liver is the major site of PCB metabolism, and the lower chlorinated metabolites could adduct to DNA, proteins and lipids, and associate with activation of various hepatic receptors; thus, liver is the major target organ for the toxic effects of PCBs exposure. The nutrient-PCB interaction also affects PCB toxicity in liver. For example, DL-PCBs interact with AhR, and induce NAFLD in normal diet, while NDL-PCBs mixture interact with nuclear receptors, and exacerbate high fat diet-induced injury, leading to NASH. Therefore, PCBs have also been classified as endocrine and metabolism disrupting chemicals (EDCs/MDCs). EDCs interfere with any aspect of hormone action, resulting in endocrine dysfunction; while MDCs promote metabolic changes, resulting in metabolic disease (66).

3. Xenobiotic receptors

The functions of xenobiotic receptors are not only related to chemical detoxification, but also contribute to glucose and lipid metabolism, which are associated with metabolic disease, including NAFLD/NASH. In the current dissertation, the xenobiotic receptors of aryl hydrocarbon receptor (AhR), constitutive androstane receptor (CAR) and pregnane x receptor (PXR) will be discussed.

The AhR is a ligand-binding activated transcription factor that belongs to the Per-Arnt-Sim family. The molecular mechanisms of AhR activation have previously been reviewed (67) (Figure 1.6). Unliganded AhR resides in cytoplasm of cells, forming a protein complex with a heat shock protein 90 (HSP90) dimer and the co-chaperone protein X-associated protein 2 (XAP2), collectively they retard AhR translocation to nucleus. Upon binding an agonist, the AhR complex translocates to the nucleus and AhR nuclear translocator (ARNT) mediates HSP90 displacement, leading to AhR-ARNT heterodimer formation. This dimer is capable of binding to a dioxin-responsive element (DRE), thereby

regulating the transcription of many genes, such as the cytochrome P4501A (*CYP1A*) family. Cypa1a1 and Cyp1a2, are the major members of Cyp1a family that metabolize the pro-carcinogenic chemicals to their carcinogenic form, which react with DNA to form mutagenic adducts, resulting in carcinogenesis. The high-affinity binding agonists for AhR are often xenobiotics, including 2,3,7,8-tetrachlorodibenzo-p-dioxin (TCDD), 1,2-benzo[a]pyrene (BA) and DL-PCBs. Moreover, low-affinity binding agonists for AhR have been discovered in diet (flavonoids and indoles), endogenously as bilirubin and tryptophan metabolites, and as products of the microflora (67, 68). On the other hand, ligand-independent indirect activation of AhR has been reported, such as that seen with omeprazole (69).

Associated with regulation of physiological functions, such as innate and adaptive immune responses (68), AhR activation also is involved in the processes of glucose and lipid metabolism. Pharmacologic activation of AhR (70) or constitutively activated AhR (71) induces hepatic steatosis via upregulation of fatty acid transport genes, such as *CD36/FAT*. Alteration of hepatic fatty acid composition (72) and decreased fatty acid oxidation (73) contribute to AhR ligand-induced liver toxicity and steatosis. On the contrary, AhR deficiency protects against high fat diet-induced obesity, improves insulin sensitivity, and attenuates hepatic steatosis (74, 75). Interestingly, liver-specific AhR knockout mice are prone to HFD-induced hepatic steatosis, inflammation and injury (76), suggesting AhR activation protects against fatty liver disease. Moreover, a disassociation of hepatic steatosis and insulin resistance has been found in constitutively activated AhR mice (77) by inducing a novel AhR target gene, fibroblast growth factor 21 (FGF21) (78). Moreover, TCDD or PCB 126 exposure-induced AhR activation suppresses hepatic

gluconeogenesis by inhibition of gluconeogenic gene expression, such as phosphoenol-pyruvate carboxykinase (*Pck1*) (73, 79, 80).
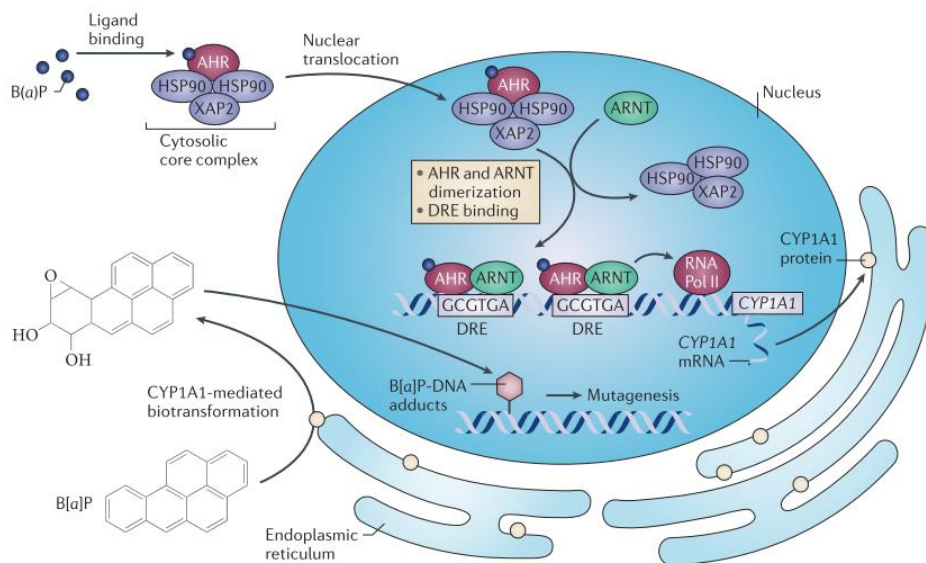
Figure 1.6 Scheme of AhR activation by agonist binding. Figure are adapted from Murray *et al*., *Nat Rev Cancer*, 2015, 14 (12): 801-814.

PXR (nuclear receptor subfamily 1, group I, member 2, NR1I2) and CAR (nuclear receptor subfamily 1, group I, member 3, NR1I3) are members of the orphan nuclear receptor subclass. The major functions of these receptors are regulating transformation and elimination of chemicals in liver by regulation of phase I and phase II drug metabolizing enzymes and drug transporters (81). The direct and indirect molecular mechanisms of CAR and PXR activation have been reviewed (82). A variety of structurally related PXR and CAR ligands has been reported, including drugs, environmental pollutants, and endobiotics. Moreover, specific ligands diversity and species diversity are well known. For example,

the CAR ligands for human and mouse are 6-(4-chlorophenyl)imidazo[2,1-b][1,3]thiazole-5-carbaldehydeO-(3,4dichlorobenzyl)oxime (CITCO) and 1,4-bis[2-(3,5-dichloropyridyl-oxy)]benzene (TCPOBOP), respectively. Activation of PXR induces expression of target genes of the *Cyp3a* family, including *Cyp3a11* in mice and *Cyp3a4* in human, while CAR target genes of the *Cyp2b* family, such as *Cyp2b10* in mice and *Cyp2b6* in human, are induced upon activation. PXR and CAR are sister xenobiotic receptors as they regulate many overlapping genes involved in chemical and drug detoxification and transportation.

Similar to AhR, PXR and CAR activities also are involved in metabolic disease by modulating glucose, fatty acid, and lipid metabolism directly or indirectly (81, 83, 84). CAR activation increases insulin sensitivity, improves type 2 diabetes and fatty liver disease (85, 86). Moreover, TCPOBOP treatment attenuates methionine choline-deficient (MCD) diet- induced NASH (87). The role of PXR activation in obesity is controversial, as ligand-induced PXR activation protects against high fat diet-induced obesity (88), while PXR ablation alleviates high fat diet-induced or genetic obesity, and improves insulin sensitivity (89). Activation of either PXR or CAR suppresses hepatic gluconeogenic gene expression by inhibition of transcriptional factors such as forkhead box protein O1 (*FoxO1*), hepatocyte nuclear factor 4 alpha (*HNF4a*), and peroxisome proliferator-activated receptor gamma coactivator 1-alpha (*PGC1a*) (90, 91). Furthermore, PXR activation suppresses inflammation and is a promising target for inflammatory diseases (92).

The detoxification of PCBs is associated with nuclear receptor CAR and PXR activation, and in turn, CAR and PXR activation affect PCBs exposure-induced metabolic disorders. Our previously published data suggest Aroclor1260, a NDL-PCB congeners mixture, activates human PXR and CAR3 variant, and is a mixed agonist/antagonist for

14

the human CAR2 variant based on cell culture model (52). In *vivo*, Aroclor 1260 treatments activate CAR and PXR, as evidenced by induced expression of their target genes, *Cyp2b10* and *Cyp3a11* at low doses, Aroclor 1260induced expression of AhR target gene *Cyp1a2* requires much higher doses due to the low amounts of DL-PCBs (59). Moreover, Aroclor 1260 treatments promote hepatic steatosis progression to steatohepatitis only at low dose, but not at high dose, under high fat diet conditions. PCB congeners apparently do not directly bind with the CAR, and the potential indirect mechanism of activation of CAR by Aroclor 1260 exposure may be EGFR signaling inhibition (93, 94), this similar to the molecular mechanisms that was shown by the CAR indirect activator, phenobarbital (95).

4. Aims and significance of current study

Although animal exposure models have typically investigated the toxic effects of only single PCB congeners or NDL-PCBs mixture treatments, humans are simultaneously exposed to mixtures of DL- and NDL-PCB congeners. Because the DL- and NDL-PCBs have different toxicological mechanisms of action, exposures to both types of PCBs might be synergistic or not. Therefore, the aims of the current dissertation are to investigate and compare DL-PCB congener (PCB 126), NDL-PCBs mixture (Aroclor 1260), and DL/NDL-PCBs mixture (Aroclor 1260 plus PCB 126) exposure related NAFLD/NASH and metabolic dysfunction. The potential role of AhR in PCB mixtures exposure-induced NAFLD/NASH will also be investigated.

As aforementioned, Aroclor 1260 best mimics PCBs that are seen in human adipose tissue (52), and Aroclor 1260 exposure is considered to be a 'second hit' in the conversion of diet-induced hepatic steatosis to the more advanced steatohepatitis. However, Aroclor 1260 (20 mg/kg) did not induce hepatic expression of prototypical AhR target genes (52,

59), because it did not contain a significant amount of DL-PCBs, such as PCB 126. To best mimic the DL/NDL-PCBs bioaccumulation pattern and the highest levels of exposure seen in humans (52), we added a small quantity of DL-PCB 126 which represents approximately 0.02% of human total PCBs exposure based on NHANES data. Because PCB 126 is not the only DL-PCB congener extant, and human exposures vary, the PCB 126 dose was increased to 0.1% (20 µg/kg).

The specific aims of my dissertation are shown as follows.

Specific Aim 1 will address whether DL-PCBs, NDL-PCBs, and DL/NDL-PCBs act differently on fatty liver disease. We will use male C57BL/6 mice on control synthetic diet to ascertain whether single treatment with Aroclor 1260, PCB 126, or Aroclor 1260/0.1% PCB 126 for 2 weeks activate AhR and downstream target genes, and lead to steatosis and liver injury (inflammatory markers, steatosis markers, and lipid metabolism markers). Next, male wild type C57BL/6 mice fed fat diet received the same PCB treatments for 12 weeks. The animals will be sacrificed and the liver mRNA levels of disease markers (receptors and their downstream targets, inflammatory markers, markers of fat metabolism), and pathological changes will be measured, to ascertain whether AhR is essential for PCBs-induced liver disease.

Specific Aim 2 will address whether human and murine AhR display the same concentration-dependence for ligand activation in response to PCBs. Initially, we will use cultured human (HepG2) and murine (Hepa1c1c7) hepatoma cells transfected with a XRE-Luc reporter to determine the relative affinity of the mixture Aroclor 1260, Aroclor 1254, selected DL-PCB congeners, including PCB 126, PCB 77, PCB 114, and PCB 81, and a mixture of DL/NDL-PCBs mixture (Aroclor 1260 plus 0.1% PCB 126, Ar1260/PCB 126).

This allows us to ascertain if the murine and human AhR are equally sensitive to PCB ligands or if the murine AhR binds ligands with higher affinity than the human receptor. We subsequently used murine and human primary hepatocytes to further test this hypothesis in an *in vitro* model. This aim is important for reverse translation studies utilizing mouse models of NAFLD.

CHAPTER II

ACUTE POLYCHLORINATED BIPHENYL TREATMENTS REGULATE HEPATIC

METABOLISM AND PANCREATIC FUNCTION: IMPLICATION FOR NON-

ALCOHOLIC FATTY LIVER DISEASE AND DIABETES

1. Introduction

The commercially manufactured PCBs mixture that best mimics human PCB (by mass) bioaccumulations patterns in adipose tissue is Aroclor 1260, which is a NDL-PCBs mixture (52). Aroclor 1260 is considered a 'second hit' in the conversion of diet-induced hepatic steatosis, to the more advanced steatohepatitis. It also decreased pancreatic insulin production (59). However, low doses of Aroclor 1260 (20 mg/kg) did not induce hepatic expression of prototypical AhR target genes (52, 59), because it should not contain a significant amount of DL-PCBs, such as PCB 126, as indicated by high doses of Aroclor 1260 (200 mg/kg) required to observe AhR activation. Therefore, a high dose of PCB 126 was used to evaluate the toxic effects on fatty liver disease (48, 96, 97).

While humans are simultaneously exposed to mixtures of DL- and NDL-PCBs, animal exposure models have typically investigated the effects of only a single congener or NDL-PCBs mixture as mentioned before. Because the DL- and NDL-PCBs have different toxicological mechanisms of action, DL/NDL-PCBs mixture exposures to both types of PCBs might be synergistic. In PCB mixtures and especially among bioaccumulated PCBs, DL-PCBs are minor constituents. Using NHANES data, PCB 126 represents approximately 0.02 % of the total PCB load in human serum (98).

18

The purpose of this subacute exposure study was to perform an integrated analysis of liver, pancreas, and serologic endpoints using exposures that better mimic high level human exposures to examine if the rodent AhR is activated and if mixtures of DL- and NDL-PCBs will behave like DL- or NDL-PCBs alone. My hypothesis is that at the highest human levels of exposure observed in literature, the rodent AhR will be activated, but that mixtures of DL- and NDL-PCBs will act differently. The mice were fed a control synthetic diet and exposed to: a low-dose of a DL-PCB congener (PCB 126, 20 µg/kg), an NDL-PCB mixture (Aroclor 1260, 20 mg/kg), an environmentally relevant mixture of low-dose PCB 126 (20 µg/kg) plus Aroclor 1260 (20 mg/kg); or vehicle. The possible impact of PCBs on novel mechanisms of endocrine and metabolic disruption [e.g., novel hepatokines (99) and genes regulating pancreatic islet cell identity and function (100)] will be investigated. This study could inform the direction of subsequent studies of combined exposures to PCB mixtures and hypercaloric diets in the metabolic syndrome.

2. Materials and Methods

Reagents

   Aroclor 1260 and PCB 126 were purchased from AccuStandard, Inc., (New Haven, CT). RNA-STAT 60 were ordered from Amsbio., (Austin, TX) and QuantiTect Reverse Transcription Kit were obtained from Qiagen, (Valencia, CA). iTaq Universal probes Supermix was supplied by Biorad, (Hercules, CA). Taqman probes for real-time polymerase chain reaction (RT-PCR) and Infinity ^{TM} Triglycerides were obtained from Thermo Fisher Scientific, Inc., (Middletown, VA). Free fatty acids test kits were purchased from Roche Dignostics, (Indianapolis, IN). Lipid panel plus kits were obtained from Abaxis, (Union City, CA). The customized Milliplex® MAP Panel was obtained from Millipore Corp, (Billerica, MA). The other reagents were obtained from Sigma-Aldrich, (St. Louis, MO).

Animal exposures

   The animal protocol used was approved by the University of Louisville Institutional Animal Care and Use Committee. Male C57BL/6j mice (10 weeks old) were obtained from The Jackson Laboratory (Bar Harbor, ME), and divided into 4 groups (n=10) based on the different exposures. All the mice were fed a control synthetic diet (20.0 %, 69.8 %, and 10.2 % of total calories come from protein, carbohydrate, and fat, TekLab TD06416). Mice were treated by one-time gavage with either Aroclor 1260 (20 mg/kg), PCB 126 (20 µg/kg), Aroclor 1260 (20 mg/kg) with 0.1 % PCB 126 (20 µg/kg) or vehicle control (corn oil) for 2 weeks. Mice were housed in a temperature- and light controlled-room (12 h light; 12 h dark) with food and water *ad libitum*. The animals were euthanized at the end of week 2 using ketamine/xylazine (100/20 mg/kg body weight, i.p.) and the blood, liver, pancreas,

and fat tissues were collected. Dual energy X-ray absorptiometry (DEXA) scanning (Lunar PIXImus densitometer, WI) was performed to analyze body fat composition prior to euthanasia.

Histological staining

The liver and pancreas tissues were fixed in 10 % neutral buffered formalin for 72 hours and embedded in paraffin for routine histological examination. Hematoxylin–eosin (H&E) staining were performed to observe histopathological changes. Photomicrographic images were acquired using a high-resolution Olympus digital scanner on an Olympus digital camera (BX41).

Real-time PCR

The liver and pancreas tissues were homogenized and total RNA was extracted using RNA-STAT 60 according to the manufacture's protocol. The purity and quantity of total RNA were assessed with Nanodrop spectromer (ND-1000, Thermo Fisher Scientific, Wilmington, DE) using ND-1000 V3.8.1 software. cDNA was synthesized using the QuantiTect Reverse Transcription Kit according to the manufacture's protocol. RT-PCR was performed on the CFX384 TM Real-Time System (Biorad, Hercules, CA) using iTaq Universal probes Supermix and Taqman probes. The probes sequence were as follows: mouse AhR (Mm00478932_m1); mouse CAR (Nr1i3) (Mm01283978_m1); mouse PXR (Nr1i2) (Mm01344139_m1); cytochrome P450s, including Cyp1a2 (Mm00487224_m1), Cyp2b10 (Mm01972453_s1), Cyp3a11 (Mm00731567_m1), and Cyp4a10 (Mm02601690_gH); carnitine palmitoyl transferase 1A (Cpt1α) (Mm01231183_m1); peroxisome proliferator-activated receptor alpha (Pparα) (Mm00440939_m1); Cd36 (Mm01135198_m1); fatty acid-binding protein 1 (Fabp1) (Mm00444340_m1); fatty acid

synthase (Fasn) (Mm00662319_m1); stearoyl coenzyme A desaturase1 (Scd1) (Mm00772290_m1); Pnpla3 (Mm00504420_m1); fibroblast growth factor 21 (Fgf21) (Mm00840165_g1); insulin-like growth factor 1 (Igf1) (Mm00439560_m1); betatrophin (Mm01175863_g1), glucose 6-phosphate (G6P) (Mm00839363_m1); phosphoenolpyruvate carboxy kinase (Pck1) (Mm01247058_m1); insulin 1(Mm01950294_s1); Nkx6-1 (Mm00454961_m1); NR4a1 (Mm01300401_m1); NR4a3 (Mm00450071_g1); pancreatic polypeptide (Mm00435889_m1); and glyceraldehyde-3-phosphate dehydrogenase (GAPDH) (Mm99999915_g1). All reactions were run in triplicate. The relative expression of each mRNA was calculated using the comparative $2^{-\triangle\triangle Ct}$ method and was normalized against GAPDH mRNA.

Measurement of hepatic lipid

The liver tissues were rinsed in neutral $1\times$ phosphate buffered saline (PBS) and homogenized in 50 mM NaCl solution. Hepatic lipids were extracted by a mixed solution of chloroform and methanol (2:1) according to a published protocol (101). Total lipid extracts were dried using nitrogen before they were dissolved in PBS containing 1 % triton X-100. Hepatic triglycerides and free fatty acid contents were measured using commercial kits and normalized to liver weight.

Measurement of plasma lipid and cytokine

Blood samples were collected by syringe with anti-coagulated EDTA. Plasma was obtained after centrifugation at 3,000 rpm for 20 min at 4 ℃. Plasma ALT, AST, triglyceride, cholesterol, high-density lipoprotein (HDL), low-density lipoprotein (LDH), very low-density lipoprotein (VLDL), and non-HDL cholesterol (nHDLc) levels were measured by Piccolo Xpress Chemistry Analyzer using the lipid panel plus kits. Plasma

cytokine and adipokine levels were measured on a Luminex® 100 system using a customized Milliplex® MAP mouse adipokine Panel.

Statistical analysis

Statistical analyses were carried out using SigmaPlot 11.0 software (Systat Software Inc., San Jose, CA). Data are presented as mean ± SEM. Statistical evaluation of the data was performed using two-way analysis of variance (ANOVA). Fold-changes are fold of vehicle control group. For all statistical comparisons, p-values less than 0.05 were considered statistically significant.

3. Results

Effects of PCB exposures on body weight and composition

There were no significant changes in body weight in either group (Fig. 2.1 A). Regarding body composition, there were no significant trends towards increased percent body fat with Aroclor 1260 (14.0 %) or PCB 126 (7.5 %). The interaction between Aroclor 1260 and PCB 126 significantly decreased percent body fat in the DL/NDL-PCBs mixture-treated group compared to either alone exposure (Fig. 2.1 B). No significant changes were observed in the liver/body weight ratio (Fig. 2.1 C) or the epididymal fat/body weight ratio (Fig. 3.1 D).
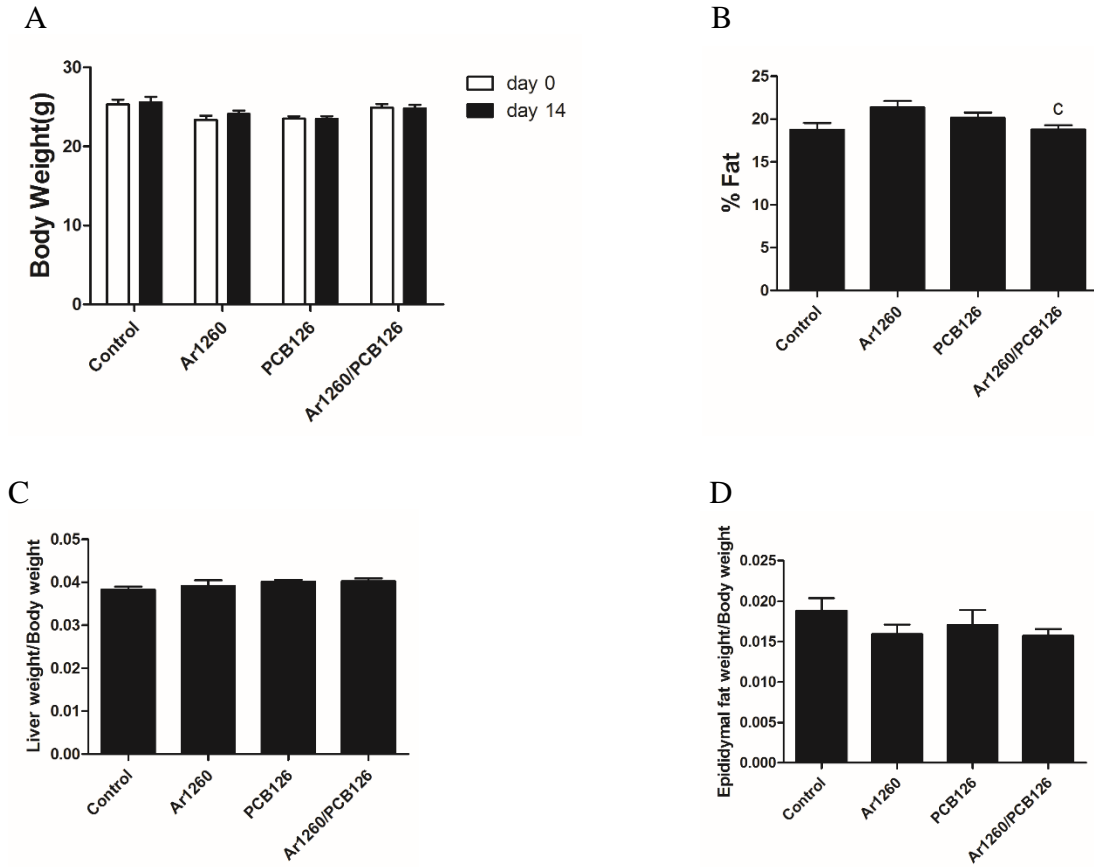
Figure 2.1 Effects of PCB exposures on liver and fat weight. (A) The body weight, (B) body fat composition, (C) the ratio of liver weight to body weight, (D) the ratio of epididymal fat weight to body weight. Data are presented as mean ± SEM. n=10. p<0.05, c= interaction between Aroclor 1260 and PCB 126.

Effects of PCB exposures on hepatic expression of AhR, CAR, PXR, and their target genes

To determine if PCB exposures affected mRNA expression of hepatic xenobiotic receptors (*AhR, CAR, PXR*) and their target genes, hepatic mRNA expression was measured by RT-PCR. *AhR* mRNA expression was significantly decreased by either Aroclor 1260 (3.3-fold) or PCB 126 (3.2-fold) exposure, while the Aroclor 1260/ PCB 126 mixture significantly increased *AhR* mRNA expression compared to either exposure alone (Fig. 2.2 A). PCB 126 alone (8.7-fold) or the Aroclor 1260/PCB 126 mixture (7.9-fold) activated AhR, as indicated by increased AhR target gene *Cyp1a2* mRNA expression. The latter data suggest that the observed changes in the *AhR* mRNA expression levels did not affect its transcriptional activity (Fig. 2.2 B). *CAR* mRNA expression was slightly increased by PCB 126 alone or by the Aroclor 1260/PCB 126 mixture, but was not changed by Aroclor 1260 (Fig. 2.2 C). The CAR target gene *Cyp2b10* mRNA expression was robustly increased by Aroclor 1260 (130,000-fold), while PCB 126 induced *Cyp2b10 mRNA* expression to a much lower degree (25.0-fold). An interaction between Aroclor 1260 and PCB 126 resulted in significantly different *Cyp2b10* mRNA levels that were intermediate between either exposure alone (50,000-fold) (Fig. 2.2 D). *PXR* mRNA expression was significantly decreased by either Aroclor 1260 or PCB 126 exposures, but was increased by the Aroclor 1260/PCB 126 mixture compared to either exposure alone (Fig. 2.2 E). PXR-dependent gene *Cyp3a11* mRNA expression was increased by Aroclor 1260 (2.0-fold), and exposure with the Aroclor 1260/PCB 126 mixture attenuated this effect (Fig. 2.2 F). These results demonstrate that PCB 126 alone or in the DL/NDL-PCBs mixture activated AhR, and Aroclor 1260 potently activated CAR and to a lesser degree PXR. The PCB exposures differentially regulated AhR and nuclear receptor expression.

Moreover, the results suggested that PCB 126 activated AhR may suppress the activation of CAR and PXR by Aroclor 1260. However, the reciprocal effect of activating either CAR or PXR did not appear to affect AhR activity.
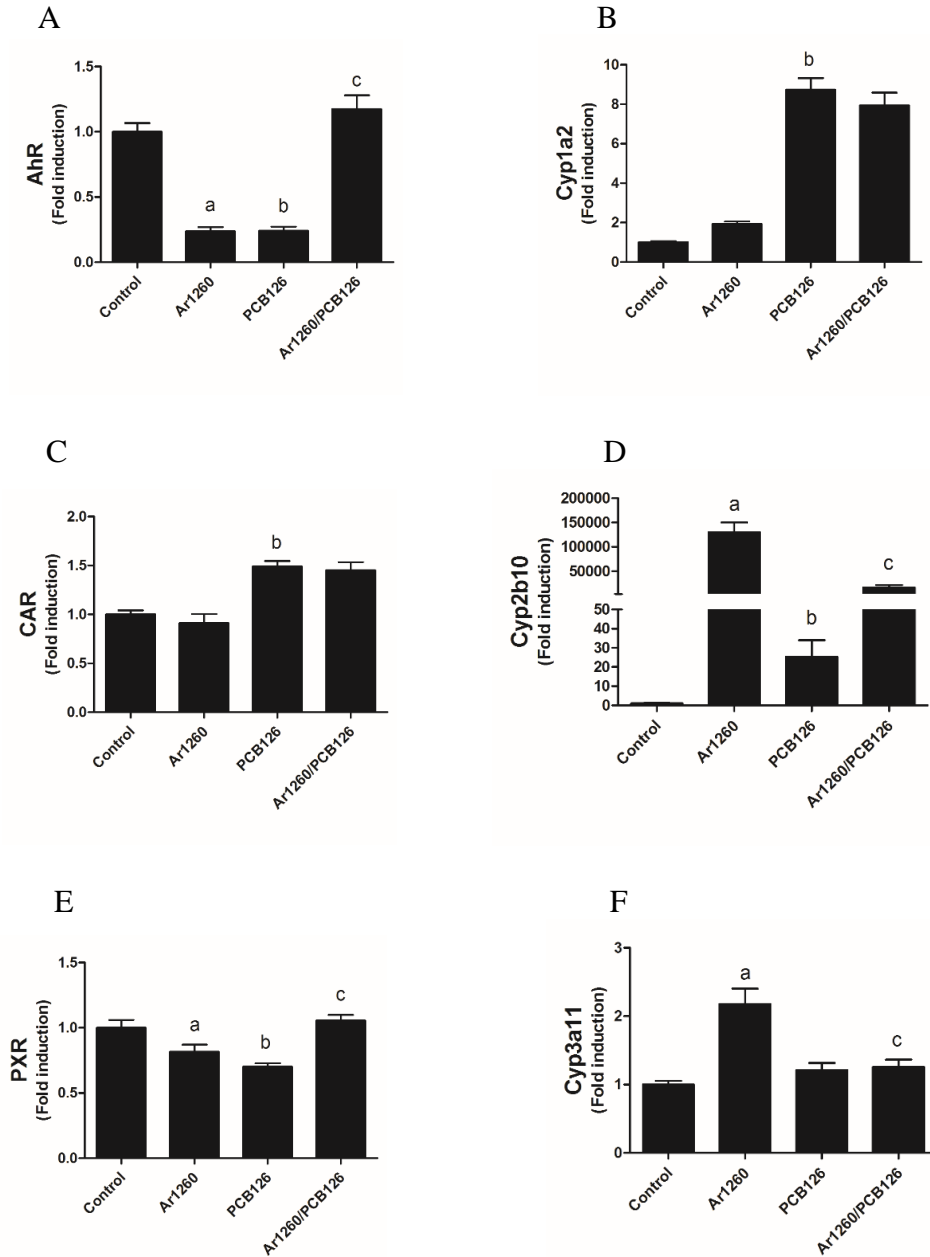
Figure 2.2 Effects of PCB exposures on levels of hepatic AhR, CAR, PXR, and their target genes expression. Hepatic mRNA levels of *AhR* (A) and target gene *Cyp1a2* (B), *CAR* (C) and target gene *Cyp2b10* (D), *PXR* (E) and target gene *Cyp3a11* (F) were measured by performing RT-PCR. Data are presented as mean ± SEM. n=10. $p < 0.05$, a= Aroclor 1260 effects, b= PCB 126 effects; c= interaction between Aroclor 1260 and PCB 126.

Effects of PCB exposures on hepatic lipids

To evaluate for hepatic steatosis, histologic staining (H&E) of liver was performed. PCB 126, but not Aroclor 1260 exposure, induced mild small droplet-macrovesicular steatosis. PCB 126-induced hepatic steatosis was attenuated in the DL/NDL-PCBs mixture (Fig. 2.3 A). These histologic steatosis results were confirmed by biochemical lipid assays. The hepatic triglyceride levels (30.7 %) (Fig. 2.3 B) and free fatty acid levels (approximately 60.0 %) (Fig. 2.3 C) were increased by PCB 126 exposure, but exposure with the mixture of Aroclor 1260 plus PCB 126 abrogated this affect. Aroclor 1260 exposure had no effect on either hepatic triglycerides or free fatty acids (Fig. 2.3 B&C). Significant hepatic necroinflammation was not observed under any exposure in histology (Fig. 2.3 A); plasma alanine or aspartate aminotransferase levels (Fig. 2.3 D&E); or serum pro-inflammatory cytokines (IL-6, MCP-1, PAI-1) were not significantly altered within any exposure group (Fig. 2.3 F-H).

A

Control　　　　　　　　　　Aroclor 1260

PCB 126　　　　　　　　　　Aroclor 1260/PCB 126
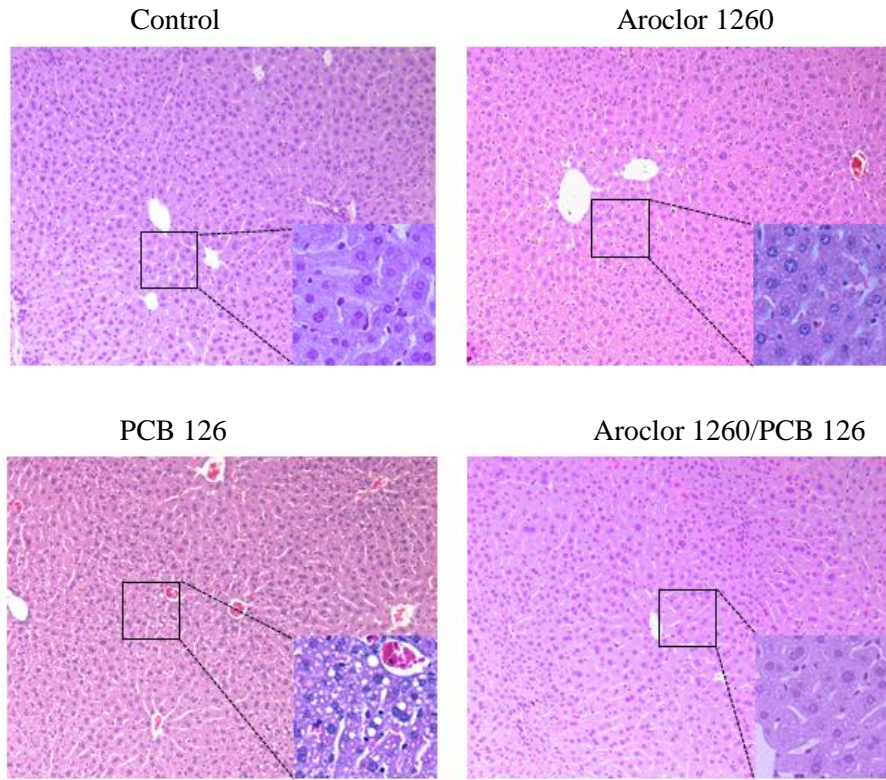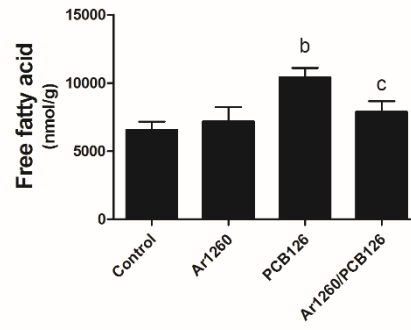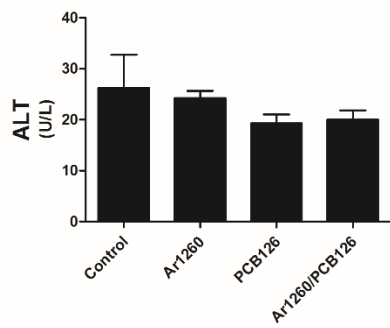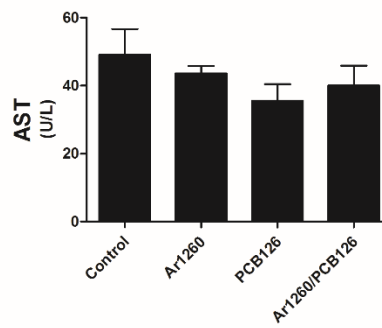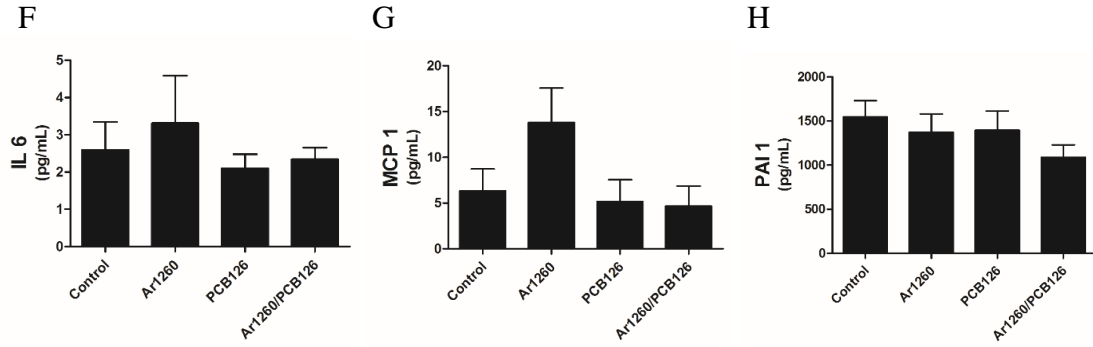
Figure 2.3 Effects of PCB exposures on hepatic lipids. (A) H&E staining of liver, (B) hepatic triglycerides levels, (C) hepatic free fatty acid levels, plasma levels of (D) ALT, (E) AST, (F) IL6, (G) MCP1, and (H) PAI1. n=10. Data are presented as mean ± SEM. $p < 0.05$, b= PCB 126 effects; c= interaction between Aroclor 1260 and PCB 126.

Effects of PCB exposures on plasma lipids

The PCB exposures had very different effects on plasma lipids. While PCB 126 increased hepatic lipids, it significantly decreased plasma triglycerides, total cholesterol, HDL, VLDL, and nHDLc cholesterol (Fig. 2.4 A-E). Blood lipids were not affected by Aroclor 1260 either alone or in the DL/NDL-PCBs mixture. In summary, these data suggested that subacute, low-dose PCB 126 exposure caused toxicant-associated fatty liver disease (steatosis) without significant necroinflammation. The fatty liver disease was associated with a paradoxical decrease in blood lipids. Aroclor 1260 in the DL/NDL-PCBs mixture abrogated PCB 126-induced changes in liver, but not the blood lipid profile.
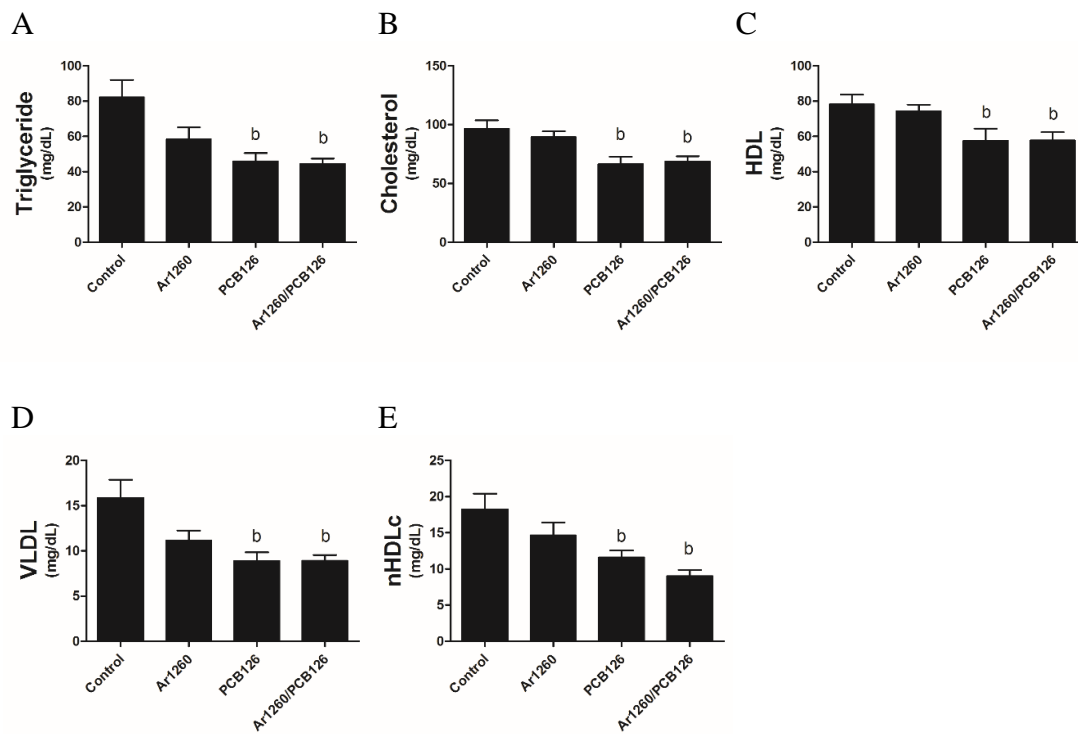
Figure 2.4 Effects of PCB exposures on plasma lipid levels. (A) Plasma triglyceride, (B) cholesterol, (C) high-density lipoprotein (HDL), (D) very low-density lipoprotein (VLDL), and (E) non-HDL cholesterol (nHDLc) levels were measured by Piccolo Xpress chemical analyzer (n=8-10). Data are presented as mean ± SEM. p<0.05, b= PCB 126 effects.

Effects of PCB exposures on hepatic fatty acid β-oxidation genes expression

Since PCB 126 exposure impacted liver and blood lipid levels, expression of lipid oxidation genes (*PPARα* and its targets, *Cyp4a10* and *Cpt1α*) were measured. There was a trend towards increased *Pparα* mRNA expression by both PCB 126 and Aroclor 1260, but the mixture of both PCB types significantly decreased *Pparα* mRNA expression compared to either alone (Fig. 2.5 A). Both mRNA levels of *Cpt1α* (1.5-fold, Fig. 2.5 B) and *Cyp4a10* (1.2-fold, Fig. 2.5 C) were significantly increased by PCB 126. Neither *Cyp4a10* nor *Cpt1α* mRNA expression was changed by Aroclor 1260 exposure. However, the DL/NDL-PCBs mixture increased *Cyp4a10* mRNA expression (Fig. 2.5 C), while decreasing *Cpt1α* mRNA expression (Fig. 2.5 B) compared to PCB 126 exposure alone. Thus, PCB 126 exposure activated PPARα to induce expression of genes implicated in hepatic fatty acid β-oxidation. While this may have contributed to the observed hypolipidemic effects of PCB 126, it cannot account for the increased hepatic lipid levels and steatosis observed with this exposure. Likewise, the decrease in hepatic *PPARα* and *Cpt1α* mRNA expression cannot account for the decreased hepatic steatosis observed when Aroclor 1260 was given along with PCB 126.
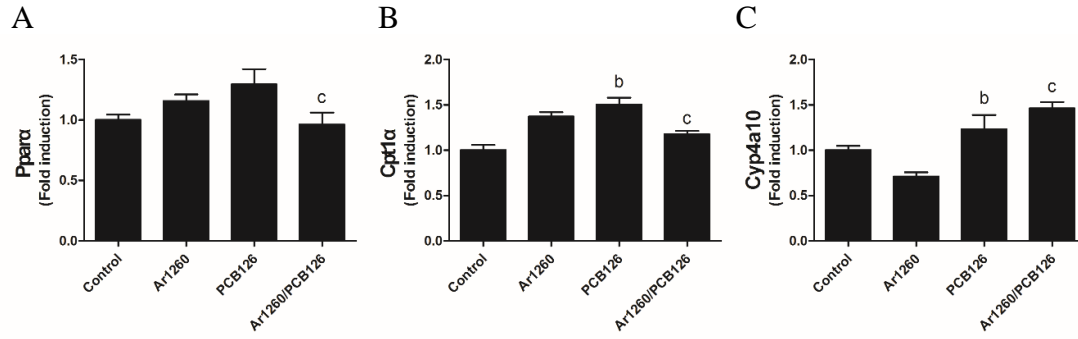
Figure 2.5 Effects of PCB exposures on hepatic fatty acid β-oxidation genes expression. Hepatic mRNA levels of *Cyp4a10* (A), *Cpt1α* (B), and *Pparα* (C) were measured by performing RT-PCR. Data are presented as mean ± SEM. n=10. p<0.05, b= PCB 126 effects; c= interaction between Aroclor 1260 and PCB 126.

Effects of PCB exposures on other genes of hepatic lipid metabolism

Because PCB 126 induced hepatic steatosis that could not be explained by a reduced β-oxidation, expression of other hepatic lipid metabolism genes was measured. These genes were involved in hepatic fatty acid import (*Cd36* and *Fabp1*), synthesis (*Fasn*), desaturation (*Scd1*), and also included the lipase implicated in NAFLD, *Pnpla3*. *Cd36* mRNA levels were significantly induced by either PCB 126 (350.0-fold) or Aroclor 1260 (300.0-fold) exposures, but surprisingly exposure to the Aroclor 1260/PCB 126 mixture attenuated these effects compared to either alone (Fig. 2.6 A). Likewise, either PCB 126 (1.5-fold) or Aroclor 1260 (1.3-fold) exposures significantly increased the mRNA levels of lipid transporter *Fabp1*, but Aroclor 1260/PCB 126 co-administration reduced *Fabp1* expression compared to either exposure alone (Fig. 2.6 B). Interestingly, there was nearly the mirror image observed between *Cd36/Fabp1* and *Fasn* mRNA expression. *Fasn* mRNA expression was significantly decreased by either Aroclor 1260 (3.3-fold) or PCB 126 (5.0-fold) exposures, but was increased by the mixture of Aroclor 1260 plus PCB 126 compared to either exposure alone (Fig. 2.6 C). Thus, mono-exposure to either PCB 126 or Aroclor 1260 increased hepatic lipid uptake while decreasing lipid biosynthesis, but these effects were abrogated by exposure to the NDL/DL-PCBs mixture. Thus, the increased steatosis observed with PCB 126 exposure was most likely due to increased hepatic lipid uptake despite decreased *de novo* lipid biosynthesis and increased β-oxidation. Exposure with either Aroclor 1260 (1.4-fold), PCB 126 (1.7-fold), or Aroclor 1260/PCB 126 (2.3-fold) resulted in significant down-regulation of *Scd1* mRNA levels (Fig. 2.6 D). This should increase the relative abundance of saturated fatty acids compared to unsaturated fatty acids. A loss of function polymorphism in the hepatic lipase, PNPLA3,

results in the accumulation of mutant protein on lipid droplets to increase human NASH (102). *Pnpla3* mRNA expression was significantly induced by Aroclor 1260 (3.0-fold) exposure, but was suppressed by either PCB 126 (2.3-fold) or Aroclor 1260/PCB 126 (7.7-fold) exposure (Fig. 2.6 E). While the impact of these effects on steatohepatitis in rodents expressing wild type Pnpla3 may not impact the degree of steatosis, the induction of mutant human PNPLA3 by Aroclor 1260 is predicted to increase NASH, while the suppression of the mutant human PNPLA3 by the other exposures is predicted to be protective (102). Pnpla3 expression may be regulated by both CAR (103) and the AhR (104). Our data suggested that there may be interaction between Aroclor 1260-activated CAR and PCB 126-activated AhR effecting the expression of Pnpla3. In summary, while all PCB exposures disrupted normal hepatic lipid metabolism, only PCB 126 exposure induced steatosis.
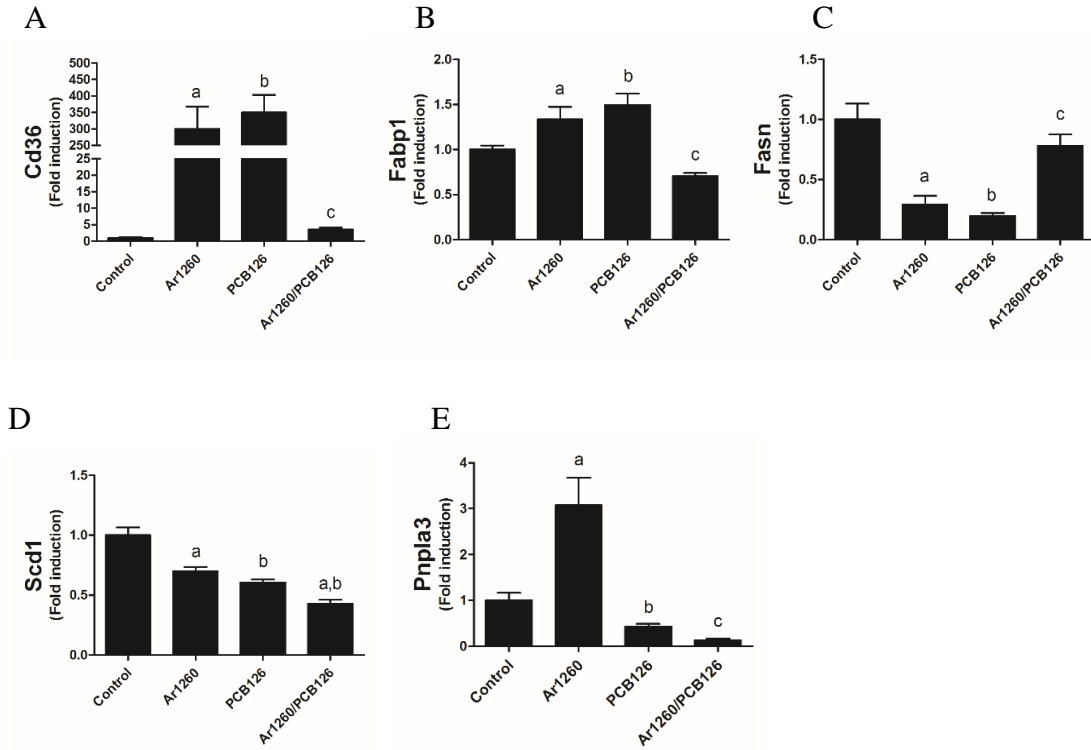
Figure 2.6 Effects of PCB exposures on genes expression of hepatic lipid metabolism. Hepatic mRNA levels of *Cd36* (A), *Fabp1* (B), *Fasn* (C), *Scd1* (D), and *Pnpla3* (E) were measured by performing RT-PCR. Data are presented as mean ± SEM. n=10. p<0.05, a= Aroclor 1260 effects, b= PCB 126 effects; c= interaction between Aroclor 1260 and PCB 126.

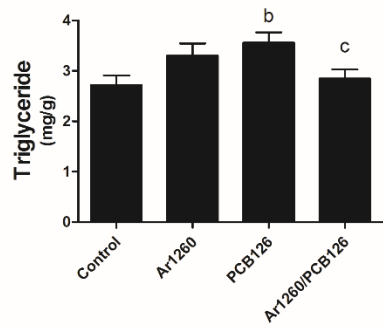Effects of PCB exposures on hepatokine expression

The liver also functions as an endocrine organ that plays a major role in the development of obesity, diabetes, and metabolic syndrome. Hepatic mRNA expression levels of several protective hepatokines previously implicated in these processes (e.g., *Fgf21*, *Igf1*, and *betatrophin*) were measured. The *Fgf21* mRNA expression was significantly down-regulated by either Aroclor 1260 (10.0- fold) or PCB 126 (4.0-fold) exposure compared to control groups. In contrast, administration of Aroclor 1260/PCB 126 mixture increased *Fgf21* mRNA expression compared to either alone (Fig. 2.7 A). Hepatic *Igf1* mRNA expression was significantly increased after exposure with either Aroclor 1260 (1.2-fold) or PCB 126 (1.6-fold) compared to control groups, while Aroclor 1260/PCB 126 mixture administration resulted in a reduction of *Igf1* mRNA expression compared to either alone (Fig. 2.7 B). Although it is controversial whether betatrophin promotes islet β cells expansion (105, 106), the expression of *betatrophin* mRNA was affected by PCBs exposure. Aroclor 1260 exposure (2.1-fold) significantly induced *betatrophin* mRNA expression, but not by PCB 126 exposure. Mixture of PCB 126 of Aroclor 1260 abolished Aroclor 1260-induced *betatrophin* mRNA expression (Fig. 2.7 C). These results suggested that environmental PCBs exposure may disrupt the liver-pancreas axis, leading to the development of NAFLD/NASH and diabetes. In summary, Aroclor 1260 increased mRNA expression of *Igf1* and *betatrophin* while decreasing mRNA expression of *Fgf21*. Addition of PCB 126 to Aroclor 1260 produced the opposite effects. PCB 126 exposure alone increased *Igf1* and decreased *Fgf21* mRNA expression. These results demonstrated that the liver is a causal target organ for PCB-related endocrine disruption.
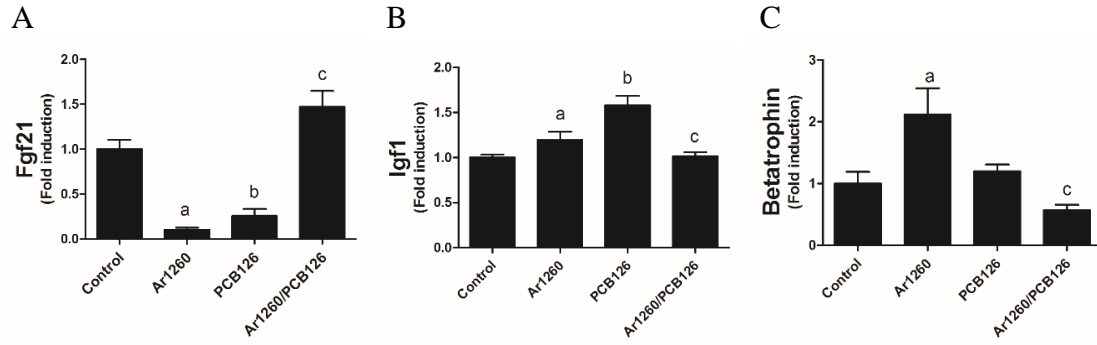
Figure 2.7 Effects of PCB exposures on hepatokines expression. Hepatic mRNA levels of *Fgf21* (A), *Igf1* (B), and *betatrophin* (C) were measured by performing RT-PCR. Data are presented as mean ± SEM. n=10. p<0.05, a= Aroclor 1260 effects, b= PCB 126 effects; c= interaction between Aroclor 1260 and PCB 126.

Effects of PCB exposures on pancreas structure

Because PCB exposures have been associated with diabetes, the effects of the PCB exposures on the pancreatic structure were evaluated. The pancreas weight to body weight ratio was unaffected by either Aroclor 1260 or PCB 126 exposures (Fig. 2.8 A). However, it was significantly decreased (25.3 %) by Aroclor 1260 / PCB 126 co-exposure (Fig. 2.8 A). H&E staining demonstrates pancreatic structural changes following exposure with the NDL/DL PCB mixture (Fig. 2.8 B). Specifically, this co-exposure was associated with pancreatic degeneration with acinar cell steatosis and atrophy occurring in the absence of ductal changes or inflammation. These changes did not occur with the other PCB exposures (Fig. 2.8 B). To further evaluate the pancreatic pathology associated with Aroclor 1260/PCB 126 co-exposure, trichrome stain was performed. The co-exposed mice had mildly increased pancreatic fibrosis compared to mice treated with vehicle control (Fig. 2.8 C).

A

B
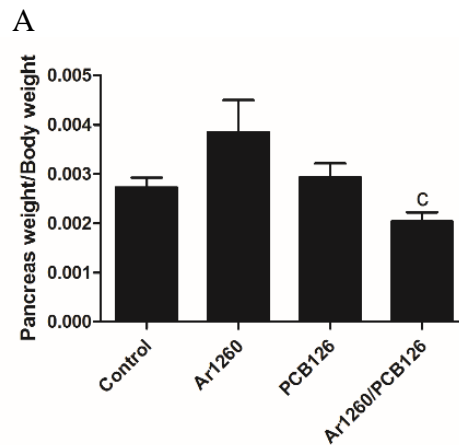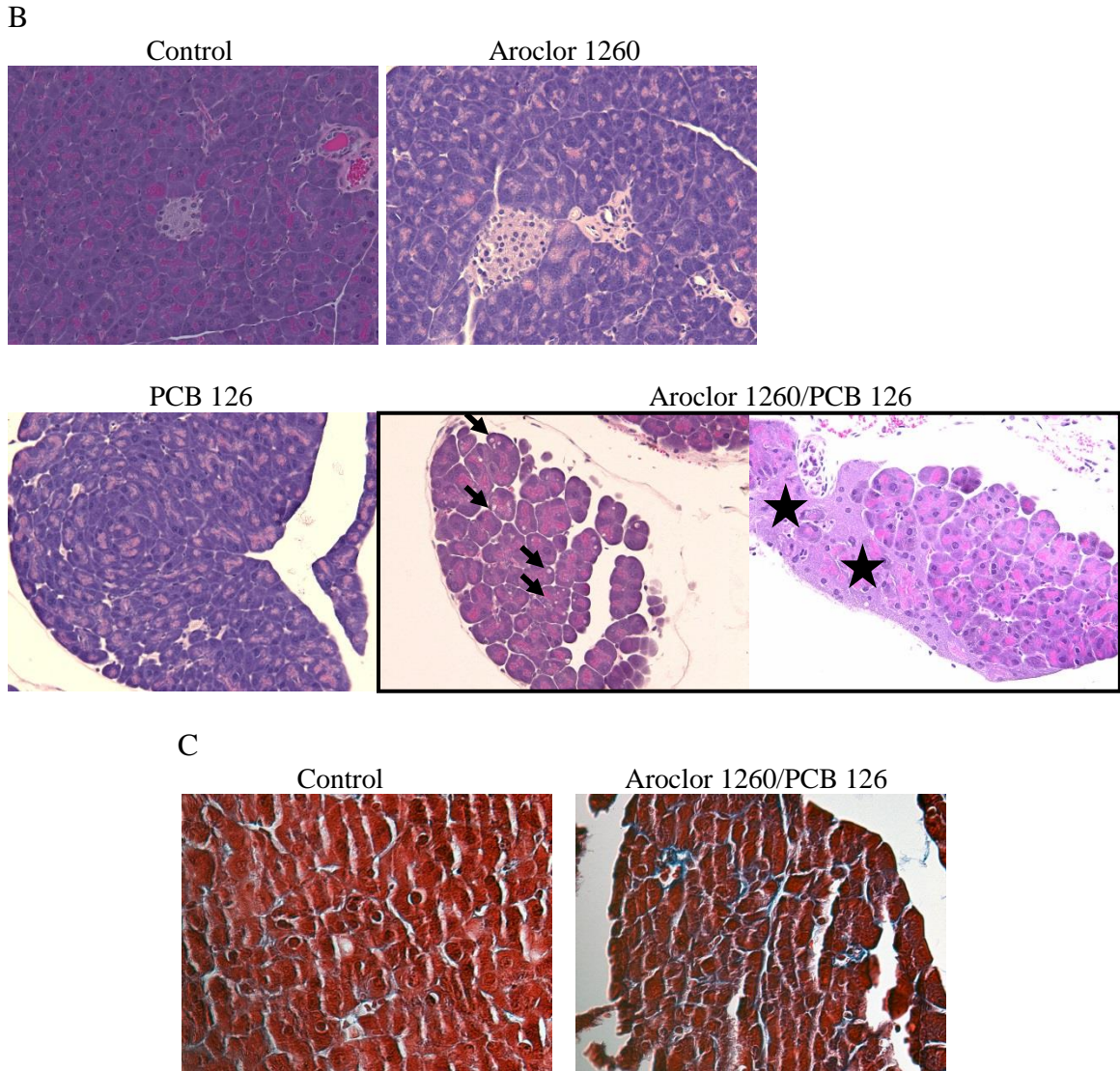
Figure 2.8 Effects of PCB exposures on pancreatic structure. (A) The ratio of pancreas weight to body weight, (B) H&E staining of pancreas (20 ×), and (C) trichrome staining (40 ×). Blank arrow indicates lipid droplet and blank star means degeneration in pancreas. c= interaction between Aroclor 1260 and PCB 126.

Effect of PCB exposures on pancreatic function

The pancreatic *insulin 1* mRNA expression was significantly up-regulated by either Aroclor 1260 (5.8-fold) or PCB 126 (1.4-fold) exposure, but was signficantly down-regulated by the Aroclor 1260/PCB 126 mixture (0.25-fold) (Fig. 2.9 A). A similar pattern was seen for the beta cell identity gene, *Nkx6-1* (Fig. 2.9 B), and for the F-cell gene product, *pancreatic polypeptide* (Fig. 2.9 C). The nuclear receptors NR4a1 and NR4a3 are involved in Nkx6-1 regulated islet beta cell proliferation (107). As with mRNA expression of *Nkx6-1*, the mRNA expression levels of *NR4a1* and *NR4a3* were increased by either Aroclor 1260 (2.0-fold and 3.1-fold, respectively) or PCB 126 (1.8-fold and 3.0-fold, resectively), while the Aroclor 1260/PCB 126 exposure reduced *NR4a1* and *NR4a3* mRNA expression compared to either exposure alone (Fig. 2.9 D&E). These findings demonstrate that exposure to the NDL/DL-PCB mixture was associated with decreased expression of genes regulating pancreatic beta cell identity, and this was associated with decreased expression of insulin and pancreatic polypeptide, and pancreatic histopathologic changes.
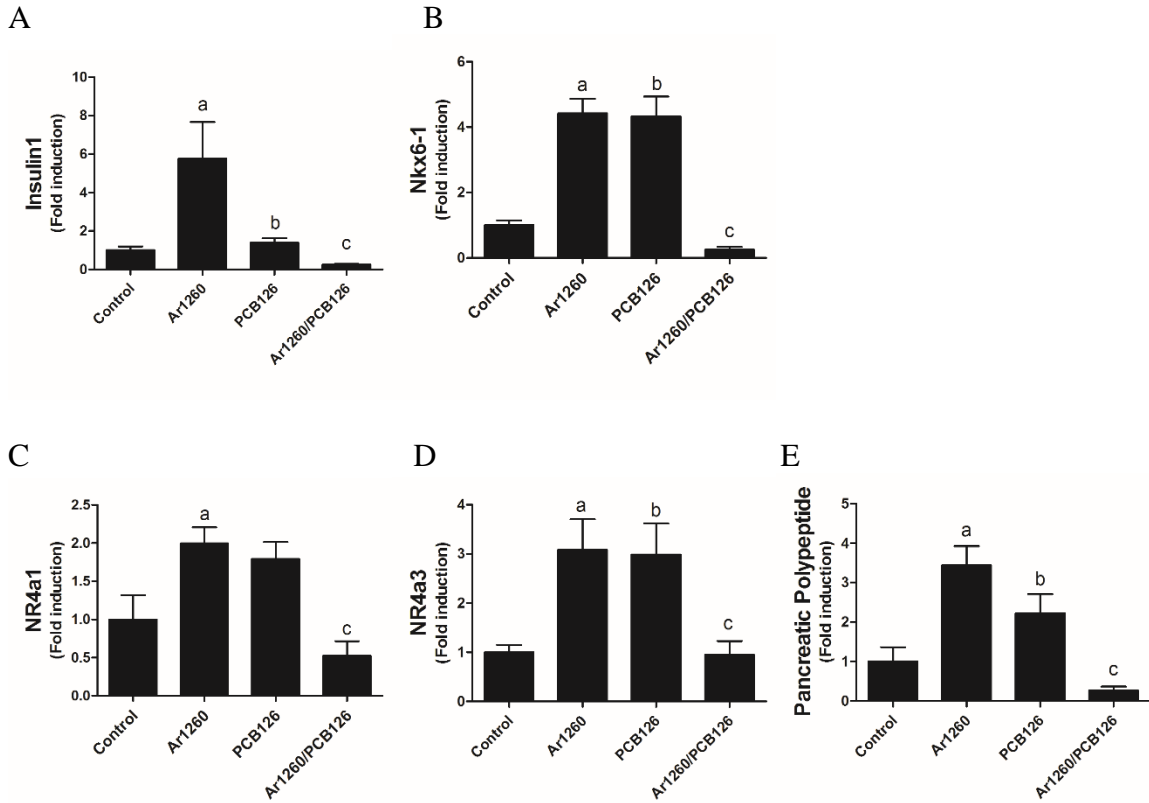
Figure 2.9 Effects of PCB exposures on pancreatic gene expression. Pancreatic mRNA levels of *insulin1*(A), *Nkx6-1* (B), *pancreatic polypeptide* (C), *NR4a1* (D) and *NR4a3* (E) were measured by performing RT-PCR. Data are presented as mean ± SEM. n=10. $p<0.05$, a= Aroclor 1260 effects, b= PCB 126 effects; c= interaction between Aroclor 1260 and PCB 126.

Effects of PCB exposures on hepatic gluconeogenic gene expression

Hepatic gluconeogenesis, contributes significantly to glycaemia, particularly in the fasting state. The hepatic mRNA level of *Pck1*, a regulator of gluconeogenesis, was significantly increased by PCB 126 exposure (1.6-fold), but was down-regulated by the Aroclor 1260/PCB 126 mixture (Fig. 2.10 A). The hepatic gluconeogenic gene, *G6P* mRNA, was significantly down-regulated by either Aroclor 1260 (1.7-fold) or PCB 126 (1.3-fold) exposure compared to vehicle control group; while the Aroclor 1260/PCB 126 mixture up-regulated *G6P* mRNA expression compared to either exposure alone (Fig. 2.10 B). Thus, hepatic carbohydrate metabolism was also affected by PCB exposures. Perhaps consistent with decreased hepatic gluconeogenesis, the fasting blood glucose was decreased by PCB 126 exposure, either alone or along with Aroclor 1260 (Fig. 2.10 C).
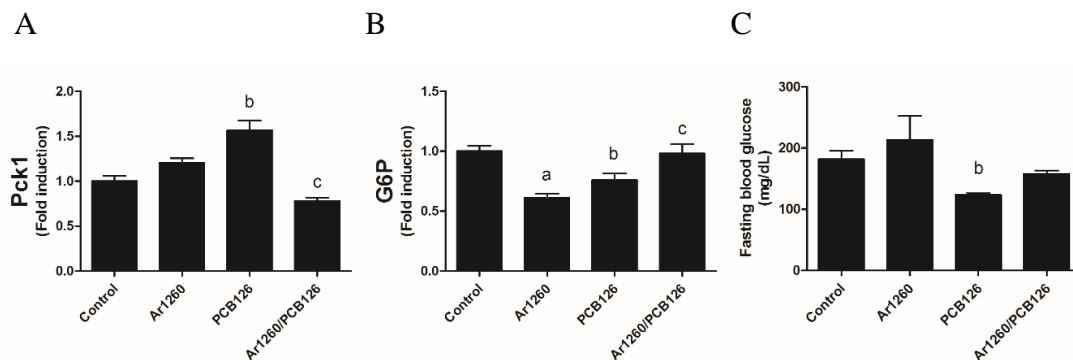
Figure 2.10 Effects of PCB on gluconeogenic genes expression. Hepatic mRNA levels of gluconeogenic genes *G6P* (A) and *Pck1* (B) were measured by performing RT-PCR. (C) Fasting blood glucose. Data are presented as mean ± SEM. n=10. $p<0.05$, a= Aroclor 1260 effects, b= PCB 126 effects; C= interaction between Aroclor 1260 and PCB 126.

4. Discussion

The exposure protocol to Aroclor 1260 used in this study is the same, which we have used in previous 12-week studies (59, 108). This exposure was designed to mimic the PCB bioaccumulation pattern and the highest levels of exposure seen in humans (52). However, Aroclor 1260 has lower levels of DL-PCBs than in human bioaccumulation patterns. To compensate for lower levels of DL-PCBs, we added a small quantity of PCB 126 that represents approximately 0.02 % of a human's total PCB exposure based on NHANES data (42). Because PCB 126 is not the only DL-PCB and human exposures vary, the PCB 126 dose was increased to 0.1 % (20 µg/kg).

This PCB 126 dose is much lower (20 µg/kg) than that used in other studies (1.6 mg/kg) in the literature (48), but it was sufficient to activate the prototypical AhR target gene, *Cyp1a2*. The induction of *Cyp1a2* mRNA was equal in both the PCB 126 alone group and in the Aroclor 1260/PCB 126 mixture-exposed groups. This confirms our previous results that Aroclor 1260 at this dose does not activate AhR (59), most likely due to the low levels of DL-PCBs in the commercial Aroclor 1260 mixture.

Activation of CAR can either occur from direct by ligand binding or indirect activation via inhibition of EGFR (95). The consequences of the different modes of activation of CAR are significant as direct CAR activation may have more limited effects in the cell than indirect activation. PCB dependent inhibition of EGFR signaling causes extensive changes in the mouse phosphoproteins, which includes PI3K. ERK, STAT3, raf (93). In this study, all exposures increased CAR target gene *Cyp2b10* mRNA expression. The increases were far greater with Aroclor 1260 or the Aroclor 1260/PCB 126 mixture exposure > 1000-fold while PCB 126 exposure increased *Cyp2b10* mRNA expression a more modest 20-fold.

This most likely reflects the large difference in dose (mg vs. µg), but confirms our observation that PCB 126 is a good inhibitor of EGFR (94). Interestingly, the induction of *Cyp2b10* mRNA by Aroclor 1260 alone was greater than the induction by the Aroclor 1260/PCB 126 mixture, indicating that mixtures do not behave in the same way as either PCB preparation alone. These results suggest that activation of AhR affected other PCB-regulated transcription factors. Similar results were obtained with Cyp3a11, where only Aroclor 1260 induced this gene and the effects of the mixture appeared no different than that seen in the control animals. Thus, it appears that there is interaction between the AhR and the nuclear receptors, CAR and PXR.

The effects of the various PCB exposures on biomarkers of liver disease are more complex. Exposure to PCB 126 alone increased liver triglycerides and free fatty acids, while the addition of Aroclor 1260 reduced liver triglycerides and fatty acids to close to control levels. This is consistent with previous studies in the literature demonstrating that activation of AhR in mice spontaneously induced hepatic steatosis (70, 71) and caused mice to be much more sensitive to methionine choline-deficient (MCD)-induced NASH (109). Likewise, this is consistent with our previous 12-week study in Aroclor 1260 exposed animals in which steatosis did not get worse. However, Aroclor 1260 exacerbated steatohepatitis in 42 % calories from fat mice but had little effect on 10.2 % calories from fat control diet. In contrast, direct activators of CAR, such as TCPOBOP, decrease hepatic steatosis in HFD-fed type 2 diabetic models and in the ob/ob mice (85, 86). All of these data likely reflect the different modes of activation of CAR as PCBs in murine systems are indirect activators.

Activation of the AhR is known to be associated with dyslipidemia and a wasting syndrome. In our current study we observed reductions in serum cholesterol and both HDL and nHDLc form, suggesting both increased hepatic import and decreased secretion. Likewise, serum triglycerides and VLDL were also reduced. This is consistent with a wasting syndrome in which peripheral fat is being mobilized and steatosis results. Interestingly, these affects occur in all groups that received PCB 126 and are independent of effects caused by Aroclor 1260 exposure. The hypolipidemia induced by PCB 126 exposure is clearly different from the steatosis caused by hypercaloric diets where these parameters rise in concert with the development of steatosis.

The effects of each exposure on genes involved in lipid metabolism are also more complex. For example, the mixture of PCB 126 and Aroclor 1260 slightly decreased the level of *PPARα*, while PCB 126 slightly induced *CPT1*a and *Cyp4a11*, and the mixture slightly attenuated the effect with *CPT1a*. In fact, it augments the effect with *Cyp4a11*. Thus, it is highly unlikely this is a PPARα-dependent process but more likely other transcription factors are involved in the promotors of these gene are involved.

Many other genes involved in fat mobilization are affected by PCB exposure. As anticipated from previously published studies exposure to either Aroclor 1260 or PCB 126 induced mRNA expression of *Cd36*. Interestingly, the mixture of both of these exposures actually reduced the expression of this gene that may in part explain why the steatosis was less pronounced in the Aroclor 1260/PCB 126 mixture group. A similar pattern is observed in the *Fabp1* mRNA expression, suggesting a conservation of mechanism while the opposite pattern is observed with Fasn. Other genes in fat metabolism and disposition are also affected including *Scd1*, which is negatively regulated by both Aroclor 1260 and PCB

126 in a simple additive fashion suggesting independent mechanisms. Finally, the mutated Pnpla3 gene results in accumulated lipids and inhibited VLDL secretion. These mutant versions are strongly linked to the development of NASH in the human population. This gene is induced by Aroclor 1260, but suppressed by PCB 126 and the combination of both suppresses the mRNA expression further. In concert these results clearly demonstrate that mixtures of DL/NDL-PCBs mixture do not act like their individual components and that considerable crosstalk exists between these signaling mechanisms.

In our study, NDL/DL-PCB mixtures definitely caused structural alterations in pancreas, as indicated by pancreatic fibrosis, acinar atrophy and acinar cell steatosis. However, there was no definite evidence of diabetes (normal HOMA-B, and decreased fasting glucose). Regarding translation to human disease, acinar cell steatosis has not been described in humans. However, PCB mixtures seem to cause a pancreatopathy, similar to that seen in diabetes, named diabetic exocrine pancreatopathy (110), and also exposures to pancreato-toxins such as smoking and alcohol, neither of which is associated with diabetes. We propose the term PCB-induced pancreatopathy to describe this condition. Just as in other forms of pancreatopathy, the clinical significance of the findings need further study. The unchanged HOMA-B in mice may be due to sufficient beta cell reserve at this timepoint in mice that were not stressed by obesity. The histological changes were paralleled by decreased mRNA expression of *insulin 1, pancreatic polypeptide*, and islet identity factors (e.g., *Nkx6-1, NR4a1*, and *NR4a3*). The combination of molecular and histological changes suggest that the Aroclor 1260/PCB 126 mixture exerted pancreatic endocrine and exocrine toxicity. However, neither Aroclor 1260 nor PCB 126 alone demonstrated this pancreatic toxicity. These results are broadly consistent with those of

earlier studies in which long-term PCB 126 exposure caused early β-cell failure (111). Lin *et al.* reported that chronic exposure to Aroclor 1254, caused pancreatic atrophy by reducing proliferation (112). Aroclor 1254 altered islet β-cell mass and impaired insulin receptor signaling, and ultimately disrupted glucose homeostasis (113). Our findings extend these observation by demonstrating that PCB exposure can possibly affect the genetic programing responsible for islet differentiation and function (e.g. islet identity factors). The islet identity factors are transcription factors involved in pancreatic differentiation and beta cell homeostasis in utero and in the adult. In rat islets, Nkx6-1 regulates the expression of glucagon, and controls glucose-stimulated insulin secretion (GSIS) (114). The alteration of Nkx6-1 expression was observed in type 2 diabetes patients (115). These results suggest alteration of islet identity factors may be involved in endocrine disruption by endocrine and metabolism disrupting chemicals (EDCs/MEDs) exposure. In the present study, the observed islet identity factors changes were a novel finding in PCB exposed mice, and more work is required to determine mechanisms of action.

Hepatokines have been proposed as being involved in mechanisms involved in the development of diabetes, as well as, NAFLD/NASH. These hepatokines include FGF21, IGF1 and betatrophin. FGF21 is a member of fibroblast growth factors (FGF) family, and plays a critical role in regulation of obesity, insulin resistance and fatty liver disease (116) by increasing brown adipose levels and adiponectin secretion. In the current study, mRNA levels of *Fgf21* were downregulated in both Aroclor 1260 and PCB 126 treated groups, while Aroclor 1260/PCB 126 mixture exposure resulted in increased *Fgf21* mRNA levels compared to individual exposures. As our mice were fasted, the *Fgf21* expression in the

PCB 126-exposed mice is consistent with the concept that AhR induces FGF21 in the fed-state, but suppresses FGF21 in the fasted-state (117).

Another hepatokine that has been implicated both in diabetes and the control of serum triglycerides and LDL metabolism is betatrophin (ANGPT8) as reviewed (118). Betatrophin expression is low in fasted animals and rises in the fed state and regulates triglyceride metabolism (119) by inhibiting lipoprotein lipase (LPL), thereby, decreasing LDL sand VLDL uptake by adipocytes. The functions of betatrophin in diabetes are controversial but studies suggest it promotes pancreatic β cell proliferation, expanding β cell mass, and improves glucose tolerance (105). Regardless, in the current study, expression of *betatrophin* mRNA was significantly upregulated by Aroclor 1260 exposure, but not by PCB 126 exposure. Adding PCB 126 to Aroclor 1260 abolished Aroclor 1260-induced betatrophin expression. PCBs exposure-induced dysregulation of hepatokines clearly demonstrates that PCBs and potentially other endocrine and metabolism disrupting chemicals (EDCs/MDCs) may affect expression of those hepatokines, such as FGF21 and betatrophin.

In conclusion, even an exposure as low as 20 µg/kg of PCB 126 induced AhR-dependent genes in mouse liver. Mixtures of DL and NDL PCBs exhibited different effects on gene expression, fatty liver disease, and diabetes endpoints, likely due to receptor interaction with each other. This suggests that studying single congeners in isolation may lead to potentially misleading results when modeling the metabolic disease associated with human PCB exposures. PCB 126 produced phenotypically were liver disease, while exposure to the mixture of PCB 126 plus Aroclor 1260 induced were pancreatic disease. Several novel targets for endocrine/metabolic disruption were identified including

PNPLA3, islet identity factors, and hepatokines. The latter implied that the liver is both a target and effect organ for endocrine disruption. More research is required to better understand the molecular mechanisms involved in complex mixtures of EDCs/MEDs, including DL/NDL-PCB mixtures.

CHAPTER III

THE INTERACTION OF DIET AND POLYCHLORINATED BIPHENYLS IN

REGULATION OF NON-ALCOHOLIC STEATOHEPATITIS

1. Introduction

High calorie intake or a Western diet induces NAFLD, and environmental pollutants serve as "second hit" to exacerbate high fat diet-induced liver injury in murine models (37). For example, a 20 mg/kg exposure to Aroclor 1260 has no effect on liver injury and hepatic pathological changes in control diet fed mice, but a high fat diet fed mice developed neutrophil infiltration, liver injury. Thus, Aroclor 1260 drives hepatic steatosis progression to steatohepatitis in high fat diet fed mice. Moreover, a high fat diet suppresses CAR activation, and decreases its target genes' expression induced by Aroclor 1260 exposure. Our acute exposure results demonstrated either Aroclor 1260 or PCB 126 exposure affected hepatic lipid metabolism, while only PCB 126 exposure induced mild hepatic steatosis. Co-administration of Aroclor 1260 and PCB 126 reduced the mild steatosis. With the increasing incidence of obesity and type 2 diabetes patients worldwide, a higher incidence of NAFLD is being observed, and the role of PCB exposures in these require investigation (42). The purpose of this chronic exposure study was to perform an analysis of liver and serologic endpoints using exposures that better mimic a high level human exposure to examine if the murine AhR is preferentially activated and whether or not mixtures of DL- and NDL-PCBs will behave like each component alone in high fat diet fed mice will be investigated. The animal groups and PCB treatments were the same as the acute exposure

study, but the control diet was replaced by high fat diet, and mice were exposed for 12 weeks.

2. Materials and Methods

Reagents

Please refer to Chapter 3 section for details. Humulin R (100 U/mL) was obtained from Eli Lilly, (Indianapolis, IN). Primary antibody (F4/80, ab6640) and second antibody were supplied by Abcam, (Cambridge, MA). CAE, Naphthol AS-D Chloroacetate (Specific Esterase) Kit were obtained from Sigma-Aldrich, (St. Louis, MO).

Animal exposures

The animal protocol used was approved by the University of Louisville Institutional Animal Care and Use Committee. Male C57BL/6j mice (10 weeks old) were obtained from The Jackson Laboratory, (Bar Harbor, ME), and divided into 4 groups (n=10). All the mice were fed a high fat diet (15.2 %, 42.7 %, and 42.0 % of total calories come from protein, carbohydrate, and fat, TekLab TD88137). Mice were treated by one-time gavage with either Aroclor 1260 (20 mg/kg), PCB 126 (20 µg/kg), Aroclor 1260 (20 mg/kg) with 0.1 % PCB 126 (20 µg/kg) or vehicle control (corn oil) for 12 weeks. Glucose tolerance test (GTT) and insulin tolerance test (ITT) were performed at 8 and 10 weeks, respectively, prior to euthanasia. Mice were housed in a temperature- and light controlled-room (12 h light; 12 h dark) with food and water *ad libitum*. The animals were euthanized at the end of week 12 using ketamine/xylazine (100/20 mg/kg body weight, i.p.) and the blood, liver, and fat tissues were collected. Dual energy X-ray absorptiometry (DEXA) scanning (Lunar PIXImus densitometer, WI) was performed to analyze body fat composition prior to euthanasia.

Histological staining

Please refer to Chapter 3 section for detail. Additional chloroacetate esterase activity and macrophage accumulation were measured using CAE and immunohistochemistry (IHC) staining according to manufacturer's protocols, respectively.

Real-time PCR

Please refer to Chapter 3 section for detail. Additional probes and their sequence were as follows: Tgf-β1 (Mm01178820_m1), Acta2 (Mm00725412_s1), Collagen (Col) 1a1 (Mm00801666_g1), Collagen (Col) 1a2 (Mm00483888_m1), and TIMP1 (Mm00441818_m1).

Measurement of hepatic lipid

Please refer to Chapter 3 section for detail.

Measurement of plasma lipid and cytokine

Please refer to Chapter 3 section for detail.

Glucose and insulin tolerance test

For the glucose tolerance test, mice were fasted for 16 hours prior to test. The basal fasting blood glucose levels were measured using a glucometer (ACCU-CHECK Aviva, Roche, Basel, Switzerland) with one drop of tail vein blood. Then sterile glucose was administrated via intraperitoneal (i.p.) injection at dose of 1 g/kg body weight within 15 minutes, and blood glucose levels were measured at 15, 30, 60, and 120 minutes post injection.

For the insulin tolerance test, mice were fasted for 6 hours at the day of test. Following a determination of the basal glucose level, sterile insulin was administrated, via

intraperitoneal (i.p.) injection, at dose of 0.5 U/kg body weight within 15 minutes, and blood glucose levels were measured at 15, 30, 60, and 120 minutes post injection.

Statistical analysis

Please refer to Chapter 3 section for detail.

3. Results

Effects of PCB exposures on body weight and composition

AhR activation induced by a high dose of pollutant agonist exposure, such as TCDD, leads to a wasting syndrome, characterized by a loss of body weight associated with a decrease in adipose tissue mass (120). To evaluate whether PCB exposures induced a wasting syndrome, body weight was monitored weekly. The body weight gradually increased in all groups regardless of PCB exposures due to high fat diet used in this experiment (Fig. 3.1 A). However, there were no changes in body weight (Fig. 3.1 B) or fat composition (Fig. 3.1 C) in PCB exposure groups compared to control group. The liver/body weight ratio was not changed after PCB exposures (Fig. 3.1 D); and the epididymal fat/body weight ratio was increased only after Aroclor 1260 exposure, but not in other PCB exposed groups (Fig. 3.1 E).
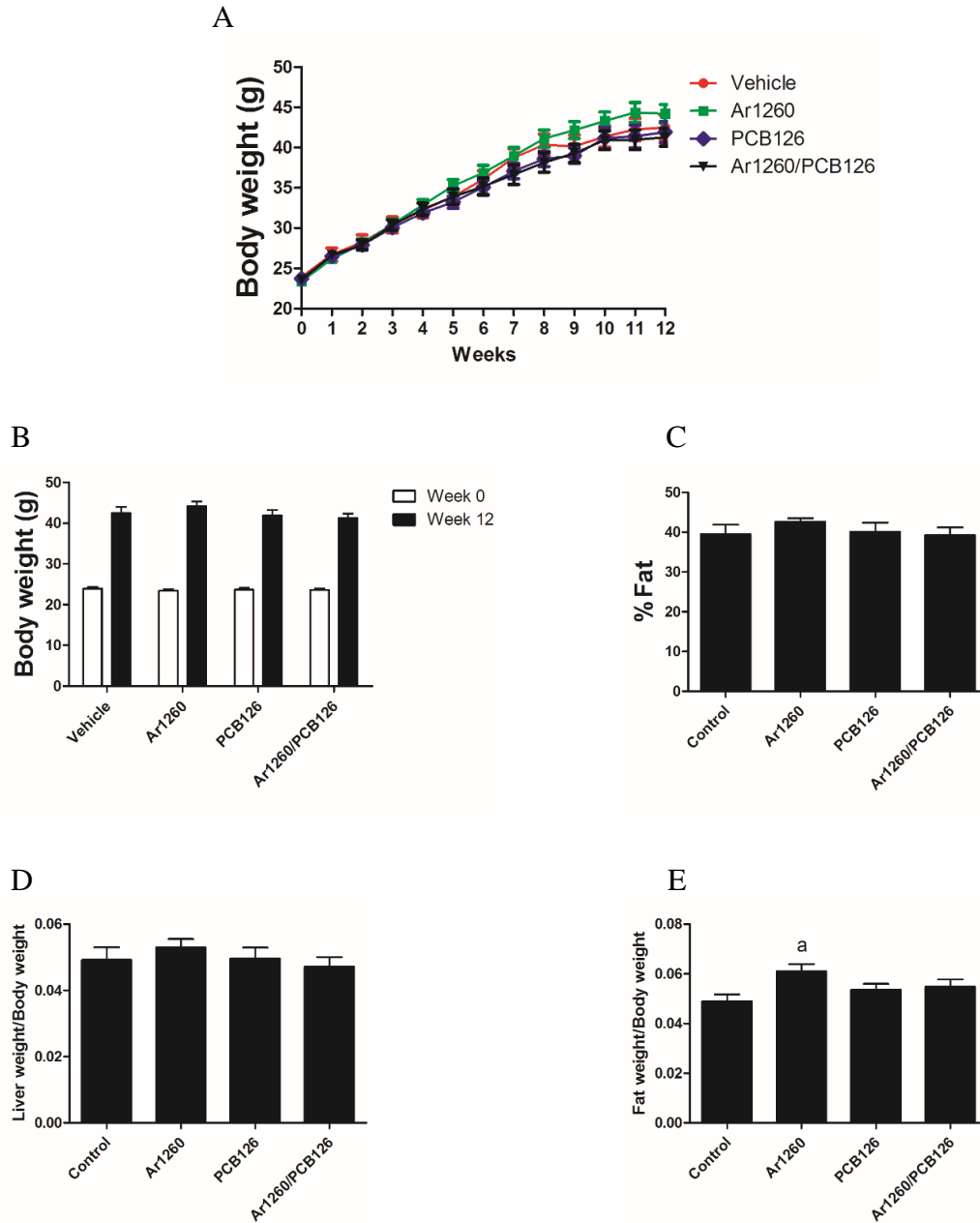
Figure 3.1 Effects of PCB exposures on body weight and composition after 12 weeks exposure. (A) Body weight changing, (B) body weight, (C) body fat composition, (D) the ratio of liver weight to body weight, (E) the ratio of epididymal fat weight to body weight. Data are presented as mean ± SEM. n=10. $p < 0.05$, a= Aroclor 1260 effects.

Effects of PCB exposures on AhR, CAR and their target genes

As shown in chapter 2, different types of PCB exposures are associated with AhR and CAR activation in mice fed control synthetic diet. *AhR* mRNA expression was decreased by PCB 126 (0.5-fold) exposure, but not by the other PCB exposed groups (Fig. 3.2 A). PCB 126 alone or Aroclor 1260/PCB 126 mixture activated AhR, as indicated by 4.0-fold or 2.6-fold induction of the AhR target gene *Cyp1a2* mRNA expression, respectively. Adding PCB 126 to Aroclor 1260 resulted in a reduction of *Cyp1a2* mRNA expression compared to PCB 126 alone (Fig. 3.2 B). *CAR* mRNA expression was significantly increased by PCB 126 alone (1.6-fold) or in the Aroclor 1260/PCB 126 mixture (2.3-fold), but was not changed by Aroclor 1260 (Fig. 3.2 C). The CAR-dependent gene *Cyp2b10* mRNA was increased by Aroclor 1260 (6.5-fold) or Aroclor 1260/PCB 126 mixture (2.3-fold) exposure (Fig. 3.2 D). Addition of PCB 126 reduced the Aroclor 1260-dependent induction of *Cyp2b10*, indicating an interaction between AhR and CAR signaling (Fig. 3.2 D). However, the extent of AhR or CAR transcriptional activities were affected by diet effects, since high fat diet suppressed PCB exposures-induction of the AhR target *Cyp1a2* slightly (≈50%). AS anticipated (37), decreased induction CAR-target *Cyp2b10* dramatically (≈1000-fold) activity when compared with control synthetic diet fed mice treated with same dose of PCBs. Moreover, the conclusions made in chapter 2 that the reciprocal effects of AhR and nuclear receptor were also found in the current study.

A

B

C

D
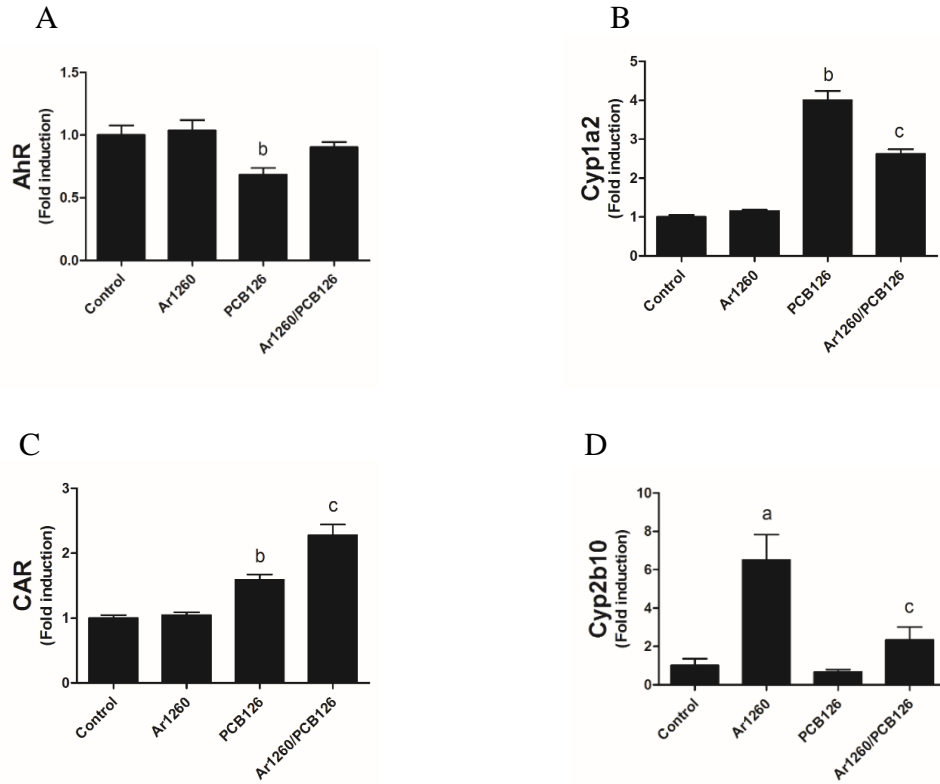
Figure 3.2 Effects of PCB exposures on AhR, CAR and their target genes. Hepatic mRNA levels of *AhR* (A) and target gene *Cyp1a2* (B), *CAR* (C) and target gene *Cyp2b10* (D) were measured by performing RT-PCR. Data are presented as mean ± SEM. n=10. $p<0.05$, a= Aroclor 1260 effects, b= PCB 126 effects, c= interaction between Aroclor 1260 and PCB 126.

Effects of PCB exposures on hepatic steatosis

H&E staining data demonstrated mice fed on high fat diet developed variable, centrilobular, macrovesicular lipidosis (hepatic steatosis), and PCB exposures did not exacerbate high fat diet-induced hepatic steatosis (Fig. 3.3 A). Neither hepatic triglyceride (Fig. 3.3 B) nor cholesterol (Fig. 3.3 C) levels were significantly affected by either PCB exposures, however, hepatic free fat acid levels were significantly increased by PCB 126 (1.3-fold) alone or Aroclor 1260/PCB 126 mixture (1.5-fold) exposures (Fig. 3.3 D).
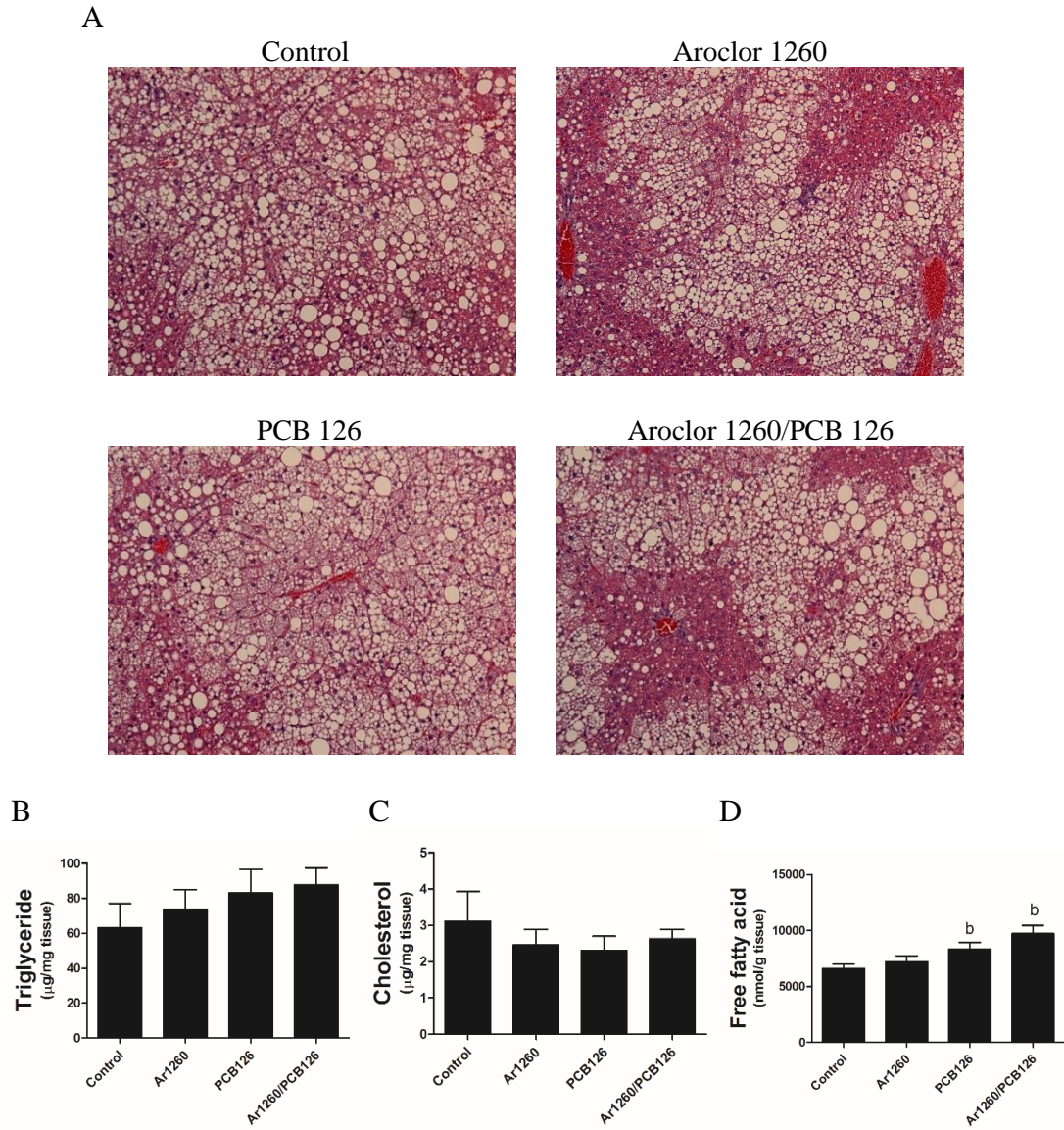
Figure 3.3 Effects of PCB exposures on hepatic steatosis. (A) H&E staining of liver (10 ×). High fat diet induced variable, centrilobular, macrovesicular lipidosis, and PCBs exposure did not exacerbate high fat diet-induced steatosis in liver. (B) hepatic triglycerides levels, (C) hepatic cholesterol levels, (D) hepatic free fatty acid levels. n=10. Data are presented as mean ± SEM. p<0.05, b= PCB 126 effects.

Effects of PCB exposures on liver injury

Previous studies showed that Aroclor 1260 exposure serves as "second hit" to drive hepatic steatosis to advanced steatohepatitis, therefore, plasma alanine (ALT) or aspartate (AST) aminotransferase levels were measured. Plasma ALT levels were elevated by Aroclor 1260 alone exposure (1.9-fold), but not by PCB 126 exposure. The mixture of PCB 126 and Aroclor 1260 attenuated Aroclor 1260-elevated plasma ALT levels (Fig. 3.4 A), suggesting that PCB 126 was protective against liver injury in this model. Likewise, PCB 126 exposure also showed a suppression of plasma AST levels when either given alone or mixed with Aroclor 1260 (Fig. 3.4 B). Hepatic mRNA expression of *Tnfα* was increased by either Aroclor 1260 exposure (1.8-fold) or Aroclor 1260/PCB 126 mixture exposure (1.9-fold) compared to vehicle group (Fig. 3.4 C). Likewise, hepatic mRNA expression of *Ccl8* was significantly induced by Aroclor 1260 exposure (3.3-fold), suppressed by PCB 126 alone exposure (0.38-fold), and mixture of PCB 126 of Aroclor 1260 abolished Aroclor 1260 exposure-induced *Ccl8* mRNA expression (Fig. 3.4 D). The similar patterns of mRNA levels of *Ccl3* (Fig. 3.4 E) and *Cxcl1* (Fig. 3.4 F) were also observed. In concert, these results demonstrated that addition of PCB 126 attenuates liver injury as evidenced by reduced ALT and AST, and by reducing hepatic inflammatory cytokines.
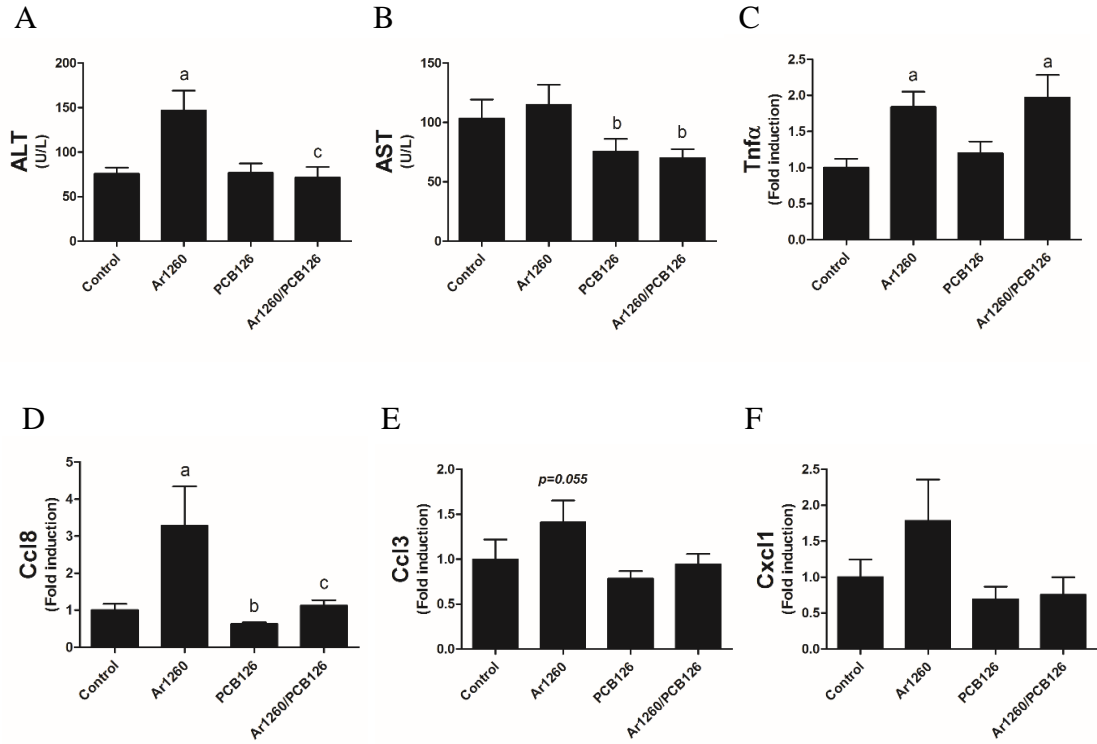
Figure 3.4 Effects of PCB exposures on liver injury. (A) Plasma ALT and (B) AST levels.

Hepatic mRNA levels of *Tnfα* (C), *Ccl8* (D), *Ccl3* (E), and *Cxcl1* (F) were measured by

performing RT-PCR. Data are presented as mean ± SEM. n=10. $p<0.05$, a= Aroclor 1260

effects, b= PCB 126 effects, c= interaction between Aroclor 1260 and PCB 126.

Effects of PCB exposures on hepatic inflammatory response

Neutrophil and macrophage infiltration lead to liver injury, thus, CAE and immunohistochemistry (F4/80, a macrophage marker) staining were performed to evaluate neutrophil infiltration and macrophage accumulation in liver, respectively. CAE staining showed high fat diet induced neutrophil infiltration, and Aroclor 1260 exposure exacerbated this effect. PCB 126 alone or in a Aroclor 1260/PCB 126 mixture did not display the elevated neutrophil infiltration (Fig. 3.5 A&B). Likewise, more F4/80 positive brown cells were found by Aroclor 1260 exposure compared to vehicle group, while PCB 126 or Aroclor 1260/PCB 126 mixture were not elevated (Fig. 3.5 C). This result was also confirmed by measurement of gene expression of another macrophage maker, CD68. Aroclor 1260 exposure increased *CD68* mRNA expression by 1.4-fold compared to vehicle group, and mixture of PCB 126 of Aroclor 1260 reversed Aroclor 1260-induced *CD68* mRNA expression (Fig. 3.5 D). These results suggested Aroclor 1260 exposure, but not PCB 126 exposure, induced inflammatory cell infiltration and led to liver injury, and PCB 126 displayed anti-inflammation effects which likely accounts for the reduced plasma liver enzyme levels.

A

Control
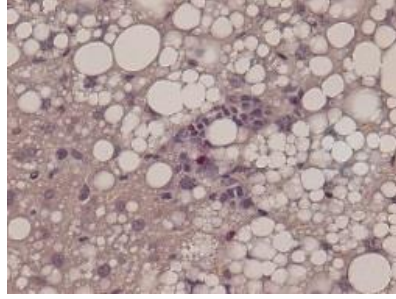
Aroclor 1260
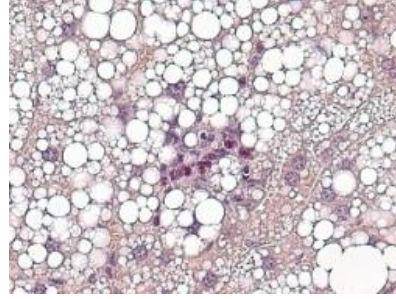
PCB 126

Aroclor 1260/PCB 126

C

Control
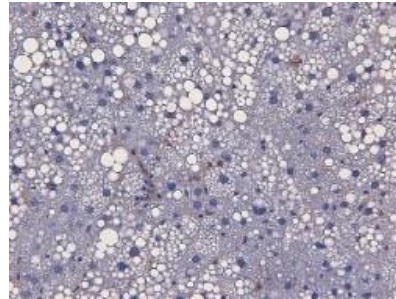
Aroclor 1260
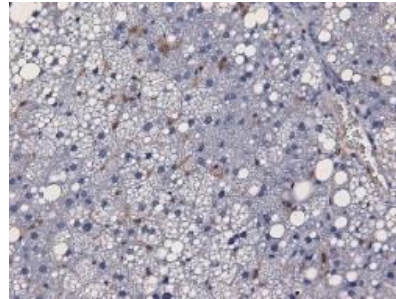
PCB 126

Aroclor 1260/PCB 126
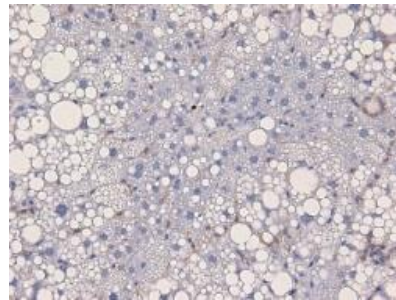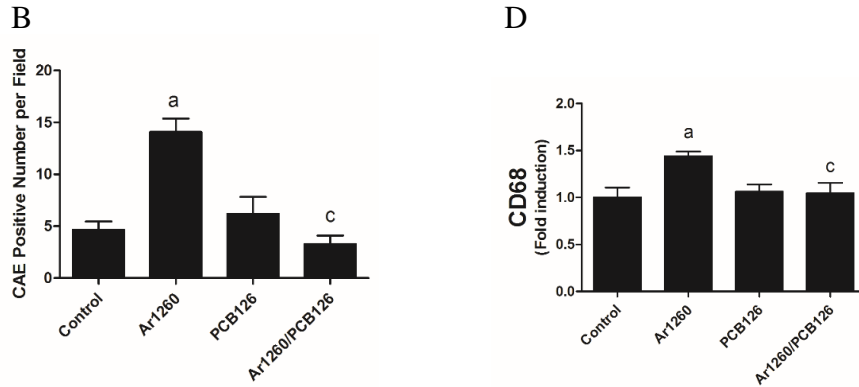
Figure 3.5 Effects of PCB exposures on hepatic inflammatory response. (A) CAE staining (40 ×). Red positive cells indicate neutrophil infiltration, (B) CAE positive number per field, (C) F4/80 immunohistochemistry staining (20 ×). Brown positive cells indicate macrophage accumulation, (D) hepatic *CD68* mRNA levels. Data are presented as mean ± SEM. n=10. p<0.05, a= Aroclor 1260 effects, c= interaction between Aroclor 1260 and PCB 126.

Effects of PCB exposures on plasma lipids and adipokines

PCB 126 exposure led to hypolipidemia in control synthetic diet fed mice in the2-week study. In high fat diet fed mice, PCB 126 alone or Aroclor 1260/PCB 126 exposure also decreased plasma triglycerides, but Aroclor 1260 exposure did not affect this variable (Fig. 3.6 A). Either Aroclor 1260 or PCB 126 exposure did not alter plasma total cholesterol, while co-administration of Aroclor 1260 and PCB 126 decreased total cholesterol (Fig. 3.6 B). The plasma levels of PAI-1, which is implicated in the pathogenesis of fibrosis (121), were significantly decreased by PCB 126 exposure (Fig. 3.6 C). Moreover, adipokines, including adiponectin (Fig. 3.6 C), leptin (Fig. 3.6 D) and resistin (Fig. 3.6 E) were not altered by any PCB exposure, suggesting PCB exposures may not cause adipose tissue dysfunction.
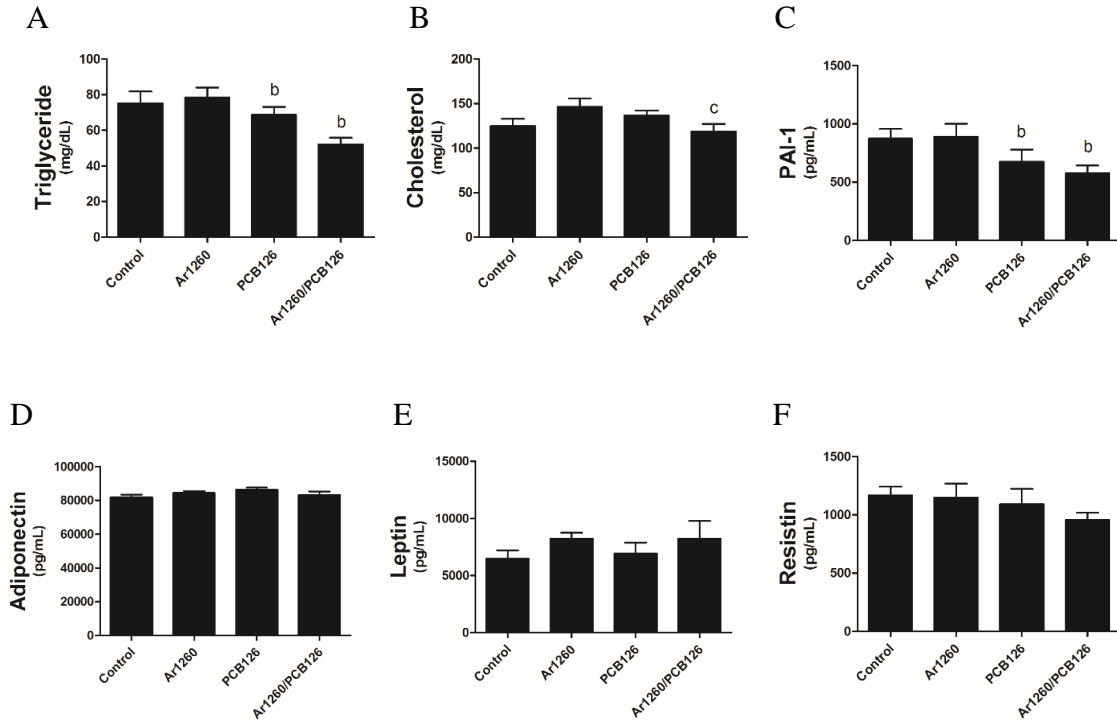
Figure 3.6 Effects of PCB exposures on plasma lipids and adipokines. Plasma levels of triglyceride (A), total cholesterol (B), PAI-1 (C), adiponectin (D), leptin (E), and resistin (F). Data are presented as mean ± SEM. n=10. p<0.05, b= PCB 126 effects, c= interaction between Aroclor 1260 and PCB 126.

Effects of PCB exposures on hepatic fatty acid β-oxidation genes expression

Unlike the effects of PCB exposures on fatty acid β-oxidation genes expression in the 2-week study, hepatic mRNA levels of *Pparα* and target gene *Cpt1α* were decreased by either Aroclor 1260, PCB 126 or Aroclor 1260/PCB 126 mixture exposure (Fig. 3.7 A&B*). Pparα* mRNA expression was decreased by 9.1 %, 11.6 % and 20.1 % by Aroclor 1260, PCB 126, and Aroclor 1260/PCB 126, respectively (Fig. 3.7 A). *Cpt1α* mRNA expression was decreased by 5.1 %, 2.8 % and 13.6 % by Aroclor 1260, PCB 126, and Aroclor 1260/PCB 126, respectively (Fig. 3.7 B). However, the mRNA expression of *Cyp4a10* had the same pattern as my 2-wwek study. PCB 126 increased *Cyp4a10* mRNA expression 1.2-fold while the Aroclor 1260/PCB 126 mixture increased 1.5-fold (Fig. 3.7 C). These data suggested that the interaction of diet and PCB exposures affect reduction of mitochondrial fatty acid β-oxidation but increased peroxisomal fatty acid β-oxidation.
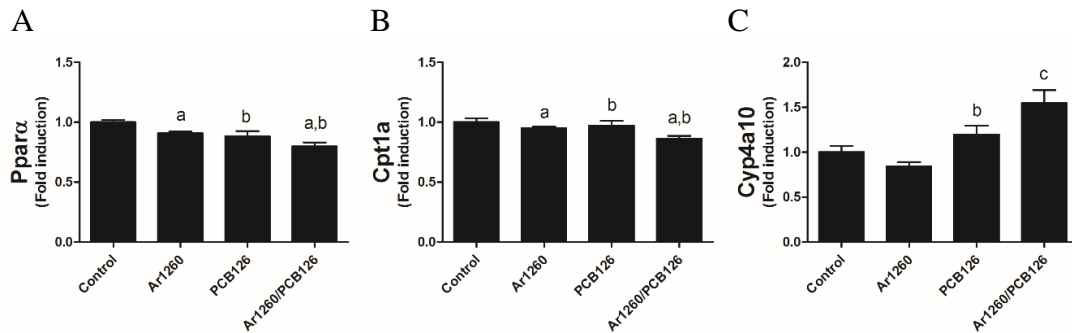
Figure 3.7 Effects of PCB exposures on hepatic fatty acid β-oxidation genes expression. Hepatic mRNA levels of *Pparα* (A), *Cpt1a* (B), and *Cyp4a10* (C)were measured by performing RT-PCR. Data are presented as mean ± SEM. n=10. p<0.05, a= Aroclor 1260 effects, b= PCB 126 effects, c= interaction between Aroclor 1260 and PCB 126.

Effects of PCB exposures on other genes of hepatic lipid metabolism

mRNA levels of *Cd36* were significantly increased by either PCB 126 (1.3-fold) or Aroclor 1260 (1.3-fold) exposures, and the additive induction by PCB 126 and Aroclor 1260 on *Cd36* mRNA levels were found with the Aroclor 1260/PCB 126 mixture exposure (1.5-fold) (Fig. 3.8 A). Either PCB 126 exposure slightly suppressed *Fabp1* mRNA expression, but Aroclor 1260/PCB 126 mixture exposure induced *Fabp1* mRNA expression compared to either exposure alone (Fig. 3.8 B). Both *Srebp1* (13.9 %) and *Fasn* (25.2 %) mRNA levels were decreased by PCB 126 exposure, but not by the Aroclor 1260 exposure. However, co-administration of PCB 126 and Aroclor 1260 resulted in slightly increased *Srebp1* mRNA compared to PCB 126 alone exposure, and suppressed *Fasn* mRNA expression compared to vehicle group (Fig. 3.8 C&D). Likewise, *Scd1* mRNA expression was decreased by either Aroclor 1260 (9.3 %) or PCB 126 (14.5 %) exposure, and in an additive manner by the Aroclor 1260/PCB 126 mixture (23.9 %) exposure (Fig. 3.8 E). *Pnpla3* mRNA expression was significantly upregulated by Aroclor 1260 (1.6-fold) exposure, but was suppressed by either PCB 126 (42.2 %) or Aroclor 1260/PCB 126 (37.5 %) exposure (Fig. 3.8 F). These data suggested that PCB exposures increased hepatic lipid levels due to increased lipid uptake, not by increasing *de novo* lipogenesis. Moreover, high fat diet suppressed PCB exposures-induced lipid metabolic gene expression when compared to chow diet fed mice in my 2-week study.
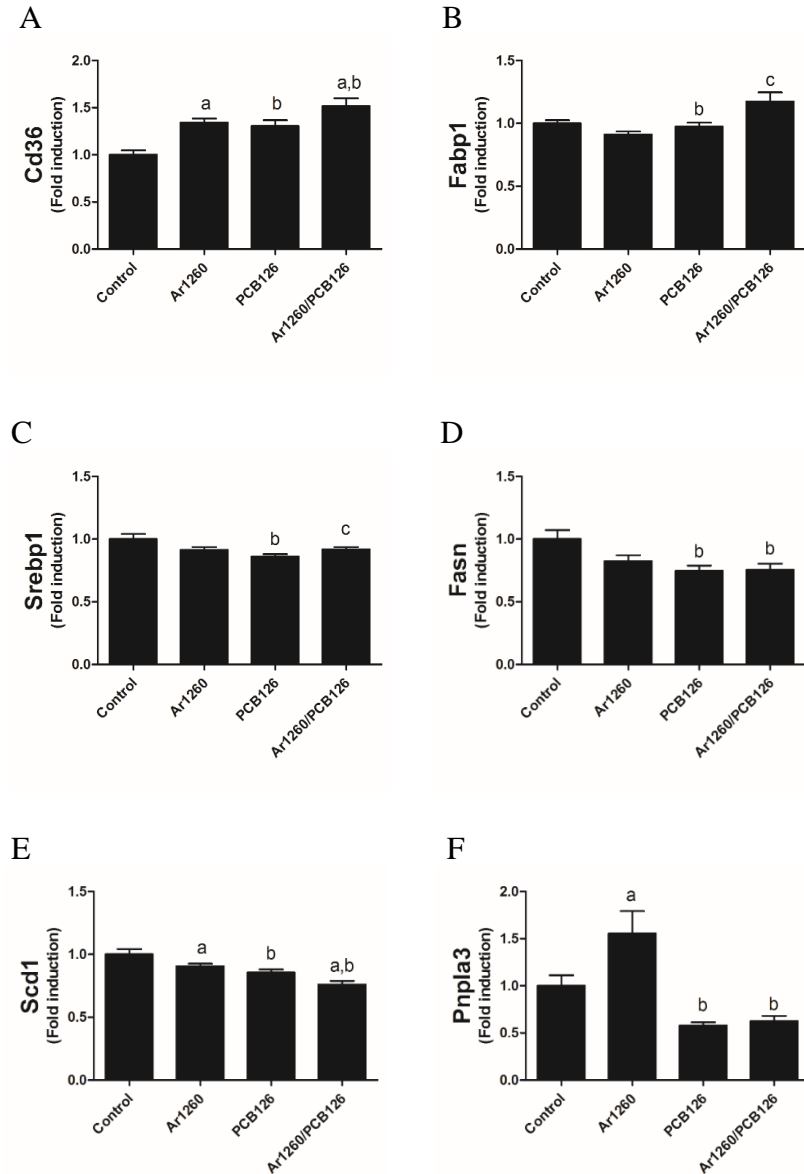
Figure 3.8 Effects of PCB exposures on other genes of hepatic lipid metabolism. Hepatic mRNA levels of *Cd36* (A), *Fabp1* (B), *Srebp1* (C), *Fasn* (D), *Scd1* (E), and *Pnpla3* (F) were measured by performing RT-PCR. Data are presented as mean ± SEM. n=10. $p < 0.05$, a= Aroclor 1260 effects, b= PCB 126 effects, c= interaction between Aroclor 1260 and PCB 126.

Effects of PCB exposures on glucose metabolism

PCB exposures are associated with diabetes in human populations. To determine whether PCB exposures affect glucose metabolism, glucose and insulin tolerance tests were performed. PCB exposures did not impair glucose tolerance and insulin sensitivity, as indicated by similar area under curves (AUCs) for all PCB exposures compared to the control group (Fig. 3.9 A&B). However, PCB 126 exposure suppressed gluconeogenic gene (*Pck1*) mRNA expression, and decreased fasting blood glucose levels (Fig. 3.9 C&D). Our current data are consistent with the published results by Diani-Moore S *et al* that activation of AhR suppressed gluconeogenic genes (*Pck1*) mRNA expression by TCDD via TCDD-inducible poly(ADP-ribose)-polymerase (*TiPARP*) (122).
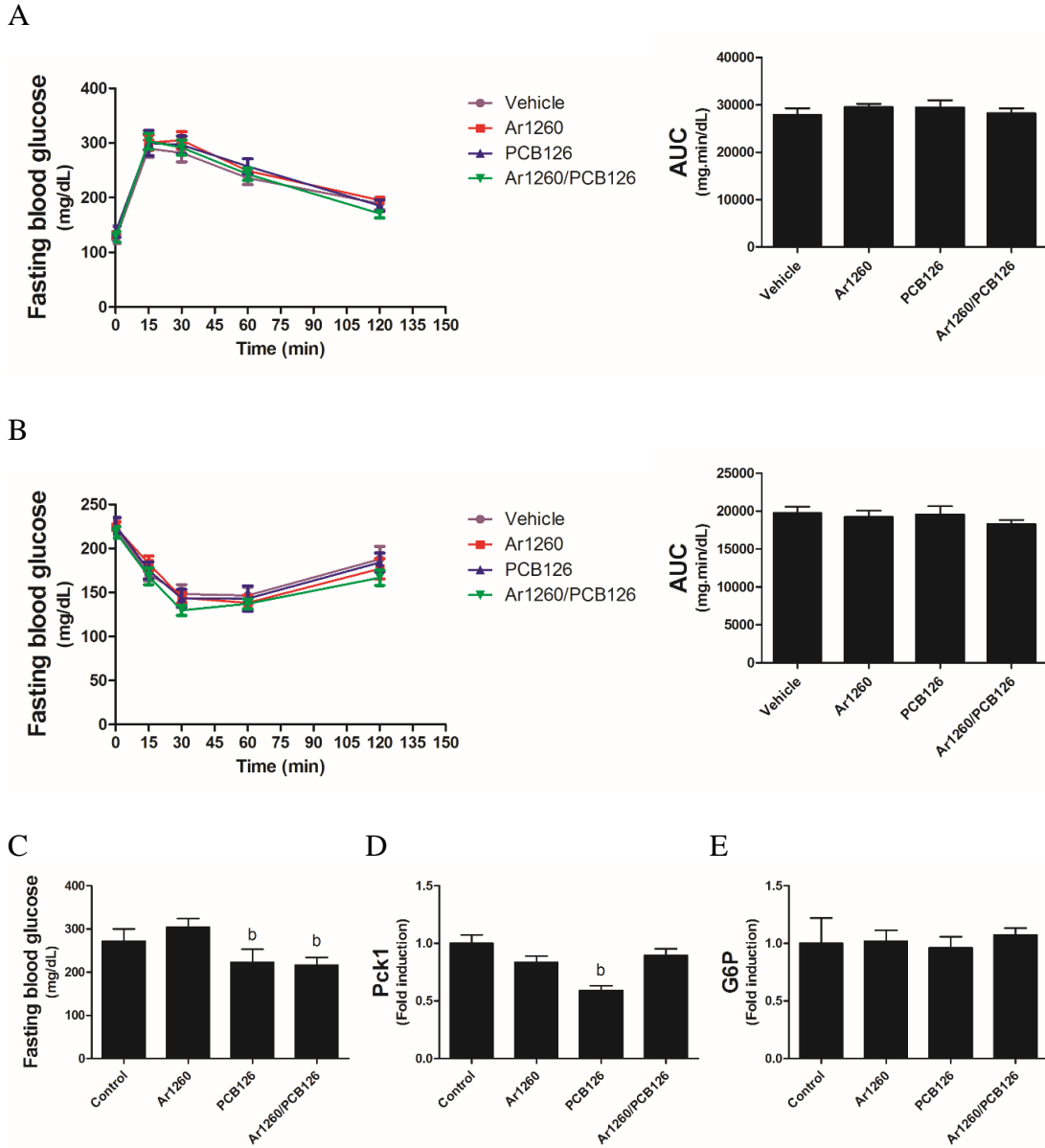
Figure 3.9 Effects of PCB exposures on glucose metabolism. (A) Glucose tolerance test and area under curve (AUC); (B) insulin tolerance test and area under curve (AUC); (C) fasting blood glucose levels; hepatic mRNA levels of *Pck1* (D) and *G6P* (E) were measured by performing RT-PCR. Data are presented as mean ± SEM. n=10. p<0.05, b= PCB 126 effects.

Effects of PCB exposures on hepatic fibrosis

Activated HSCs are the major source of extracellular matrix (ECM), including collagen, deposition in liver fibrosis. The balance of ECM is regulated by MMPs and TIMPs. To evaluate whether PCB exposures induced hepatic fibrosis, mRNA expression levels of fibrosis genes (e.g., *TGF-β1*, *Acta2*, *Col 1a1*, *Col 1a2*, MMPs, *TIMP1*, and *PAI1*) were measured. Although *TGF-β1* mRNA expression was not affect by all PCB exposures (Fig. 3.10 A), PCB 126 alone exposure suppressed hepatic stellate cells (HSCs) activation, as indicated by decreased *Acta2* (48.3 %) mRNA expression (Fig. 3.10 B). Moreover, mRNA expression of *Col 1a1* (40.5 %) (Fig. 3.10 C), *Col 1a2* (55.6 %) (Fig. 3.10 D), *TIMP1* (64.6 %) (Fig. 3.10 E), and *PAI1* (72.5 %) (Figure 3.10 F) were significantly decreased by PCB 126 exposure, but not by Aroclor 1260 exposure. The mRNA levels of ECM degradation genes, including *MMP2* (Fig. 3.10 G), *MMP9* (Fig. 3.10 H), and *MMP14* (Fig. 3.10 I), were not significantly changed by all PCB exposures. Co-administration of Aroclor 1260 and PCB 126 did not attenuate PCB 126 exposure-induced changes in mRNA levels of these genes. Surprisingly, although PCB 126 exposure alone suppressed fibrotic genes mRNA levels, histological data showed that the collagen deposition was similar with all PCB exposures, as shown by picrosirius red staining (Fig. 3.10 J). However, mRNA changes may proceed pathological changes. These data suggested that fibrotic genes were altered by PCB exposures, but failed to cause phenotypical changes in fibrosis. Longer time and/or higher dose exposure, or the carbon tetrachloride-induced fibrosis model, should be considered to evaluate the fibrotic effects of PCB exposures.
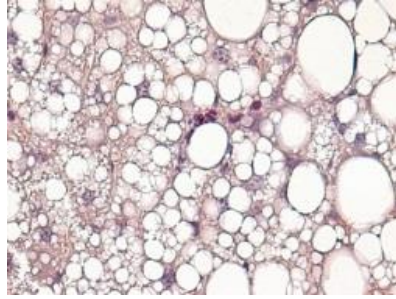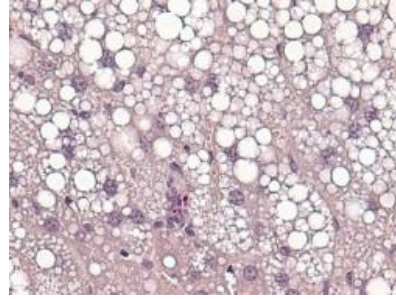
J

Control

Aroclor 1260

PCB 126

Aroclor 1260/PCB 126

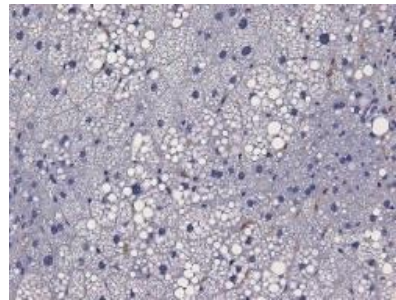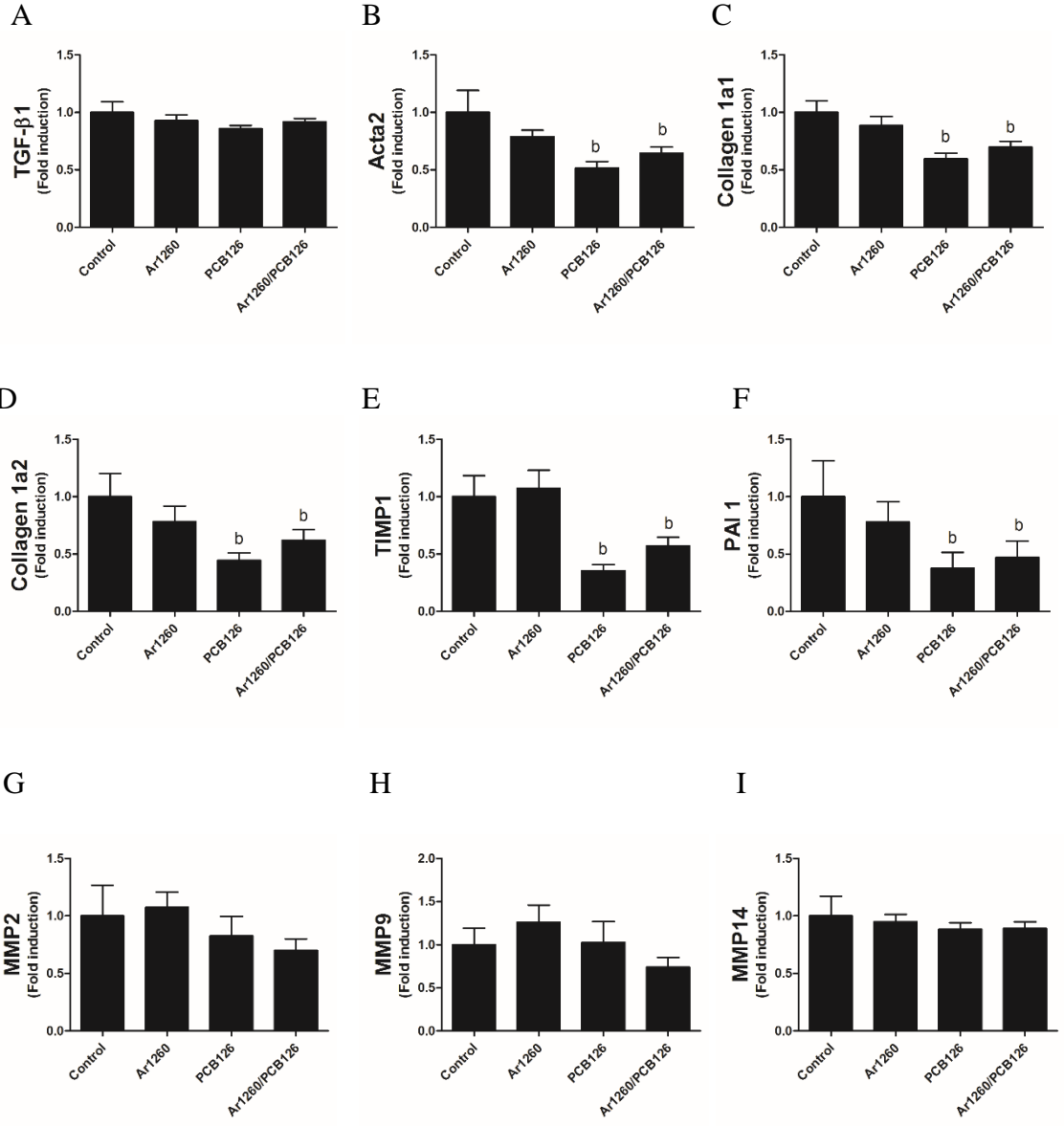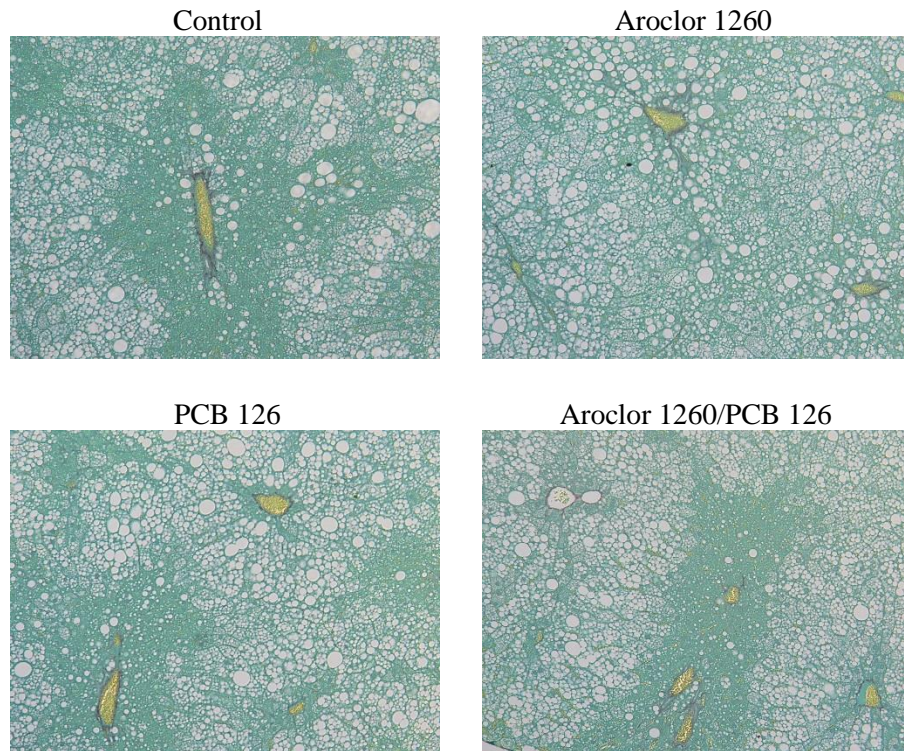Figure 3. 10 Effects of PCB exposures on hepatic fibrosis. Hepatic mRNA levels of *TGF-β1* (A), *Acta2* (B), *Col 1a1* (C), *Col 1a2* (D), *TIMP1* (E), *PAI1* (F), *MMP2* (G), *MMP9* (H), and *MMP14* (I) were measured by performing RT-PCR. (J) picrosirius red staining of liver (10 ×). Data are presented as mean ± SEM. n=10. $p < 0.05$, b= PCB 126 effects.

4. Discussion

The acute PCB exposure study (chapter 3), mice fed control synthetic diet developed hepatic steatosis and activation of AhR with PCB 126 exposure. Aroclor 1260/PCB 126 exposure also activated AhR, but failed to induce hepatic steatosis. In the current study, the interactions of diet and PCB exposures in regulation of NAFLD/NASH were investigated. I hypothesize that activation of AhR is involved in the development and progression of NAFLD/NASH after PCB exposures in high fat diet fed mice. The results demonstrated that high fat diet induced hepatic steatosis regardless of PCB exposure, Aroclor 1260 (20 mg/kg) exposure promoted progression of hepatic steatosis to steatohepatitis, while PCB 126 (20 µg/kg) exposure appeared to reverse HFD-induced hepatic fibrosis. Co-administration of PCB 126 of Aroclor 1260 abrogated Aroclor 1260 exposure-induced steatohepatitis.

Aroclor 1260 is a mixture of NDL-PCB congeners. It contains low amounts of DL PCB congeners. Aroclor 1260 exposure at this level failed to induce the AhR target gene, *Cyp1a2* mRNA level in mice on either chow diet in 2-week study or with a high fat diet in the current study. These data are consistent with previous results demonstrating that Aroclor 1260 (20 mg/kg) did not activate AhR, but a high exposure of Aroclor 1260 (200 mg/kg) did (59). In the acute study (chapter 3), either PCB 126 or Aroclor 1260/PCB 126 mixture activated AhR, and co-administration of Aroclor 1260 with PCB 126 did not affect PCB 126-induced AhR activity. In the current study, AhR activity was increased by PCB 126 alone exposure, but the magnitude of AhR-dependent induction was decreased compared to the results seen in the acute study. Co-administration of Aroclor 1260 in the Aroclor 1260/PCB 126 mixture attenuated PCB 126 exposure-induced AhR activity. These

data suggested that high fat diet affects the magnitude of PCB 126 exposure-induced AhR activity. Moreover, high fat diet also impacted Aroclor 1260 exposure-induced CAR and PXR target gene expression. For example, CAR target gene *Cyp2b10* mRNA was induced at least 1000-fold by either Aroclor 1260 or Aroclor 1260/PCB 126 mixture in mice fed on control chow diet as shown in chapter 3. However, less than 10-fold induction of *Cyp2b10* mRNA by either Aroclor 1260 or Aroclor 1260/PCB 126 mixture was found. The magnitude of induction of *Cyp2b10* mRNA by PCB 126 exposure, as shown in chapter 3, was also abolished by high fat diet.

High dose of TCDD (120) or PCB 126 (123) exposure causes a wasting syndrome. However, in the current study, neither PCB 126 nor Aroclor 1260/PCB 126 mixture exposure resulted in a wasting syndrome, as indicated by no significant body weight or epididymal fat tissue weight changes compared to the control group, although activation of AhR can be observed at lower doses of PCB 126 exposure (20 µg/kg *VS.* 4.9 mg/kg). Moreover, epididymal fat tissue weight was significantly increased by Aroclor 1260 exposure, possibly due to NDL-PCB 153 serving as an obesogen (124). Similar results were found in control synthetic diet fed mice in chapter 3. In low fat diet fed rats, PCB 126 exposure induced hepatic steatosis (73, 125), associated with altered hepatic micronutrients (96, 126). Our previous acute study results confirm these data that only PCB 126 exposure led to hepatic steatosis in control synthetic diet fed mice. However, in the current study, histological results showed that high fat diet induced hepatic steatosis alone, and PCB exposures did not exacerbate high fat diet-induced hepatic steatosis. These results were also confirmed by hepatic lipid levels measurement. As shown above, no PCBs exposure had effects on hepatic triglycerides or total cholesterol levels. However, PCB 126 exposure

increased hepatic free fatty acid levels compared to control group. These data suggest interactions between diet and PCB 126 exposure may affect AhR activation-induced hepatic steatosis. This may be due to the lipophilic property of PCBs, which may restrict PCBs distribution in high fat diet conditions and metabolic stress.

As mentioned in the discussion section of chapter 3, activation of CAR can be direct by ligand binding or indirect via inhibition of EGFR signaling (95). Direct activation of CAR by agonist, TCPOBOP, ameliorates metabolic syndromes, such as obesity, type 2 diabetes and NAFLD/NASH in mice under pathological conditions (85-87). However, mice administered TCPOBOP displayed hepatic lipogenesis and positive regulation of Pnpla3 gene expression. These results suggest the consequences of activation of CAR are varied under different conditions by direct ligand activation. Although Aroclor 1260 exposure induced CAR activation under either physiological condition (low fat diet) or pathological condition (high fat diet), Aroclor 1260 exposure had no effects on hepatic steatosis or glucose or insulin tolerance. However, Aroclor 1260 alone exposure promoted hepatic steatosis progression to steatohepatitis in high fat diet fed mice, which conflicts with the fact that direct activation of CAR attenuates NAFLD/NASH. These data suggest CAR is indirectly activated by Aroclor 1260 exposure. These data have been confirmed by our previous study demonstrating that Aroclor 1260 inhibits hepatic EGFR signaling (93). Other data to support this conclusion are that hepatic gluconeogenesis regulation occurs by direct CAR activation. CAR activation by agonists suppresses gluconeogenic genes (*Pck1* and *G6p*) mRNA levels, and suppresses hepatic gluconeogenesis via degradation of PGC1alpha protein (91), or inhibition of *HNF4a* and *FOXO1* transcriptional activity (127). In my study, Aroclor 1260 exposure did not affect hepatic gluconeogenic genes expression

and fasting blood glucose levels in either chow diet or high fat diet fed mice. In addition, PCB 126 exposure suppressed gluconeogenic genes expression, and decreased fasting blood glucose levels, consistent with previous published data (73, 79, 122).

In chapter 2, not all PCB exposures caused liver injury, as documented by similar plasma ALT and ALT levels compared to the mice on control synthetic diet fed mice, even though PCB 126 alone exposure induced mild hepatic steatosis. In the current study, Aroclor 1260 exposure induced neutrophils infiltration and macrophages accumulation in liver, and increased plasma ALT levels, which has been confirmed by our previous study (59). Interestingly, it appears that PCB 126 exposure protected against high fat diet-induced liver injury, as PCB 126 alone exposure decreased plasma AST levels, and attenuated Aroclor 1260 exposure-elevated plasma ALT levels by co-exposure of Aroclor 1260 and PCB 126. This may be due to anti-inflammatory due to AhR activation (128). This phenomenon was also found in our previous study that high dose of Aroclor 1260 (200 mg/kg) activates AhR and fails to cause liver injury (59). These results suggested that AhR activation regulates lipid metabolism and immune response through different signaling pathways.

Liver injury activates hepatic stellate cells (HSCs), and results in hepatic fibrosis by environmental pollutant exposure. TCDD exposure activates AhR, induces HSCs activation, and facilitates liver fibrosis (129, 130). However, TCDD exposure fails to exacerbate experimental liver fibrosis, although it increases necroinflammation and HSCs activation (131). This may be due to enhanced ECM turnover (132). In addition, high dose of PCB 126 exposure exacerbates MCD-induced liver fibrosis (123). In the current study, all PCB exposures did not increase collagen deposition or cause liver fibrosis, even though

Aroclor 1260 exposure increased liver injury. Surprisingly, PCB 126 exposure suppressed fibrotic gene mRNA levels, such as *col 1a1*, *col 1a2*, and *TIMP1*. It also decreased plasma PAI1 levels. The reasons for this are unknown, and need further investigation.

The effects of PCBs exposure on genes involved in lipid metabolism are not like the data in acute study. For example, the fatty acid β-oxidation genes mRNA levels are increased by either Aroclor 1260 or PCB 126 exposure, but inhibited by Aroclor 1260/PCB 126 exposure compared to either exposure alone. In the current study, all PCBs exposure suppressed fatty acid β-oxidation genes mRNA expression. The gene expression of fatty acid transporters mRNA was upregulated by either Aroclor 1260 or PCB 126 exposure in both diet, but the Aroclor 1260/PCB 126 mixture exposure displayed opposite results. The similar pattern also was found in *Pnpla3* and fatty acid synthesis (*Fasn*) gene. These data suggest that unlike Aroclor 1260 or PCB 126 exposure, Aroclor 1260/PCB 126 mixture exposure exhibits different effects on genes involved in lipid metabolism with diet interaction. The DL/NDL-PCBs mixture should be used to evaluate metabolic endpoints in animal model, to allow for better prediction of the endocrine and metabolism disruption effects in humans.

In summary, high fat diet affects AhR, and CAR expression, as well as, their transcriptional activity. Aroclor 1260 exposure may indirectly activates CAR, and induces liver inflammation and injury; while PCB 126 exposure activates AhR and reduces hepatic inflammation, and attenuates Aroclor 1260 exposure-induced liver injury, and fibrosis. Moreover, both DL- and NDL-PCBs affect genes of lipid metabolism, which are associated with fatty liver disease. Mixtures of DL- and NDL-PCBs exhibit different effects on fatty liver disease compared to either alone exposure.

CHAPTER IV

COMPARISON OF CONCENTRATION-DEPENDENCE OFHUMAN AND MOUSE

ARYL HYDROCARBON RECEPTOR ACTIVATION IN RESPONSE TO

POLYCHLORINATED BIPHENYL EXPOSURES

1. Introduction

PCB congeners can be classified into dioxin-like (DL) and non-dioxin-like (NDL) classes. DL-PCBs have non-ortho or mono-ortho substitution and are ligands for the AhR since their planar structure allows them to fit well in the binding pocket of that receptor. The AhR plays an important role in allowing the liver to be a target for PAH metabolic action. Furthermore, other studies have shown that PCBs exposure is associated with liver disease (42), diabetes (57), and vascular disease (133), association with AhR activation.

The AhR is a transcription factor that belongs to the Per-Arnt-Sim family (67). Unliganded AhR resides in the cytoplasm of cells and upon ligand binding, translocates to the nucleus, forming a heterodimer with AHR nuclear translocator protein (ARNT). The AhR-ARNT heterodimer binds to the dioxin response element (DRE) on the 5'-flanking regions of most dioxin-responsive genes, and regulates expression of target genes, prototypically the Cyp1 family.

To estimate human risk due to AhR activation by these chemical exposure, the World Health Organization (WHO) has established toxic equivalency factors (TEFs) for AhR ligands (134). TCDD is considered the prototypical ligand for AhR and therefore, is assigned a TEF of 1. The TEFs of other chemicals are calculated based on relative effect

potency (REP) values relative to that of TCDD. PCB 126, a non-ortho substituted PCB, which has highest AhR binding affinity of DL-PCBs, has the TEF 0.1 and is the major contributor to the total TEQ from PCBs. The TEFs of 29 AhR ligands have been calculated and have much lower TEFs than PCB 126. For example, all the TEFs of all mono-ortho substituted PCBs are 0.00003 (135).

However, TEFs are calculated for each AhR ligand in a species-specific manner, so if differences exist between the affinity for TCDD or the PCBs relative to TCDD, then there will be differences in the exposure levels required to activate the AhR. Previous Studies have compared the potency of DL-PCB congeners and/or TCDD in inducing CYP mRNA levels in the human and rodent immortalized cell lines and primary hepatocytes (136, 137). These data support the conclusion that the sensitivity of human AhR is lower than that of the rat in response to TCDD or some DL-PCB congeners exposure. The differences in primary amino acid sequence of AhR in ligand-binding pocket (138) and the different ability to recruit coactivators by AhR (139) were thought to be responsible for the different AhR sensitivity across species. Relatively, less is known about the murine AhR which was the species used in our animal studies (59, 140).

My hypothesis is that the murine AhR activation will respond to DL/NDL-PCBs mixture and DL-PCBs with lower concentration-dependence than the human AhR. To evaluate the difference of TEFs across human and mouse AhR in response to DL-PCBs exposure, human (HepG2) and mouse (Hepa1c1c7) hepatoma-derived cell line were used for AhR-dependent luciferase activity, as well as, primary human and mouse hepatocytes were used for native *Cyp1a1* gene expression. Our results demonstrated that the maximal

response for human AhR in increasing gene expression was higher than that in mouse, but

concentration-dependence of the human AhR is higher than that of mouse AhR.

2. Materials and Methods

Reagents

TCDD, Aroclor 1260, Aroclor 1254 (lot # 124-191) and DL-PCB congeners (PCBs 77, 81, 114, 126, 169) were purchased from AccuStandard (New Haven, CN). Lipofectamine, Opti-MEM and Wamouth's medium, fetal bovine serum (FBS), Hank's Balanced Salt Solution (HBSS, 10X), probes for human CYP1a1 (Hs01054797_g1) and GAPDH (Hs02786624_g1), mouse Cyp1a1 (Mm00487218_m1) and GAPDH (Mm99999915_g1) for Taqman Gene Expression Assays were ordered from Thermo Fisher Scientific (Waltham, MA). Dulbecco's Modified Eagle's Medium (DMEM) was purchased from VWR (Radnor, PA), whereas antibiotics, 0.25 % trypsin with EDTA, Type 1 collagen , and ITS^{TM} + Premix Universal Culture Supplement were obtained from Corning Inc. (Corning, NY). Cell culture Lysis 5x buffer and Luciferase Assay System were obtained from Promega (Madison, WI). Chlorophenol red-β-D-galactopyranoside and Collagenase D were from Sigma-Aldrich, (St. Louis, MO). RNA STAT-60 was from amsbio (Austin, TX), and QuantiTect Reverse Transcription Kit was obtained from QIAGEN (Qiagen, Valencia, CA). iTag Universal Probes Supermix was purchased form Bio-Rad (Hercules, CA). 1,2-benz[a]anthracene (BA), dimethyl sulfoxide (DMSO), ethanol, 2-propanol, chloroform and all other reagents were obtained from Sigma Aldrich.

Cell culture

The human male HepG2 and mouse Hepa1c1c7 cells were purchased from the American Type Culture Collection (Manassas, MD). Cells were cultured in DMEM complete medium supplemented with 10 % FBS and 1 % antibiotics, and incubated in 5 %

CO_2 and 95 % humidity at 37 °C. HepG2 cells and Hepa1c1c7 cells were sub-cultured every 3-4 days.

Cell transfection

The HepG2 and Hepa1c1c7 cells were plated into 24-well plates, and transfected at 40 %-50 % confluence. In brief, DMEM medium was replaced by Opti-MEM medium 30 min prior to transfection. Cells were transfected with 150 ng of a pGl3-promoter-based reporter plasmid pXRE-SV40-Luc that has been described previously (52) and 150 ng of pCMV-β (Stratagene, CA) using lipofectamine (Thermo-Fisher) according to the manufacturer's instructions. Following an overnight recovery period, the chemicals of interest were then added and the cells were grown for 24 hours prior to harvest. DMSO was used as a solvent control, and the final concentration was less than 0.2 %. Cells were harvested using 1x cell culture lysis buffer. Chlorophenol red β-D-galactopyranoside was used to determine β-galactosidase activity to normalize transfection efficiency. Following incubation, β-galactosidase enzyme activity was determined spectrophotometrically at 595 nm using the Bio-Tek Synergy HT multi-mode micro plate reader (Bio-Tek USA, Winooski, VT). Luciferase reporter assays were performed with a Promega Luciferase Assay System on an Orion L micro plate luminometer (Berthold Detection Systems, Pforzheim, Germany).

Primary mouse hepatocytes isolation

Livers from 10-week-old male C57BL/6 mice were used to prepare hepatocytes by digestion with collagenase D on basis of published protocol (141). Hepatocytes were resuspended in cold Waymouth's medium, and cultured for 12 hours in type 1 collagen pre-coated 12-well plates.

Cell treatment and RT-PCR

Primary human hepatocytes were obtained from BioreclamationIVT (Baltimore, MD). Primary human hepatocytes were plated according to the supplier's instructions in 12-well plates and cultured overnight. Chemicals of interest at indicated concentration were added to primary human and mouse hepatocytes for 24 hours. Cells were lysed and mRNA was isolated using STAT-60. RNA purity and quantity were assessed with a Nanodrop spectrometer (ND-1000, Thermo Scientific, Wilmington, DE) using ND-1000 V3.8.1 software. cDNA was synthesized using a Qiagen QuantiTect Reverse Transcription Kits. PCR reaction was performed using iTag Universal Probes Supermix, with CYP1a1 and GAPDH primers Taqman probe sets on a Bio-Rad CFX384TM Real-Time System (Hercules, CA). CYP1a1 expression level was determined using $2^{-\Delta\Delta Ct}$ methods.

Statistical analysis

Concentration-response analyses were performed on SigmaPlot 11.0 software (Systat Software Inc., San Jose, CA) using a Four Parameter Logistic Curve. Other statistical analyses performed using Graphpad Prism software (GraphPad Software Inc., La Jolla, CA). All data were normalized to uninduced control group. Data are presented as mean ± SEM. Statistical evaluation of the data was performed using one-way analysis of variance (ANOVA) followed by the Dunnett's post hoc test to compare all groups with the control sample for multiple groups. For all statistical comparisons, p-values of less than 0.05 were considered statistically significant.

3. Results

Concentration-response curves for the luciferase assay activated by TCDD

Based on the concentration-response data, TCDD displayed an EC_{50} value of 0.4 ± 0.1 nM in HepG2 cells, whereas the EC_{50} value in Hepa1c1c7 cells was 0.03 ± 0.01 nM (Fig. 4.1 A&B). TCDD was much more potent, and induced luciferase activity to a significantly greater level in HepG2 cells (maximal response 83-fold compared to uninduced control group) compared to Hepa1c1c7 cells (maximal response 2.2-fold compared to uninduced control group).

A   B

$EC_{50} = 0.4 \pm 0.1$ nM $EC_{50} = 0.03 \pm 0.01$ nM

Figure 4.1 Concentration-response curves for the luciferase assay activated by TCDD. AhR-dependent luciferase activity in HepG 2 cells (A) and Hepa1c1c7 cells (B) treated with various of concentrations of TCDD. Data are presented as mean $\pm$ SEM.

Concentration-response curves for the luciferase assay and Cyp1a1 expression activated by non-ortho PCB 126

Because PCB 126 is thought to be the congener with the greatest contribution to the overall TEQ provided by PCBs, we examined the concentration dependence in both human HepG2 cells and mouse Hep1c1c7 cells. Our results show that PCB 126 had an EC_{50} value of 250 ± 150 nM in HepG2 cells, while EC_{50} value in Hepa1c1c7 cells was 4.7 ± 3.2 nM (Fig. 4.2 A&B). PCB 126 induced luciferase activity to a significantly greater level in HepG2 cells (maximal response 31.6-fold compared to uninduced control group) compared to Hepa1c1c7 cells (maximal response 5.9-fold compared to uninduced control group).

Using primary human and mouse hepatocytes, real-time PCR was used to measure *CYP1A1* and *Cyp1a1* mRNA levels, respectively, when treated with PCB 126. PCB 126 induced expression of *CYP1A1* with an EC_{50} value of 195 ± 35 nM in primary human hepatocytes. The EC_{50} value for *Cyp1a1* in primary mouse hepatocytes was 12.3 ± 7.9 nM (Fig. 4.2 C&D). The maximal fold *Cyp1a1* mRNA induction did not display a significant difference between primary human (45.1-fold compared to uninduced control group) and mouse hepatocytes (53.3-fold compared to uninduced control group).

A

HepG2

$EC_{50} = 250.0 \pm 150.0$ nM

B

Hepa1c1c7

$EC_{50} = 4.7 \pm 3.2$ nM

C

Primary human hepatocytes

$EC_{50} = 194.5 \pm 35.2$ nM

D

Primary mouse hepatocytes

$EC_{50} = 12.3 \pm 7.9$ nM
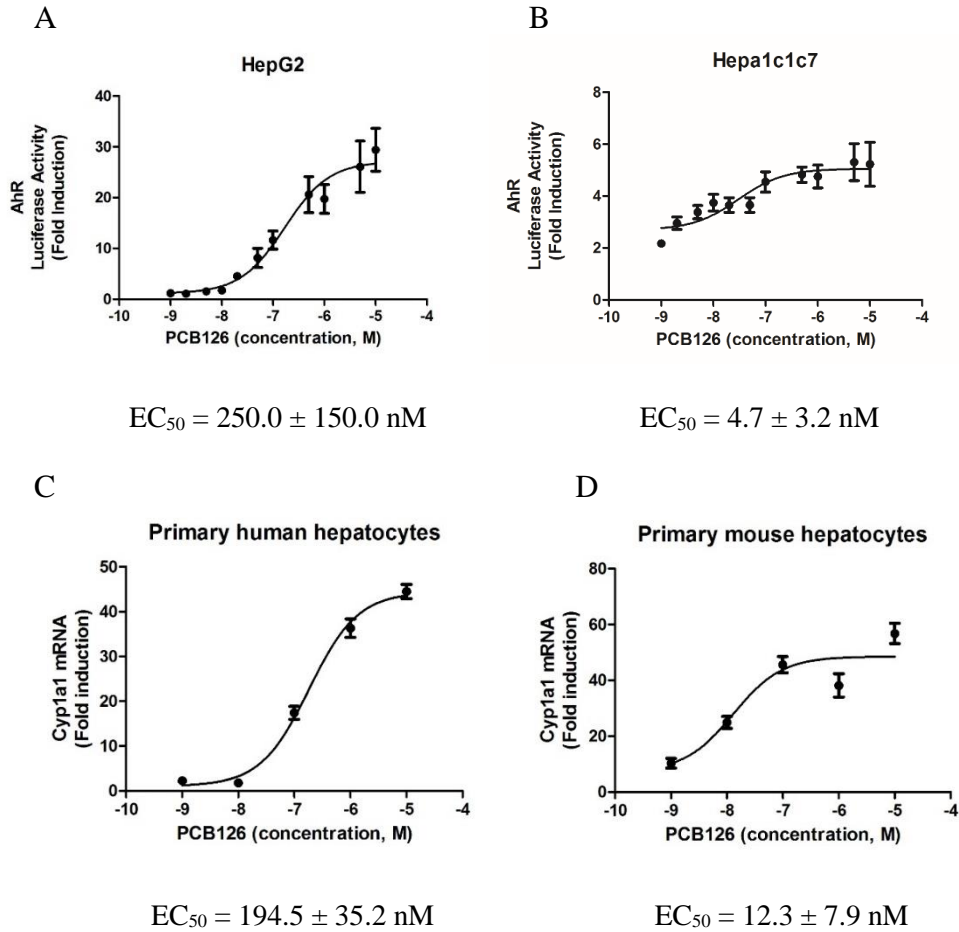
Figure 4.2 Concentration-response curves for the luciferase assay and *Cyp1a1* expression activated by non-ortho PCB 126. AhR-dependent luciferase activity in HepG2 cells (A) and Hepa1c1c7 cells (B) treated with various of indicated concentration of PCB 126. AhR target gene *Cyp1a1* induction in primary human (C) and mouse (D) hepatocytes after the same treatment with the indicated concentration of PCB 126. Data are presented as mean ± SEM.

Concentration-response curves for the luciferase assay activated by non-ortho PCB 169

PCB 169 was tested using the reporter gene assay, in which HepG2 and Hepa1c1c7 cells were treated with various of concentrations of PCB 169 up to 10 µM (Fig. 4.3 A&B). Based on the concentration-response data, the EC_{50} value was 25.7 ± 4.6 nM in Hepa1c1c7 cells, whereas the EC_{50} value in HepG2 cells could not be determined, because of the failure to reach the maximum effect.

A

B

EC_{50} = None $EC_{50} = 25.7 \pm 4.6$ nM
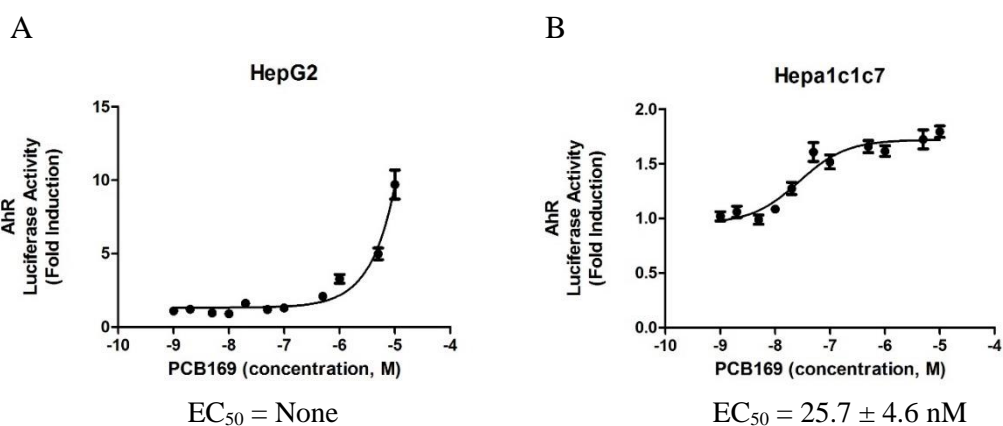
Figure 4.3 Concentration-response curves for the luciferase assay activated by non-ortho PCB 169. AhR-dependent luciferase activity in HepG2 cells (A) and Hepa1c1c7 cells (B) treated with the indicated concentration of PCB 169. Data are presented as mean $\pm$ SEM.

Concentration-response curves for the luciferase assay activated by non-ortho PCB 81

Unlike others dioxin-like PCB congeners, PCB 81 had approximately 5-fold higher EC_{50} value in Hepa1c1c7 cells (32.0 ± 17.7 nM), compared to the EC_{50} value in HepG2 cells (6.8 ± 2.7 nM) (Fig. 4.4 A&B).

A   B

$EC_{50} = 6.8 \pm 2.7$ nM $EC_{50} = 32.0 \pm 17.7$ nM
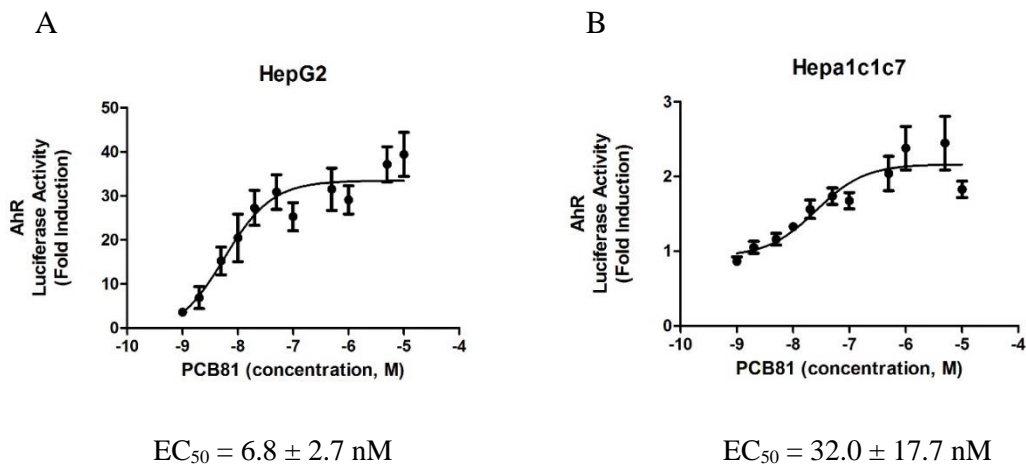
Figure 4.4 Concentration-response curves for the luciferase assay activated by non-ortho PCB 81. AhR-dependent luciferase activity in HepG2 cells (A) and Hepa1c1c7 cells (B) treated with various of concentrations of PCB 81. Data are presented as mean $\pm$ SEM.

Concentration-response curves for the luciferase assay activated by mono-ortho PCB 114

PCB 114 induced luciferase activity to a significantly greater level in HepG2 cells, compared to Hepa1c1c7 cells. Based on the concentration-response data, the EC_{50} value of PCB 114 was 796 ± 661 nM in Hepa1c1c7 cells, whereas the EC_{50} value in HepG2 cells was not attained because of the inability to reach the maximal effects, like PCB 169 (Fig. 4.5 A&B).

A   B

EC_{50} = None $EC_{50} = 796.5 \pm 660.5$ nM
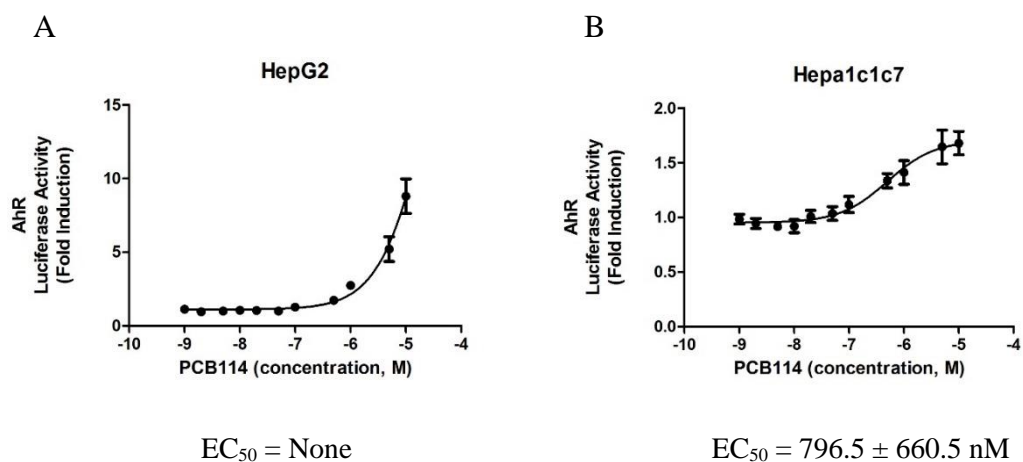
Figure 4.5 Concentration-response curves for the luciferase assay activated by mono-ortho PCB 114. AhR-dependent luciferase activity in HepG2 cells (A) and Hepa1c1c7 cells (B) treated with the indicated concentration of PCB 114. Data are presented as mean $\pm$ SEM.

Concentration-response curves for the luciferase assay activated by non-ortho PCB 77

PCB 77 induced luciferase activity to a higher level in HepG2 cells, compared to Hepa1c1c7 cells. The EC_{50} value for PCB 77 was 108 ± 39 nM in Hepa1c1c7 cells, whereas EC_{50} value in HepG2 cells was again not attained because of failure to reach the maximal effect (Fig. 4.6 A&B).

A   B

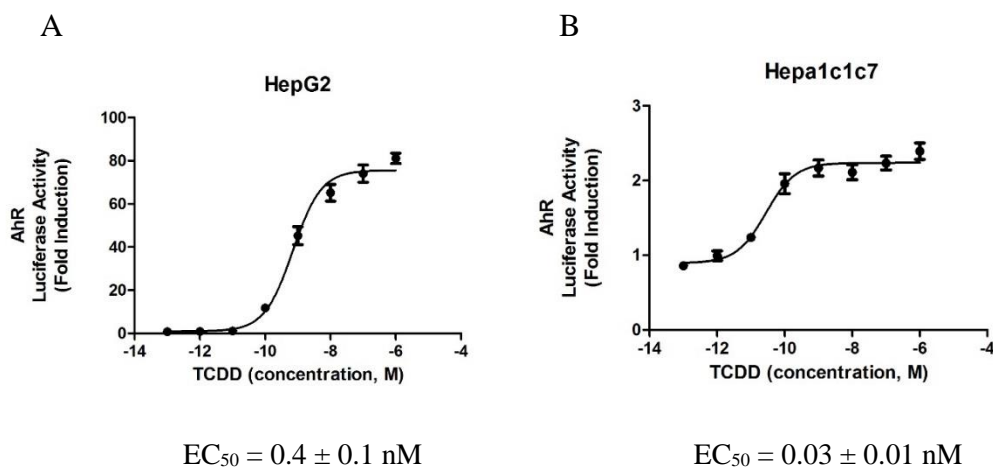EC_{50} = None EC_{50} = 108.2 ± 38.8 nM
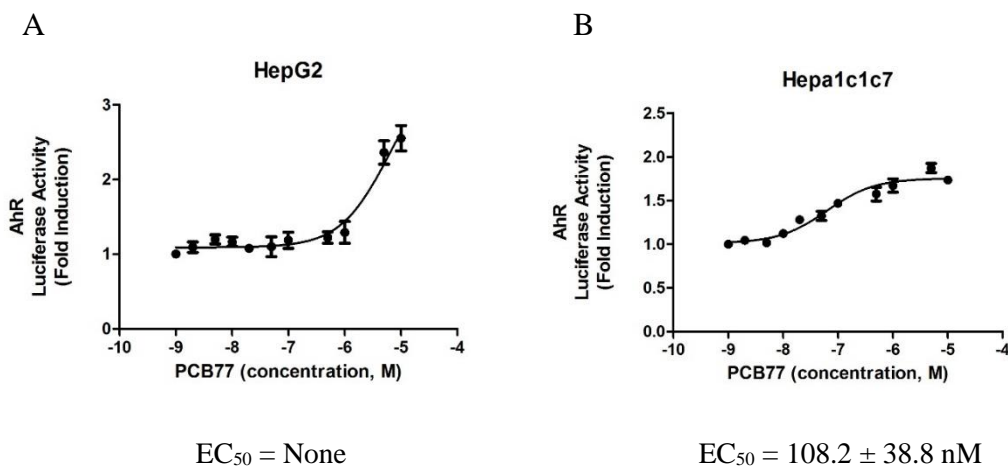
Figure 4.6 Concentration-response curves for the luciferase assay activated by non-ortho PCB 77. AhR-dependent luciferase activity in HepG2 cells (A) and Hepa1c1c7 cells (B) treated with various of concentrations of PCB 77. Data are presented as mean $\pm$ SEM.

DL/NDL-PCBs mixture activates mouse AhR

HepG2 and Hepa1c1c7 cells were transfected with AhR-dependent (pXRE-SV40-Luc) reporter plasmid, then treated with Aroclor 1260 (10 µg/ml), Aroclor 1254 (10 µg/ml), PCB 126 (3.26 µg/ml; 10 µM), or the DL/NDL-PCBs mixture (Aroclor 1260 (10 µg/ml) plus 0.1 % PCB 126 (10 ng/ml; 0.0306 µM), Aroclor 1260/PCB 126), and positive control 1,2-benz[a]anthracene (BA, 2.28 µg/ml; or 50 µM). These concentrations have been shown not to cause cellular toxicity (52). As anticipated, BA increased luciferase activity 67.4-fold in HepG2 cells and 5.1-fold in Hepa1c1c7 cells when compared with vehicle group. Likewise, PCB 126 induced a 42.2-fold increase in luciferase activity in HepG2 cells and a 3.7-fold increase in Hepa1c1c7 cell lines. Neither Aroclor 1260 nor Aroclor 1254 induced luciferase activity in either HepG2 or Hepa1c1c7. In contrast, the mixture of Aroclor 1260/PCB 126 induced luciferase in only the Hepa1c1c7 cell line by 3.0-fold. It is important to note that the concentration of PCB 126 (0.0306 µM) is much lower in the DL/NDL-PCBs mixture than the 10 µM used as a control (Fig. 4.7 A&B).

The expression of the prototypical AhR target gene *CYP1a1* was measured using RT-PCR in primary human and mouse hepatocytes treated with chemicals of interest. As anticipated, BA increased the expression of *CYP1A1* message 616-fold in human primary hepatocytes and 398-fold in murine primary hepatocytes. Likewise, addition of 10 µM PCB 126 induced *CYP1A1* message 225-fold in human hepatocytes and 187-fold in murine hepatocytes. Neither Aroclor 1260 nor Aroclor 1254 induced mRNA expression of either *CYP1A1* or *Cyp1a1* in human and murine hepatocytes, respectively. Consistent with the luciferase assay results, the DL/NDL-PCBs mixture group showed no significant elevation of *CYP1A1* mRNA expression in primary human hepatocytes, but exhibited markedly

increased expression of *Cyp1a1* message in primary mouse hepatocytes (112-fold) (Fig. 4.7 C&D). These data demonstrated that regardless of using isolated hepatocytes or immortalized cell lines, the trends are consistently similar among these treatments. The results suggested that the maximal response of human AhR was higher than that of mouse AhR, but ligands were more potent for the murine AhR.
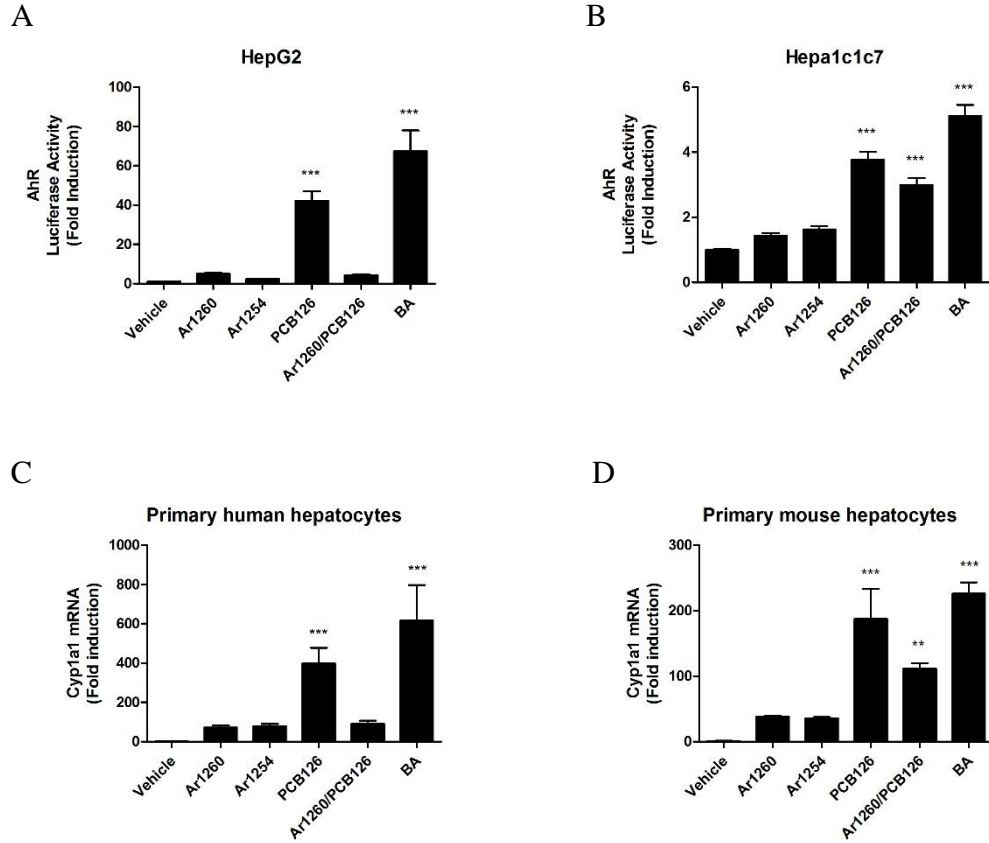
Figure 4.7 DL/NDL-PCBs mixture activates mouse AhR. AhR-dependent luciferase activity in HepG2 cells (A) and Hepa1c1c7 cells (B) treated with Aroclor 1260 (10 µg/ml), Aroclor 1254 (10 µg/ml), PCB 126 (10 µM), DL/NDL-PCBs mixture (Aroclor 1260 (10 µg/ml) plus 0.1 % PCB 126 (10 ng/ml; 0.0306 µM), Aroclor 1260/PCB 126), and positive control 1,2-benz[a]anthracene (BA, 10 µM). AhR target gene *CYP1a1* induction in primary human (C) and mouse (D) hepatocytes after the same treatment with luciferase activity assay. Data are presented as mean ± SEM. [**]p<0.01, and [***]p<0.001 *VS* vehicle.

4. Discussion

The main objective of the current study was to test the hypothesis that DL-PCBs exhibited higher concentration-dependence for the mouse AhR activation than for human AhR. Neither, Aroclor 1260 nor 1254 activated AhR or induced AhR-dependent gene expression in either cell line, suggesting that the major PCB congeners in this mixture are not effective AhR ligands. This was expected for Aroclor 1260 as it contains low levels of DL-PCBs and requires exposures over 20 mg/kg to induce Cyp1a2 in murine whole animal models (59). In contrast, we expected Aroclor 1254 would activate AhR as it contains more penta- and less-highly chlorinated PCBs than the hexa- and hepta-substituted PCBs that predominate in Aroclor 1260; therefore, Aroclor 1254 should have higher levels of DL-PCBs. The amounts of DL-PCBs in Aroclor 1254 varies considerably (142) by lot and we used lot 124-191 rather than lots like lot 6024 which contains approximately 10-fold higher DL-PCBs. Thus, it is possible that induction may have been observed with Aroclor 1254, had we used another lot.

We designed a DL/NDL-PCBs mixture containing more dioxin-like congeners (Aroclor 1260 plus 0.1% PCB 126) to approximate the human PCB exposure profiles seen in the general U.S. population (98). We found that this fortified DL/NDL-PCBs mixture activated AhR in murine cells, but failed to induce human AhR in transfection experiments in immortalized cell lines and in primary human or mouse hepatocytes. This suggests that the affinity values for DL-PCBs, i.e., EC_{50} values, are considerably lower in murine systems than in human cells (Table 4.1).

As anticipated, PCB 126, the most potent DL-PCB ligand for the AhR, increased AhR luciferase activity in immortal cells or increased *Cyp1a1* mRNA levels in primary

hepatocytes regardless of species at 10 µM. The fold induction with either BA or PCB 126 was significantly lower in the Hepa1c1c7 cell line than in the HepG2 cell line, but similar in the primary hepatocytes. This most likely is a cell line-dependent effect, possibly as a result of a rapid decrease in AhR protein after translocation to the nucleus in Hepa1c1c7 cells (143). The more relevant fold-inductions from primary mouse and human hepatocytes were similar. This likely reflects similarities in the activation domains between the two receptors and similarities in the number and sequence of the AhR responsive elements of either CYP1A1 or Cyp1a1.

In this study, the EC_{50} value for TCDD in both cell lines was not similar, 0.4 ± 0.1 nM in HepG2 cells and 0.03 ± 0.01 nM in Hepa1c1c7 cells. This was approximately 4-fold higher than previously published studies (144-146).

The EC_{50}-based potencies for DL-PCBs in HepG2 cells in rank order was TCDD > PCB 81 > PCB 126, consistent with previous studies (136) that used CYP 1A1 activity assays to determine EC_{50}-based potencies in HepG2 cells (Table 4.2). The EC_{50}-based relative potency values (REPs) were calculated (Table 4.2). In HepG2 cells, the REPs of PCB 126 and PCB 81were 0.002 and 0.06, respectively within species, consistent with previous studies (136). The EC_{50} values of various DL-PCB congeners were lower in Hepa1c1c7 cells except for PCB 81 that displayed a lower EC_{50} in HepG2 cells than PCB 126, but a higher EC_{50} in Hepa1c1c7 cells. The rank order of EC_{50}-based potencies in mouse Hepa1c1c7 cells was TCDD > PCB 126 > PCB 169 > PCB 81 > PCB 77 > PCB 114 (145). This is nearly identical to results observed with the rat H4IIE cell line (136). In our study with Hepa1c1c7 cells, the REPs in table 4.2 for PCB 126 was 0.006, PCB 81 was

0.0009, PCB 77 was 0.0003, PCB 114 was 0.00004, and PCB 169 was 0.001 which are much lower than the rat REPs.

In contrast to the mouse and human REPs, the rat REPs are reported to be much higher for DL-PCBs in rat H4IIE cells and rat primary hepatocytes. The WHO 2005 TEF values are based on a combination of rodent and human REPs. The species most commonly used in PCB studies is the rat, so the WHO 2005 TEF values likely reflect this and may vary considerably from that observed in humans. With TEF, the toxicity of a mixture of dioxins or dioxin-like chemicals could be defined by the toxic equivalency (TEQ); it can be calculated by the sum of the concentrations of individual chemicals (Ci) multiplied by their relative toxicity (TEF). Thus, the WHO 2005 TEF for PCB 126 is 0.1, far higher than our human REP of 0.002. In contrast to the PCBs, published consensus toxicity factors for polychlorinated dibenzo-p-dioxins and dibenzofurans (145) are much more closely aligned to WHO 2005 TEFs, suggesting that the human TEQ may represent a result dominated by these compounds with PCBs having only a small effect. Of relevance to humans, the PCB load we receive from food consumption (147) in which PCBs make up approximately 30 % of the TEQ using WHO 2005 TEFs. If this where adjusted using our REPs and that of others (145), it would only be a few percent at best.

Likewise, in our previous animal studies (59), Aroclor 1260 made steatohepatitis worse in animals fed a high fat diet at exposures that did not appear to significantly induce *Cyp1a2* gene expression. In mice, the different AhR ligands activate different subsets of genes leading to the concept of selective modulation of the AhR (148) and it is unclear whether the human AhR behaves in a similar manner. As the human AhR has higher affinity for either dietary indole metabolites or tryptophan metabolites than the mouse AhR

(149), it may be important to determine whether PCBs act like the dietary and endogenous ligands or like dioxin-like compounds.

In summary, the results demonstrated the sensitivity of mouse AhR, as indicated by lower EC_{50} value, is higher than human AhR in response to dioxin exposure and even more so with DL-PCBs like PCB 126. In addition, the DL/NDL-PCBs mixture designed to approximate human exposures and bioaccumulation patterns activated the mouse AhR, but not the human AhR. These results suggest that the animal exposure models in chapter 2 and 3 should be referred to increase human relevance. This could be accomplished by using humanized AhR mice.

Table 4.1 AhR EC_{50} values in human and mouse

Chemical	Type [a]	HepG2 (nM)	Hepa1c1c7 (nM)	Primary human hepatocytes (nM)	Primary mouse hepatocytes (nM)
TCDD		0.4±0.1	0.03±0.01	n.d.	n.d.
PCB 77	n	n.d.[b]	108.2 ±38.8	n.d.	n.d.
PCB 81	n	6.8±2.7	32.0±17.7	n.d.	n.d.
PCB 126	n	250±150	4.7±3.2	194.5±35.2	12.3±7.9
PCB 169	n	n.d.	25.7 ±4.6	n.d	n.d
PCB 114	m	n.d.	796.5 ±660.5	n.d	n.d

Note. EC_{50} values calculated 24 hours after treatment with TCDD and DL-PCB congeners.

[a] n means non-*ortho*; m means mono-*ortho*.

[b] n.d. means not/no detectable.

Table 4.2 Relative Effect Potency Values (REPs)

Chemical	Type [a]	HepG2	Hepa1c1c7	WHO-TEF [c]
TCDD		1	1	1
PCB 77	n	n.d.[b]	0.0003	0.0001
PCB 81	n	0.06	0.0009	0.0003
PCB 126	n	0.002	0.006	0.1
PCB 169	n	n.d.	0.001	0.03
PCB 114	m	n.d.	0.00004	0.00003

[a] n means non-*ortho*; m means mono-*ortho*.

[b] n.d. means not/no detectable.

[c] Van den Berg *et al.* (2006)

CHAPTER V

CONCLUSIONS

1. Overall goals and specific aims

The goals of the current dissertation are to investigate and compare low doses of DL-PCB congener (PCB 126, 20 µg/kg), NDL-PCBs mixture (Aroclor 1260, 20 mg/kg), and DL/NDL-PCBs mixture exposure (mixture of Aroclor 1260 and PCB 126)-induced NAFLD/NASH and metabolic dysfunction, as well as, to investigate the role of AhR in PCBs exposure-induced NAFLD/NASH. The outcomes of these studies have provided us a better understanding of different PCB exposures-induced NAFLD/NASH. The specific aims are shown as follows:

Specific Aim 1 addressed whether DL-PCBs, NDL-PCBs, and DL/NDL-PCBs act differently on fatty liver disease.

1a. Determined the activation of AhR and liver injury stimulated by DL-PCB and DL/NDL-PCBs mixture in a two-week treatment in mice on control synthetic diet.

1b. Determined the effects of DL-PCB and DL/NDL-PCBs mixture in NAFLA/NASH in a twelve-week treatment in mice on high fat diet via interaction with AhR.

Specific Aim 2 addressed whether human and murine AhR display the same concentration-dependence for ligand activation in response to PCBs.

2a. Determined the half maximal effective concentration (EC_{50}) for DL-PCB congeners in HepG2 cells and Hepa1c1c7 cells transfected with a XRE-luciferase reporter.

2b. Determined the concentration-dependence of AhR activation in murine and human primary hepatocytes treated with DL-PCBs and DL/NDL-PCBs mixture.

2. Major findings of current dissertation

In my dissertation, specific aim 1 addressed whether DL-PCBs, NDL-PCBs, and DL/NDL-PCBs act differently on fatty liver disease. A new human relevant PCB exposures animal model was established to evaluate different outcomes of DL-, NDL-, and DL/NDL-PCBs mixture exposure in NAFLD/NASH. In the control synthetic diet acute PCB exposures model, DL-PCB 126 exposure induced AhR activation, and caused mild hepatic steatosis (lean NAFLD), and DL/NDL-PCBs mixture exposure targeted pancreas, and caused pancreatic dysfunction, a condition termed PCB exposure-induced pancreatopathy. In high fat diet chronic PCB exposures model, Aroclor 1260 promoted steatosis progression to steatohepatitis (obese NASH), while DL-PCB 126 attenuated Aroclor 1260 exposure-induced steatohepatitis. Novel mechanisms of PCB exposures-induced toxicity related to NAFLD/NASH, such as liver-pancreas axis, β cell identity, hepatokines, and Pnpla3 were observed in the animal models. Please refer to supplemental table 1 &2 for detailed information. Specific aim 2 addressed whether human and murine AhR display the same concentration-dependence for ligand activation in response to PCBs. The results demonstrated that the concentration-dependence of mouse AhR activation by DL-PCBs is much lower than human AhR, suggesting species difference for AhR activation, and the same difference was also found in REPs in response to PCBs exposure. Difference between human and mouse AhR relative ligand affinity indicated that humanized AhR mouse model should be used relevant to specific aim 1to better evaluate risks of PCB exposures in humans.

3. Strengths and limitations of this dissertation

Strengths

There are several strengths in this dissertation. First strength is environmentally relevant DL/NDL-PCBs mixture exposure induces AhR activation in vivo, and the extent of AhR activation by this PCBs mixture is similar to low dose of PCB 126 exposure, and the histological changes and molecule level of lipid metabolism gene expression are different with this PCBs mixture exposure compared to either exposure alone. This result may be due to the interaction of transcription factors, as well as diet effects. In addition, DL/NDL-PCBs mixture also induces pancreatic structure changes and dysfunction, termed PCBs exposure-induced pancreatopathy. These data suggest to us that DL/NDL-PCBs mixture should be used when we evaluate a PCB exposures-induced metabolic disease, providing data that more closely reflect in human. Another strength is that our AhR relative ligand affinity assay demonstrates activation of mouse AhR is much more sensitive to dose than human AhR by dioxin-like PCB congeners exposure. Moreover, DL/NDL-PCBs mixture at the concentration tested only activates mouse AhR, not human AhR. These data suggest a species difference between human and mouse that should be considered when evaluating the risk of PCBs mixture exposure that contain dioxin-like PCB congeners, and the data generated could provide us better understanding of PCB exposure-induced disease in humans.

Limitations

Although the phenotypic changes are significantly different by specific PCB exposures, we will not be able to provide a molecular mechanism that is responsible for these changes. However, our results suggest nuclear receptor, AhR, hepatokines, and Pnpla3 could be

influenced. A proteomic and/or RNA sequencing analysis could be done to identify different proteins and/or genes that might provide us an insight for these phenotypical changes. PCB exposures-induced AhR, PXR, and CAR activation, were associated with phenotypic changes; however, the exact role of these receptors' activation in PCB exposures-induced liver disease is unclear. In addition, potential sex differences were also not considered in this dissertation, as PCBs interact with estrogen receptor (51) and AhR activation causes loss of liver specific and sexually dimorphic gene expression (150). AhR is also expressed in gut, and may impact liver disease through gut-liver axis. Thus, the hepatocyte AhR-specific knockout mice, and/or combination with CAR/PXR double knockout mice might be used to better understand the potential mechanisms. (151). Moreover, PCBs exposure disrupts intestinal integrity (152) and induces dysbiosis of the gut microbiota (153, 154). Therefore, investigation of gut microbiota would be performed with the varying PCB exposures. These data may distinguish the causative of various of changes by different PCB exposures. Lastly, the humanized AhR mouse should be used to better evaluate risk of PCBs exposure, due to the different AhR relative ligand affinity across species.

4. Summary

   Taken together, both PCB 126 or the DL/NDL-PCBs mixture activated AhR, while Aroclor 1260 exposure activated CAR and PXR in either control synthetic diet or high fat diet. However, high fat diet abrogated PCB exposures-induced xenobiotic receptor activation. The effects of PCB exposures on liver lipid homeostasis were summarized in Figure 5.1. PCB 126 exposure induced mild hepatic steatosis in control synthetic diet model (lean NAFLD), while Aroclor 1260 exposure promoted steatosis progression to

steatohepatitis (obese NASH) in high fat diet model. Regardless of the diet effects, PCB exposures increased lipid influx to liver, and decreased *de novo* lipogenesis. Moreover, PCB 126 exposure decreased fasting blood glucose via inhibition of hepatic gluconeogenic gene mRNA expression, and induced hypolipidemia. For fatty acid β-oxidation, PCB exposures exhibited different effects on mRNA expression for these genes. Other potential mechanisms include hepatokines, Pnpla3 mRNA transcription. The DL/NDL-PCBs mixture caused pancreatopathy which warrant future study. Difference in ligand concentration-dependence of AhR activation between human and mouse was observed by DL-PCB congeners exposure, and DL/NDL-PCBs mixture exposure activated mouse AhR. These results suggested that utilizing an environmentally relevant mixture of PCBs containing both DL-and NDL-PCB congeners is important in the study of endocrine and metabolic disruption because the combined effects may be different than the effects of either type of PCB alone. Due to species difference in PCB-ligand activation of AhR, humanized AhR mice should be used in the future study.
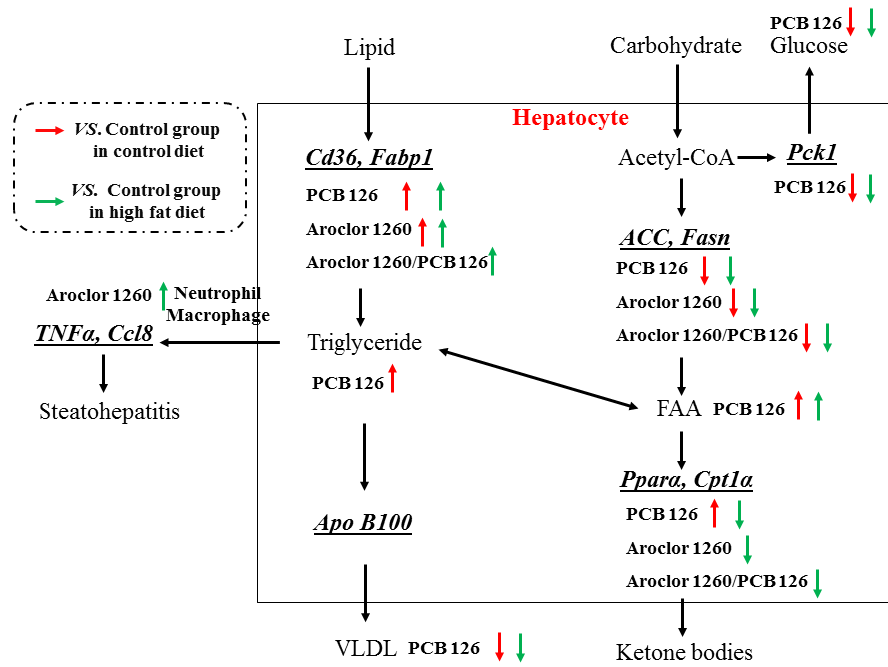
Figure 5.1 PCB exposures affected homeostasis of liver lipid metabolism.

Supplemental Table 1 Effects of PCB exposures on liver, pancreas and blood in mice fed on control synthetic diet for 2 weeks.

Targets	Effects		Aroclor 1260	PCB 126	Aroclor 1260/PCB 126
Liver	Cytochrome P450s	Cyp1a2 induction	↔	↑	↑
		Cyp2b10 induction	↑ (+/+)	↑ (-/-)	↑ (+/-) *
		Cyp3a11 induction	↑	↔	↔ *
	Steatosis		↔	↑	↔ *
	Injury		↔	↔	↔
	Lipid uptake gene mRNA levels		↑	↑	↔ *
	Fatty acid β-oxidation gene mRNA levels		↔	↑	↔ *
	Fatty acid synthesis gene mRNA levels		↓	↓	↔ *
	Hepatokine gene mRNA levels	FGF21	↓	↓	↑ *
		IGF1	↑	↑	↔ *
		Betatrophin	↑	↔	↓ *
	Gluconeogenesis gene mRNA levels		↔	↓	↔ *
Pancreas	Atrophy		↔	↔	↑
	Acinar cell steatosis		↔	↔	↑
	Fibrosis		↔	↔	↑
	Insulin1 gene mRNA levels		↑	↑	↓ *
	Pancreatic polypeptide gene mRNA levels		↑	↑	↓ *
	Islet identity gene mRNA levels		↑	↑	↓ *
Blood	Fasting glucose		↔	↓	↓
	Lipid		↔	↓	↓
	Insulin		↔	↔	↔
	Systemic inflammation		↔	↔	↔

Notes:
1. ↔ indicates no change; ↑ indicates increase; ↓ indicates decrease *versus* vehicle control;
2. + indicates numerical high; - indicates numerical low;
3. * indicates interaction between Aroclor 1260 and PCB 126.

Supplemental Table 2 Effects of PCB exposures on liver and blood in mice fed on high

fat diet for 12 weeks.

Targets	Effects		Aroclor 1260	PCB 126	Aroclor 1260/PCB 126
Liver	Cytochrome P450s	Cyp1a2 induction	↔	↑	↑ *
		Cyp2b10 induction	↑ (+)	↔	↑(-) *
	Steatosis		↔	↔	↔
	Injury		↑	↓	↓
	Inflammation		↑	↔	↔*
	Lipid uptake gene mRNA levels		↑	↑	↑
	Fatty acid β-oxidation gene mRNA levels		↓	↓	↓
	Fatty acid synthesis gene mRNA levels		↓	↓	↓
	Fibrosis	Fibrotic gene mRNA levels	↔	↓	↓
		Phenotype	↔	↔	↔
	Gluconeogenesis gene mRNA levels		↔	↓	↔
Blood	Fasting glucose		↔	↓	↓
	Lipid (triglyceride)		↔	↓	↓
	Adipokines		↔	↔	↔
	Tolerance test		↔	↔	↔

Notes:
1. ↔ indicates no change; ↑ indicates increase; ↓ indicates decrease *versus* vehicle
   control;
2. + indicates numerical high; - indicates numerical low;
3. * indicates interaction between Aroclor 1260 and PCB 126.

REFERENCES

1.	Michelotti GA, Machado MV, Diehl AM. NAFLD, NASH and liver cancer. Nat Rev Gastroenterol Hepatol 2013;10:656-665.
2.	Kim GA, Lee HC, Choe J, Kim MJ, Lee MJ, Chang HS, Bae IY, et al. Association between non-alcoholic fatty liver disease and cancer incidence rate. J Hepatol 2017.
3.	Bradbury MW. Lipid metabolism and liver inflammation. I. Hepatic fatty acid uptake: possible role in steatosis. Am J Physiol Gastrointest Liver Physiol 2006;290:G194-198.
4.	Pohl J, Ring A, Ehehalt R, Herrmann T, Stremmel W. New concepts of cellular fatty acid uptake: role of fatty acid transport proteins and of caveolae. Proc Nutr Soc 2004;63:259-262.
5.	Abumrad N, Coburn C, Ibrahimi A. Membrane proteins implicated in long-chain fatty acid uptake by mammalian cells: CD36, FATP and FABPm. Biochim Biophys Acta 1999;1441:4-13.
6.	Solinas G, Borén J, Dulloo AG. De novo lipogenesis in metabolic homeostasis: More friend than foe? Molecular Metabolism 2015;4:367-377.
7.	Strable MS, Ntambi JM. Genetic control of de novo lipogenesis: role in diet-induced obesity. Critical reviews in biochemistry and molecular biology 2010;45:199-214.
8.	Meex RCR, Watt MJ. Hepatokines: linking nonalcoholic fatty liver disease and insulin resistance. Nature Reviews Endocrinology 2017;13:509.
9.	J D McGarry a, Foster DW. Regulation of Hepatic Fatty Acid Oxidation and Ketone Body Production. Annual Review of Biochemistry 1980;49:395-420.
10.	Younossi ZM, Koenig AB, Abdelatif D, Fazel Y, Henry L, Wymer M. Global epidemiology of nonalcoholic fatty liver disease-Meta-analytic assessment of prevalence, incidence, and outcomes. Hepatology 2016;64:73-84.
11.	Younossi Z, Anstee QM, Marietti M, Hardy T, Henry L, Eslam M, George J, et al. Global burden of NAFLD and NASH: trends, predictions, risk factors and prevention. Nature Reviews Gastroenterology &Amp; Hepatology 2017;15:11.
12.	Buzzetti E, Pinzani M, Tsochatzis EA. The multiple-hit pathogenesis of non-alcoholic fatty liver disease (NAFLD). Metabolism 2016;65:1038-1048.
13.	Nobili V, Alisi A, Raponi M. Pediatric non-alcoholic fatty liver disease: Preventive and therapeutic value of lifestyle intervention. World Journal of Gastroenterology : WJG 2009;15:6017-6022.
14.	Dongiovanni P, Lanti C, Riso P, Valenti L. Nutritional therapy for nonalcoholic fatty liver disease. The Journal of Nutritional Biochemistry 2016;29:1-11.
15.	Eslam M, Valenti L, Romeo S. Genetics and epigenetics of NAFLD and NASH: Clinical impact. J Hepatol 2018;68:268-279.

16.   Smith BW, Adams LA. Nonalcoholic fatty liver disease and diabetes mellitus: pathogenesis and treatment. Nature Reviews Endocrinology 2011;7:456.

17.   Ono M, Okamoto N, Saibara T. The latest idea in NAFLD/NASH pathogenesis. Clin J Gastroenterol 2010;3:263-270.

18.   Arab JP, Arrese M, Trauner M. Recent Insights into the Pathogenesis of Nonalcoholic Fatty Liver Disease. Annual Review of Pathology: Mechanisms of Disease 2018;13:321-350.

19.   Romeo S, Kozlitina J, Xing C, Pertsemlidis A, Cox D, Pennacchio LA, Boerwinkle E, et al. Genetic variation in PNPLA3 confers susceptibility to nonalcoholic fatty liver disease. Nat Genet 2008;40:1461-1465.

20.   BasuRay S, Smagris E, Cohen JC, Hobbs HH. The PNPLA3 Variant Associated with Fatty Liver Disease (I148M) Accumulates on Lipid Droplets by Evading Ubiquitylation. Hepatology 2017.

21.   Younossi ZM, Blissett D, Blissett R, Henry L, Stepanova M, Younossi Y, Racila A, et al. The Economic and Clinical Burden of Non-alcoholic Fatty Liver Disease (NAFLD) in the United States and Europe. Hepatology 2016.

22.   Vilar-Gomez E, Martinez-Perez Y, Calzadilla-Bertot L, Torres-Gonzalez A, Gra-Oramas B, Gonzalez-Fabian L, Friedman SL, et al. Weight Loss Through Lifestyle Modification Significantly Reduces Features of Nonalcoholic Steatohepatitis. Gastroenterology;149:367-378.e365.

23.   Sumida Y, Yoneda M. Current and future pharmacological therapies for NAFLD/NASH. J Gastroenterol 2017.

24.   Musso G, Cassader M, Gambino R. Non-alcoholic steatohepatitis: emerging molecular targets and therapeutic strategies. Nat Rev Drug Discov 2016;15:249-274.

25.   Sookoian S, Pirola CJ. Elafibranor for the treatment of NAFLD: One pill, two molecular targets and multiple effects in a complex phenotype. Ann Hepatol 2016;15:604-609.

26.   Ratziu V, Harrison SA, Francque S, Bedossa P, Lehert P, Serfaty L, Romero-Gomez M, et al. Elafibranor, an Agonist of the Peroxisome Proliferator-Activated Receptor-alpha and -delta, Induces Resolution of Nonalcoholic Steatohepatitis Without Fibrosis Worsening. Gastroenterology 2016;150:1147-1159.e1145.

27.   Neuschwander-Tetri BA, Loomba R, Sanyal AJ, Lavine JE, Van Natta ML, Abdelmalek MF, Chalasani N, et al. Farnesoid X nuclear receptor ligand obeticholic acid for non-cirrhotic, non-alcoholic steatohepatitis (FLINT): a multicentre, randomised, placebo-controlled trial. Lancet 2015;385:956-965.

28.   Ray K. NAFLD: obeticholic acid for the treatment of fatty liver disease--NASH no more? Nat Rev Gastroenterol Hepatol 2015;12:1.

29.   Loomba R, Lawitz E, Mantry PS, Jayakumar S, Caldwell SH, Arnold H, Diehl AM, et al. The ASK1 inhibitor selonsertib in patients with nonalcoholic steatohepatitis: A randomized, phase 2 trial. Hepatology 2018;67:549-559.

30.   Ray K. NAFLD: Early promise for ASK1 inhibition in NASH. Nat Rev Gastroenterol Hepatol 2017;14:631.

31.   Friedman SL, Ratziu V, Harrison SA, Abdelmalek MF, Aithal GP, Caballeria J, Francque S, et al. A randomized, placebo-controlled trial of cenicriviroc for treatment of nonalcoholic steatohepatitis with fibrosis. Hepatology 2017.

32.   Tacke F. Cenicriviroc for the treatment of non-alcoholic steatohepatitis and liver fibrosis. Expert Opin Investig Drugs 2018;27:301-311.

33.   Day CP, James OF. Steatohepatitis: a tale of two "hits"? Gastroenterology 1998;114:842-845.

34.   Tilg H, Moschen AR. Evolution of inflammation in nonalcoholic fatty liver disease: the multiple parallel hits hypothesis. Hepatology 2010;52:1836-1846.

35.   Cave M, Falkner KC, Ray M, Joshi-Barve S, Brock G, Khan R, Bon Homme M, et al. Toxicant-associated steatohepatitis in vinyl chloride workers. Hepatology 2010;51:474-481.

36.   Wahlang B, Beier JI, Clair HB, Bellis-Jones HJ, Falkner KC, McClain CJ, Cave MC. Toxicant-associated steatohepatitis. Toxicol Pathol 2013;41:343-360.

37.   Al-Eryani L, Wahlang B, Falkner KC, Guardiola JJ, Clair HB, Prough RA, Cave M. Identification of Environmental Chemicals Associated with the Development of Toxicant-associated Fatty Liver Disease in Rodents. Toxicol Pathol 2015;43:482-497.

38.   Breivik K, Sweetman A, Pacyna JM, Jones KC. Towards a global historical emission inventory for selected PCB congeners — a mass balance approach: 1. Global production and consumption. Science of The Total Environment 2002;290:181-198.

39.   Risebrough RW, Rieche P, Peakall DB, Herman SG, Kirven MN. Polychlorinated Biphenyls in the Global Ecosystem. Nature 1968;220:1098.

40.   Oliveira T, Santacroce G, Coleates R, Hale S, Zevin P, Belasco B. Concentrations of polychlorinated biphenyls in water from US Lake Ontario tributaries between 2004 and 2008. Chemosphere 2011;82:1314-1320.

41.   Rogan WJ, Gladen BC, McKinney JD, Carreras N, Hardy P, Thullen J, Tingelstad J, et al. Polychlorinated biphenyls (PCBs) and dichlorodiphenyl dichloroethene (DDE) in human milk: effects of maternal factors and previous lactation. American Journal of Public Health 1986;76:172-177.

42.   Cave M, Appana S, Patel M, Falkner KC, McClain CJ, Brock G. Polychlorinated biphenyls, lead, and mercury are associated with liver disease in American adults: NHANES 2003-2004. Environ Health Perspect 2010;118:1735-1742.

43.   Johnson-Restrepo B, Kannan K, Rapaport DP, Rodan BD. Polybrominated Diphenyl Ethers and Polychlorinated Biphenyls in Human Adipose Tissue from New York. Environmental Science & Technology 2005;39:5177-5182.

44.   Vorkamp K. An overlooked environmental issue? A review of the inadvertent formation of PCB-11 and other PCB congeners and their occurrence in consumer products and in the environment. Sci Total Environ 2016;541:1463-1476.

45.   Ampleman MD, Martinez A, DeWall J, Rawn DF, Hornbuckle KC, Thorne PS. Inhalation and dietary exposure to PCBs in urban and rural cohorts via congener-specific measurements. Environ Sci Technol 2015;49:1156-1164.

46.   Schecter A, Pavuk M, Malisch R, Ryan JJ. Are Vietnamese food exports contaminated with dioxin from Agent Orange? J Toxicol Environ Health A 2003;66:1391-1404.

47.   Liu H, Nie FH, Lin HY, Ma Y, Ju XH, Chen JJ, Gooneratne R. Developmental toxicity, oxidative stress, and related gene expression induced by dioxin-like PCB 126 in zebrafish (Danio rerio). Environ Toxicol 2014.

48.	Klaren WD, Gadupudi GS, Wels B, Simmons DL, Olivier AK, Robertson LW. Progression of micronutrient alteration and hepatotoxicity following acute PCB126 exposure. Toxicology 2015;338:1-7.

49.	Yoshizawa K, Brix AE, Sells DM, Jokinen MP, Wyde M, Orzech DP, Kissling GE, et al. Reproductive lesions in female Harlan Sprague-Dawley rats following two-year oral treatment with dioxin and dioxin-like compounds. Toxicol Pathol 2009;37:921-937.

50.	Hassoun EA, Periandri-Steinberg S. Assessment of the roles of antioxidant enzymes and glutathione in 3,3',4,4',5-Pentachlorobiphenyl (PCB 126)-induced oxidative stress in the brain tissues of rats after subchronic exposure. Toxicol Environ Chem 2010;92:301.

51.	Gjernes MH, Schlenk D, Arukwe A. Estrogen receptor-hijacking by dioxin-like 3,3'4,4',5-pentachlorobiphenyl (PCB126) in salmon hepatocytes involves both receptor activation and receptor protein stability. Aquat Toxicol 2012;124-125:197-208.

52.	Wahlang B, Falkner KC, Clair HB, Al-Eryani L, Prough RA, States JC, Coslo DM, et al. Human receptor activation by aroclor 1260, a polychlorinated biphenyl mixture. Toxicol Sci 2014;140:283-297.

53.	Luthe G, Jacobus JA, Robertson LW. Receptor interactions by polybrominated diphenyl ethers versus polychlorinated biphenyls: A theoretical structure–activity assessment. Environmental Toxicology and Pharmacology 2008;25:202-210.

54.	Grimm FA, Hu D, Kania-Korwel I, Lehmler H-J, Ludewig G, Hornbuckle KC, Duffel MW, et al. Metabolism and metabolites of polychlorinated biphenyls. Critical Reviews in Toxicology 2015;45:245-272.

55.	Pavuk M, Olson JR, Sjödin A, Wolff P, Turner WE, Shelton C, Dutton ND, et al. Serum concentrations of polychlorinated biphenyls (PCBs) in participants of the Anniston Community Health Survey(,). The Science of the total environment 2014;0:286-297.

56.	Sjödin A, Wong L-Y, Jones RS, Park A, Zhang Y, Hodge C, DiPietro E, et al. Serum Concentrations of Polybrominated Diphenyl Ethers (PBDEs) and Polybrominated Biphenyl (PBB) in the United States Population: 2003–2004. Environmental Science & Technology 2008;42:1377-1384.

57.	Silverstone AE, Rosenbaum PF, Weinstock RS, Bartell SM, Foushee HR, Shelton C, Pavuk M. Polychlorinated biphenyl (PCB) exposure and diabetes: results from the Anniston Community Health Survey. Environ Health Perspect 2012;120:727-732.

58.	Rosenbaum PF, Weinstock RS, Silverstone AE, Sjödin A, Pavuk M. Metabolic syndrome is associated with exposure to organochlorine pesticides in Anniston, AL, United States. Environment international 2017;108:11-21.

59.	Wahlang B, Song M, Beier JI, Falkner KC, Al-Eryani L, Clair HB, Prough RA, et al. Evaluation of Aroclor 1260 exposure in a mouse model of diet-induced obesity and non-alcoholic fatty liver disease. Toxicology and Applied Pharmacology 2014;279:380-390.

60.	Aoki Y. Polychlorinated Biphenyls, Polychloronated Dibenzo-p-dioxins, and Polychlorinated Dibenzofurans as Endocrine Disrupters—What We Have Learned from Yusho Disease. Environmental Research 2001;86:2-11.

61.   Hsu ST, Ma CI, Hsu SK, Wu SS, Hsu NH, Yeh CC, Wu SB. Discovery and epidemiology of PCB poisoning in Taiwan: a four-year followup. Environ Health Perspect 1985;59:5-10.
62.   Tsukimori K, Uchi H, Mitoma C, Yasukawa F, Chiba T, Todaka T, Kajiwara J, et al. Maternal exposure to high levels of dioxins in relation to birth weight in women affected by Yusho disease. Environ Int 2012;38:79-86.
63.   Lin K-C, Guo N-W, Tsai P-C, Yang C-Y, Guo YL. Neurocognitive Changes among Elderly Exposed to PCBs/PCDFs in Taiwan. Environmental Health Perspectives 2008;116:184-189.
64.   Yu M-L, Guo YL, Hsu C-C, Rogan WJ. Increased mortality from chronic liver disease and cirrhosis 13 years after the Taiwan "yucheng" ("oil disease") incident. American Journal of Industrial Medicine 1997;31:172-175.
65.   Tsai P-C, Ko Y-C, Huang W, Liu H-S, Guo YL. Increased liver and lupus mortalities in 24-year follow-up of the Taiwanese people highly exposed to polychlorinated biphenyls and dibenzofurans. Science of The Total Environment 2007;374:216-222.
66.   Heindel JJ, Blumberg B, Cave M, Machtinger R, Mantovani A, Mendez MA, Nadal A, et al. Metabolism disrupting chemicals and metabolic disorders. Reprod Toxicol 2017;68:3-33.
67.   Murray IA, Patterson AD, Perdew GH. Aryl hydrocarbon receptor ligands in cancer: friend and foe. Nat Rev Cancer 2014;14:801-814.
68.   Esser C, Rannug A. The aryl hydrocarbon receptor in barrier organ physiology, immunology, and toxicology. Pharmacol Rev 2015;67:259-279.
69.   Daujat M, Peryt B, Lesca P, Fourtanier G, Domergue J, Maurel P. Omeprazole, an inducer of human CYP1A1 and 1A2, is not a ligand for the Ah receptor. Biochem Biophys Res Commun 1992;188:820-825.
70.   Kawano Y, Nishiumi S, Tanaka S, Nobutani K, Miki A, Yano Y, Seo Y, et al. Activation of the aryl hydrocarbon receptor induces hepatic steatosis via the upregulation of fatty acid transport. Arch Biochem Biophys 2010;504:221-227.
71.   Lee JH, Wada T, Febbraio M, He J, Matsubara T, Lee MJ, Gonzalez FJ, et al. A novel role for the dioxin receptor in fatty acid metabolism and hepatic steatosis. Gastroenterology 2010;139:653-663.
72.   Angrish MM, Jones AD, Harkema JR, Zacharewski TR. Aryl hydrocarbon receptor-mediated induction of Stearoyl-CoA desaturase 1 alters hepatic fatty acid composition in TCDD-elicited steatosis. Toxicol Sci 2011;124:299-310.
73.   Gadupudi GS, Klaren WD, Olivier AK, Klingelhutz AJ, Robertson LW. PCB126-Induced Disruption in Gluconeogenesis and Fatty Acid Oxidation Precedes Fatty Liver in Male Rats. Toxicol Sci 2016;149:98-110.
74.   Wang C, Xu CX, Krager SL, Bottum KM, Liao DF, Tischkau SA. Aryl hydrocarbon receptor deficiency enhances insulin sensitivity and reduces PPAR-alpha pathway activity in mice. Environ Health Perspect 2011;119:1739-1744.
75.   Xu CX, Wang C, Zhang ZM, Jaeger CD, Krager SL, Bottum KM, Liu J, et al. Aryl hydrocarbon receptor deficiency protects mice from diet-induced adiposity and metabolic disorders through increased energy expenditure. Int J Obes (Lond) 2015;39:1300-1309.

76.   Wada T, Sunaga H, Miyata K, Shirasaki H, Uchiyama Y, Shimba S. Aryl Hydrocarbon Receptor Plays Protective Roles against High Fat Diet (HFD)-induced Hepatic Steatosis and the Subsequent Lipotoxicity via Direct Transcriptional Regulation of Socs3 Gene Expression. J Biol Chem 2016;291:7004-7016.

77.   Lu P, Yan J, Liu K, Garbacz WG, Wang P, Xu M, Ma X, et al. Activation of aryl hydrocarbon receptor dissociates fatty liver from insulin resistance by inducing fibroblast growth factor 21. Hepatology 2015;61:1908-1919.

78.   Cheng X, Vispute SG, Liu J, Cheng C, Kharitonenkov A, Klaassen CD. Fibroblast growth factor (Fgf) 21 is a novel target gene of the aryl hydrocarbon receptor (AhR). Toxicol Appl Pharmacol 2014;278:65-71.

79.   Zhang W, Sargis RM, Volden PA, Carmean CM, Sun XJ, Brady MJ. PCB 126 and other dioxin-like PCBs specifically suppress hepatic PEPCK expression via the aryl hydrocarbon receptor. PLoS One 2012;7:e37103.

80.   Diani-Moore S, Ram P, Li X, Mondal P, Youn DY, Sauve AA, Rifkind AB. Identification of the aryl hydrocarbon receptor target gene TiPARP as a mediator of suppression of hepatic gluconeogenesis by 2,3,7,8-tetrachlorodibenzo-p-dioxin and of nicotinamide as a corrective agent for this effect. J Biol Chem 2010;285:38801-38810.

81.   Wada T, Gao J, Xie W. PXR and CAR in energy metabolism. Trends Endocrinol Metab 2009;20:273-279.

82.   Chai SC, Cherian MT, Wang Y-M, Chen T. Small-molecule modulators of PXR and CAR. Biochimica et Biophysica Acta (BBA) - Gene Regulatory Mechanisms 2016;1859:1141-1154.

83.   Hakkola J, Rysä J, Hukkanen J. Regulation of hepatic energy metabolism by the nuclear receptor PXR. Biochimica et Biophysica Acta (BBA) - Gene Regulatory Mechanisms 2016;1859:1072-1082.

84.   Yan J, Chen B, Lu J, Xie W. Deciphering the roles of the constitutive androstane receptor in energy metabolism. Acta Pharmacol Sin 2015;36:62-70.

85.   Dong B, Saha PK, Huang W, Chen W, Abu-Elheiga LA, Wakil SJ, Stevens RD, et al. Activation of nuclear receptor CAR ameliorates diabetes and fatty liver disease. Proc Natl Acad Sci U S A 2009;106:18831-18836.

86.   Gao J, He J, Zhai Y, Wada T, Xie W. The constitutive androstane receptor is an anti-obesity nuclear receptor that improves insulin sensitivity. J Biol Chem 2009;284:25984-25992.

87.   Baskin-Bey ES, Anan A, Isomoto H, Bronk SF, Gores GJ. Constitutive androstane receptor agonist, TCPOBOP, attenuates steatohepatitis in the methionine choline-deficient diet-fed mouse. World J Gastroenterol 2007;13:5635-5641.

88.   Ma Y, Liu D. Activation of pregnane X receptor by pregnenolone 16 alpha-carbonitrile prevents high-fat diet-induced obesity in AKR/J mice. PLoS One 2012;7:e38734.

89.   He J, Gao J, Xu M, Ren S, Stefanovic-Racic M, O'Doherty RM, Xie W. PXR ablation alleviates diet-induced and genetic obesity and insulin resistance in mice. Diabetes 2013;62:1876-1887.

90.   Gao J, Xie W. Targeting xenobiotic receptors PXR and CAR for metabolic diseases. Trends Pharmacol Sci 2012;33:552-558.

91.   Gao J, Yan J, Xu M, Ren S, Xie W. CAR Suppresses Hepatic Gluconeogenesis by Facilitating the Ubiquitination and Degradation of PGC1alpha. Mol Endocrinol 2015;29:1558-1570.

92.   Cheng J, Shah YM, Gonzalez FJ. Pregnane X receptor as a target for treatment of inflammatory bowel disorders. Trends Pharmacol Sci 2012;33:323-330.

93.   Hardesty JE, Wahlang B, Falkner KC, Clair HB, Clark BJ, Ceresa BP, Prough RA, et al. Polychlorinated biphenyls disrupt hepatic epidermal growth factor receptor signaling. Xenobiotica 2017;47:807-820.

94.   Hardesty JE, Al-Eryani L, Wahlang B, Falkner KC, Shi H, Jin J, Vivace B, et al. Epidermal Growth Factor Receptor Signaling Disruption by Endocrine and Metabolic Disrupting Chemicals. Toxicol Sci 2018.

95.   Mutoh S, Sobhany M, Moore R, Perera L, Pedersen L, Sueyoshi T, Negishi M. Phenobarbital indirectly activates the constitutive active androstane receptor (CAR) by inhibition of epidermal growth factor receptor signaling. Sci Signal 2013;6:ra31.

96.   Wang B, Klaren WD, Wels BR, Simmons DL, Olivier AK, Wang K, Robertson LW, et al. Dietary manganese modulates PCB126 toxicity, metal status and MnSOD in the rat. Toxicol Sci 2015.

97.   Wu X, Yang J, Morisseau C, Robertson LW, Hammock B, Lehmler HJ. 3,3',4,4',5-Pentachlorobiphenyl (PCB 126) decreases hepatic and systemic ratios of epoxide to diol metabolites of unsaturated fatty acids in male rats. Toxicol Sci 2016.

98.   Cave M, Appana S, Patel M, Falkner KC, McClain CJ, Brock G. Polychlorinated Biphenyls, Lead, and Mercury Are Associated with Liver Disease in American Adults: NHANES 2003-2004. Environmental Health Perspectives 2010;118:1735-1742.

99.   Goto T, Hirata M, Aoki Y, Iwase M, Takahashi H, Kim M, Li Y, et al. The hepatokine FGF21 is crucial for peroxisome proliferator-activated receptor-alpha agonist-induced amelioration of metabolic disorders in obese mice. J Biol Chem 2017.

100.   Rutter GA. Diabetes: Controlling the identity of the adult pancreatic beta cell. Nat Rev Endocrinol 2017;13:129-130.

101.   Bligh EG, Dyer WJ. A rapid method of total lipid extraction and purification. Can J Biochem Physiol 1959;37:911-917.

102.   Smagris E, BasuRay S, Li J, Huang Y, Lai KM, Gromada J, Cohen JC, et al. Pnpla3I148M knockin mice accumulate PNPLA3 on lipid droplets and develop hepatic steatosis. Hepatology 2015;61:108-118.

103.   Marmugi A, Lukowicz C, Lasserre F, Montagner A, Polizzi A, Ducheix S, Goron A, et al. Activation of the Constitutive Androstane Receptor induces hepatic lipogenesis and regulates Pnpla3 gene expression in a LXR-independent way. Toxicol Appl Pharmacol 2016;303:90-100.

104.   Angrish MM, Mets BD, Jones AD, Zacharewski TR. Dietary fat is a lipid source in 2,3,7,8-tetrachlorodibenzo-rho-dioxin (TCDD)-elicited hepatic steatosis in C57BL/6 mice. Toxicol Sci 2012;128:377-386.

105.   Yi P, Park J-S, Melton Douglas A. Betatrophin: A Hormone that Controls Pancreatic β Cell Proliferation. Cell 2013;153:747-758.

106.   Gusarova V, Alexa Corey A, Na E, Stevis Panayiotis E, Xin Y, Bonner-Weir S, Cohen Jonathan C, et al. ANGPTL8/Betatrophin Does Not Control Pancreatic Beta Cell Expansion. Cell 2014;159:691-696.

107.   Tessem JS, Moss LG, Chao LC, Arlotto M, Lu D, Jensen MV, Stephens SB, et al. Nkx6.1 regulates islet beta-cell proliferation via Nr4a1 and Nr4a3 nuclear receptors. Proc Natl Acad Sci U S A 2014;111:5242-5247.

108.   Wahlang B, Prough RA, Falkner KC, Hardesty JE, Song M, Clair HB, Clark BJ, et al. Polychlorinated Biphenyl-Xenobiotic Nuclear Receptor Interactions Regulate Energy Metabolism, Behavior, and Inflammation in Nonalcoholic-Steatohepatitis. Toxicol Sci 2015.

109.   He J, Hu B, Shi X, Weidert ER, Lu P, Xu M, Huang M, et al. Activation of the aryl hydrocarbon receptor sensitizes mice to nonalcoholic steatohepatitis by deactivating mitochondrial sirtuin deacetylase Sirt3. Mol Cell Biol 2013;33:2047-2055.

110.   Mohapatra S, Majumder S, Smyrk TC, Zhang L, Matveyenko A, Kudva YC, Chari ST. Diabetes Mellitus Is Associated With an Exocrine Pancreatopathy: Conclusions From a Review of Literature. Pancreas 2016;45:1104-1110.

111.   Loiola RA, Dos Anjos FM, Shimada AL, Cruz WS, Drewes CC, Rodrigues SF, Cardozo KH, et al. Long-term in vivo polychlorinated biphenyl 126 exposure induces oxidative stress and alters proteomic profile on islets of Langerhans. Sci Rep 2016;6:27882.

112.   Lin M, Wu T, Sun L, Lin JJ, Zuo Z, Wang C. Aroclor 1254 causes atrophy of exocrine pancreas in mice and the mechanism involved. Environmental toxicology 2016;31:671-678.

113.   Zhang S, Wu T, Chen M, Guo Z, Yang Z, Zuo Z, Wang C. Chronic Exposure to Aroclor 1254 Disrupts Glucose Homeostasis in Male Mice via Inhibition of the Insulin Receptor Signal Pathway. Environ Sci Technol 2015;49:10084-10092.

114.   Schisler JC, Jensen PB, Taylor DG, Becker TC, Knop FK, Takekawa S, German M, et al. The Nkx6.1 homeodomain transcription factor suppresses glucagon expression and regulates glucose-stimulated insulin secretion in islet beta cells. Proc Natl Acad Sci U S A 2005;102:7297-7302.

115.   Lupi R, Bugliani M, Del Guerra S, Del Prato S, Marchetti P, Boggi U, Filipponi F, et al. Transcription factors of beta-cell differentiation and maturation in isolated human islets: effects of high glucose, high free fatty acids and type 2 diabetes. Nutr Metab Cardiovasc Dis 2006;16:e7-8.

116.   Dushay J, Chui PC, Gopalakrishnan GS, Varela-Rey M, Crawley M, Fisher FM, Badman MK, et al. Increased fibroblast growth factor 21 in obesity and nonalcoholic fatty liver disease. Gastroenterology 2010;139:456-463.

117.   Girer NG, Murray IA, Omiecinski CJ, Perdew GH. Hepatic Aryl Hydrocarbon Receptor Attenuates Fibroblast Growth Factor 21 Expression. J Biol Chem 2016.

118.   Siddiqa A, Cirillo E, Tareen SHK, Ali A, Kutmon M, Eijssen LMT, Ahmad J, et al. Visualizing the regulatory role of Angiopoietin-like protein 8 (ANGPTL8) in glucose and lipid metabolic pathways. Genomics 2017;109:408-418.

119.   Wang Y, Quagliarini F, Gusarova V, Gromada J, Valenzuela DM, Cohen JC, Hobbs HH. Mice lacking ANGPTL8 (Betatrophin) manifest disrupted triglyceride metabolism without impaired glucose homeostasis. Proceedings of the National Academy of Sciences 2013;110:16109-16114.

120.   Brewster DW, Matsumura F. Reduction of adipose tissue lipoprotein lipase activity as a result of in vivo administration of 2,3,7,8-tetrachlorodibenzo-p-dioxin to the guinea pig. Biochem Pharmacol 1988;37:2247-2253.

121.   Ghosh AK, Vaughan DE. PAI-1 in tissue fibrosis. J Cell Physiol 2012;227:493-507.

122.   Diani-Moore S, Zhang S, Ram P, Rifkind AB. Aryl hydrocarbon receptor activation by dioxin targets phosphoenolpyruvate carboxykinase (PEPCK) for ADP-ribosylation via 2,3,7,8-tetrachlorodibenzo-p-dioxin (TCDD)-inducible poly(ADP-ribose) polymerase (TiPARP). J Biol Chem 2013;288:21514-21525.

123.   Wahlang B, Perkins JT, Petriello MC, Hoffman JB, Stromberg AJ, Hennig B. A compromised liver alters polychlorinated biphenyl-mediated toxicity. Toxicology 2017;380:11-22.

124.   Wahlang B, Falkner KC, Gregory B, Ansert D, Young D, Conklin DJ, Bhatnagar A, et al. Polychlorinated biphenyl 153 is a diet-dependent obesogen that worsens nonalcoholic fatty liver disease in male C57BL6/J mice. J Nutr Biochem 2013;24:1587-1595.

125.   Chapados NA, Boucher MP. Liver metabolic disruption induced after a single exposure to PCB126 in rats. Environ Sci Pollut Res Int 2016.

126.   Klaren WD, Flor S, Gibson-Corley KN, Ludewig G, Robertson LW. Metallothionein's role in PCB126 induced hepatotoxicity and hepatic micronutrient disruption. Toxicol Rep 2016;3:21-28.

127.   Yarushkin AA, Kachaylo EM, Pustylnyak VO. The constitutive androstane receptor activator 4-[(4R,6R)-4,6-diphenyl-1,3-dioxan-2-yl]-N,N-dimethylaniline inhibits the gluconeogenic genes PEPCK and G6Pase through the suppression of HNF4alpha and FOXO1 transcriptional activity. Br J Pharmacol 2013;168:1923-1932.

128.   Monteleone I, Pallone F, Monteleone G. Aryl hydrocarbon receptor and colitis. Semin Immunopathol 2013;35:671-675.

129.   Harvey WA, Jurgensen K, Pu X, Lamb CL, Cornell KA, Clark RJ, Klocke C, et al. Exposure to 2,3,7,8-tetrachlorodibenzo-p-dioxin (TCDD) increases human hepatic stellate cell activation. Toxicology 2016;344-346:26-33.

130.   Han M, Liu X, Liu S, Su G, Fan X, Chen J, Yuan Q, et al. 2,3,7,8-Tetrachlorodibenzo-p-dioxin (TCDD) induces hepatic stellate cell (HSC) activation and liver fibrosis in C57BL6 mouse via activating Akt and NF-κB signaling pathways. Toxicology Letters 2017;273:10-19.

131.   Lamb CL, Cholico GN, Pu X, Hagler GD, Cornell KA, Mitchell KA. 2,3,7,8-Tetrachlorodibenzo-p-dioxin (TCDD) increases necroinflammation and hepatic stellate cell activation but does not exacerbate experimental liver fibrosis in mice. Toxicology and Applied Pharmacology 2016;311:42-51.

132.   Lamb CL, Cholico GN, Perkins DE, Fewkes MT, Oxford JT, Lujan TJ, Morrill EE, et al. Aryl Hydrocarbon Receptor Activation by TCDD Modulates Expression of Extracellular Matrix Remodeling Genes during Experimental Liver Fibrosis. Biomed Res Int 2016;2016:5309328.

133.   Kippler M, Larsson SC, Berglund M, Glynn A, Wolk A, Akesson A. Associations of dietary polychlorinated biphenyls and long-chain omega-3 fatty acids with stroke risk. Environ Int 2016;94:706-711.

134.   Van den Berg M, Birnbaum L, Bosveld AT, Brunstrom B, Cook P, Feeley M, Giesy JP, et al. Toxic equivalency factors (TEFs) for PCBs, PCDDs, PCDFs for humans and wildlife. Environ Health Perspect 1998;106:775-792.

135.   Van den Berg M, Birnbaum LS, Denison M, De Vito M, Farland W, Feeley M, Fiedler H, et al. The 2005 World Health Organization reevaluation of human and Mammalian toxic equivalency factors for dioxins and dioxin-like compounds. Toxicol Sci 2006;93:223-241.

136.   Zeiger M, Haag R, Hockel J, Schrenk D, Schmitz HJ. Inducing effects of dioxin-like polychlorinated biphenyls on CYP1A in the human hepatoblastoma cell line HepG2, the rat hepatoma cell line H4IIE, and rat primary hepatocytes: comparison of relative potencies. Toxicol Sci 2001;63:65-73.

137.   Silkworth JB, Koganti A, Illouz K, Possolo A, Zhao M, Hamilton SB. Comparison of TCDD and PCB CYP1A induction sensitivities in fresh hepatocytes from human donors, sprague-dawley rats, and rhesus monkeys and HepG2 cells. Toxicol Sci 2005;87:508-519.

138.   Ramadoss P, Perdew GH. Use of 2-Azido-3-[125I]iodo-7,8-dibromodibenzo-*p*-dioxin as a Probe to Determine the Relative Ligand Affinity of Human versus Mouse Aryl Hydrocarbon Receptor in Cultured Cells. Molecular Pharmacology 2004;66:129-136.

139.   Flaveny C, Reen RK, Kusnadi A, Perdew GH. The mouse and human Ah receptor differ in recognition of LXXLL motifs. Arch Biochem Biophys 2008;471:215-223.

140.   Wahlang B, Prough RA, Falkner KC, Hardesty JE, Song M, Clair HB, Clark BJ, et al. Polychlorinated Biphenyl-Xenobiotic Nuclear Receptor Interactions Regulate Energy Metabolism, Behavior, and Inflammation in Non-alcoholic-Steatohepatitis. Toxicol Sci 2016;149:396-410.

141.   Aparicio-Vergara M, Tencerova M, Morgantini C, Barreby E, Aouadi M. Isolation of Kupffer Cells and Hepatocytes from a Single Mouse Liver. Methods Mol Biol 2017;1639:161-171.

142.   Burgin DE, Diliberto JJ, Derr-Yellin EC, Kannan N, Kodavanti PR, Birnbaum LS. Differential effects of two lots of aroclor 1254 on enzyme induction, thyroid hormones, and oxidative stress. Environ Health Perspect 2001;109:1163-1168.

143.   Suzuki T, Nohara K. Regulatory factors involved in species-specific modulation of arylhydrocarbon receptor (AhR)-dependent gene expression in humans and mice. J Biochem 2007;142:443-452.

144.   Peters AK, Leonards PE, Zhao B, Bergman A, Denison MS, Van den Berg M. Determination of in vitro relative potency (REP) values for mono-ortho polychlorinated biphenyls after purification with active charcoal. Toxicol Lett 2006;165:230-241.

145.   Larsson M, van den Berg M, Brenerova P, van Duursen MB, van Ede KI, Lohr C, Luecke-Johansson S, et al. Consensus toxicity factors for polychlorinated dibenzo-p-dioxins, dibenzofurans, and biphenyls combining in silico models and extensive in vitro screening of AhR-mediated effects in human and rodent cells. Chem Res Toxicol 2015;28:641-650.

146.   Brennan JC, He G, Tsutsumi T, Zhao J, Wirth E, Fulton MH, Denison MS. Development of Species-Specific Ah Receptor-Responsive Third Generation CALUX Cell Lines with Enhanced Responsiveness and Improved Detection Limits. Environ Sci Technol 2015;49:11903-11912.

147.   Parvez S, Evans AM, Lorber M, Hawkins BS, Swartout JC, Teuschler LK, Rice GE. A sensitivity analysis using alternative toxic equivalency factors to estimate U.S. dietary exposures to dioxin-like compounds. Regul Toxicol Pharmacol 2013;67:278-284.

148. Nault R, Forgacs AL, Dere E, Zacharewski TR. Comparisons of differential gene expression elicited by TCDD, PCB126, betaNF, or ICZ in mouse hepatoma Hepa1c1c7 cells and C57BL/6 mouse liver. Toxicol Lett 2013;223:52-59.

149. Flaveny CA, Murray IA, Chiaro CR, Perdew GH. Ligand selectivity and gene regulation by the human aryl hydrocarbon receptor in transgenic mice. Mol Pharmacol 2009;75:1412-1420.

150. Nault R, Fader KA, Harkema JR, Zacharewski T. Loss of liver-specific and sexually dimorphic gene expression by aryl hydrocarbon receptor activation in C57BL/6 mice. PLoS One 2017;12:e0184842.

151. Marra F, Svegliati-Baroni G. Lipotoxicity and the gut-liver axis in NASH pathogenesis. J Hepatol 2017.

152. Choi YJ, Seelbach MJ, Pu H, Eum SY, Chen L, Zhang B, Hennig B, et al. Polychlorinated biphenyls disrupt intestinal integrity via NADPH oxidase-induced alterations of tight junction protein expression. Environ Health Perspect 2010;118:976-981.

153. Chen L, Zhang W, Hua J, Hu C, Lok-Shun Lai N, Qian PY, Lam PKS, et al. Dysregulation of Intestinal Health by Environmental Pollutants: Involvement of the Estrogen Receptor and Aryl Hydrocarbon Receptor. Environ Sci Technol 2018;52:2323-2330.

154. Matturro B, Ubaldi C, Rossetti S. Microbiome Dynamics of a Polychlorobiphenyl (PCB) Historically Contaminated Marine Sediment under Conditions Promoting Reductive Dechlorination. Front Microbiol 2016;7:1502.

ABBREVIATIONS

AhR	Aryl hydrocarbon receptor
ARNT	AhR nuclear translocator
ALT	Alanine aminotransferase
AST	Aspartate aminotransferase
BA	1,2-benz[a]anthracene
CAR	Constitutive androstane receptor
CCL8	Chemokine (C-C motif) ligand 8
Cpt1α	Carnitine palmitoyl transferase 1A
CXCL1	Chemokine (C-X-C motif) ligand 1
CYP	Cytochromes P450
CITCO	6-(4-chlorophenyl)imidazo[2,1-b][1,3]thiazole-5-carbaldehydeO-(3,4dichlorobenzyl)oxime
DL	Dioxin like
DMSO	Dimethyl sulfoxide
DRE	Dioxin-responsive element
ECM	Extracellular matrix
EDCs/MDCs	Endocrine and metabolism disrupting chemicals
FABP1	Fatty acid-binding protein 1

FASN	Fatty acid synthase
FGF21	Fibroblast growth factor 21
FoxO1	Forkhead box protein O1
G6P	Glucose 6-phosphate
GTT	Glucose tolerance test
HCC	Hepatocellular carcinoma
HDL	High-density lipoprotein
HNF4α	Hepatocyte nuclear factor 4 alpha
HFD	High fat diet
IGF1	Insulin-like growth factor 1
IL6	Interleukin 6
ITT	Insulin tolerance test
LDL	Low-density lipoprotein
MCP1	Monocyte chemoattractant protein 1
MCD	Methionine choline-deficient
MMPs	Matrix metalloproteases
NAFLD/NASH	Nonalcoholic fatty liver disease /steatohepatitis
NDL	Non-dioxin like
nHDLc	non-HDL cholesterol
NR	Nuclear receptor
PAI1	Plasminogen activator inhibitor-1
PCB	Polychlorinated biphenyl
Pck1	Phosphoenolpyruvate carboxy kinase

PGC1α	Peroxisome proliferator-activated receptor gamma coactivator 1-alpha
PNPLA3	Patatin-like phospholipase domain-containing protein 3
PPARα	Peroxisome proliferator-activated receptor alpha
PXR	Pregnane X receptor
RT-PCR	Reverse transcription-polymerase chain reaction
SCD1	Stearoyl coenzyme A desaturase1
TAFLD/TASH	Toxicant associated fatty liver disease/steatohepatitis
TCDD	2,3,7,8-tetrachlorodibenzo-p-dioxin
TCPOBOP	1,4-bis[2-(3,5-dichloropyridyloxy)]benzene
TIMPs	Tissue inhibitors of metalloproteinases
TNFα	Tumor necrosis factor-alpha
VLDL	Very low-density lipoprotein

CURRICULUM VITAE

Hongxue Shi

University of Louisville School of Medicine

Department of Pharmacology and Toxicology

Louisville, KY 40292

Email: s0hong10@louisville.edu

Phone: 502-296-5219

EDUCATION

2014-Present   University of Louisville
- Ph.D. candidate, Pharmacology and Toxicology

2010-2013   Wenzhou Medical University
- M.S., Pharmacology

2006-2010   Huaiyin Institute of Technology
- B.S., Pharmaceutical Engineering

WORK EXPERIENCE

2014- Present   Graduate Research Assistant, Program in Pharmacology & Toxicology, Graduate School, University of Louisville
2013-2014   Lab Manager, School of Pharmacology, Wenzhou Medical University

ABSTRACTS

1.   ***Hongxue Shi**, Josiah E. Hardesty, Jian Jin, Heather B. Clair, Cameron K. Falkner, Russell A. Prough, Matthew C. Cave. Chronic PCB Exposure Disrupts Hepatic Xenobiotic and Intermediary Metabolism and Increases Hepatic Inflammation/Injury. 2018; Society of Toxicology Poster

2.   ***Hongxue Shi**, Josiah E. Hardesty, Jian Jin, Heather B. Clair, Cameron K. Falkner, Russell A. Prough, Matthew C. Cave. Chronic PCB Exposure Disrupts Hepatic Xenobiotic and Intermediary Metabolism and Increases Hepatic Inflammation/Injury. 2017; AASLD

3.   ***Josiah E. Hardesty, Bradley J. Vivace, **Hongxue Shi**, Jian Jin, Cameron K. Falkner, Russell A. Prough, Matthew C. Cave. Epidemal growth factor receptor inhibition is a conserved mechanism for environmental pollutants in nonalcoholic fatty liver disease. 2017; AASLD.

4.   *Ming Song, Xiaohong Li, **Hongxue Shi**, Hong Gao, Jian Jin, Matthew C. Cave, Craig J. McClain. Aldose Reductase Gene Shapes the Gut Microbiome and Contributes to Dietary Glucose Induced Hepatic Steatosis: Effect of Environment-host Genetics Interaction on the Pathogenesis of Hepatic Steatosis. 2017; AASLD

5.   *Josiah E. Hardesty, **Hongxue Shi**, Jian Jin, Daniel Wilkey, Banrida Wahlang, Heather B. Clair, Michael L. Merchant, Cameron K. Falkner, Russell A. Prough, Matthew C. Cave. Phosphoproteomics Analysis of Animal Models of Nonalcoholic Fatty Liver Disease Reveals that Interactions between Diet and Environmental Chemicals Regulate Hepatic Nuclear Receptor Protein Levels and Phosphorylation Status. 2017; AASLD

6.   * Ming Song, Xiaohong Li, **Hongxue Shi,** Eric Rouchka, Russell Prough, Matthew Cave, Craig McClain. Dietary Copper-Fructose Interactions Alter Gut Microbial Activity in Male Rats. 2017; Research of Louisville.

7.   *Brad Vivace, Matt Cave, Cameron Falkner, Russell Prough, Josiah Hardesty, **Hongxue Shi**. Effect of Triazine Herbicides on Epidermal Growth Factor Receptor Activation. 2017; Research of Louisville.

8.   ***Shi, HX**, Clair, H.B., Hardesty, J.E., Jin, J., Falkner, K.C., Prough, R.A., Song, M., Cave, M.C. The Role of Aryl Hydrocarbon Receptor in PCB-Induced Fatty Liver Disease in Mice. 2017; Digestive Disease Week Poster.

9.   ***Shi, HX**, Clair, H.B., Hardesty, J.E., Jin, J., Falkner, K.C., Prough, R.A., Song, M., Cave, M.C. The Role of Aryl Hydrocarbon Receptor in PCB-Induced Fatty Liver Disease in Mice. The Toxicologist Supplement to Toxicological Sciences — An Official Journal of the Society of Toxicology. 2017; 2553A. Society of Toxicology Poster.

10.   *Jian, J., **Shi, HX**, Falkner, K.C., Cave, M.C. The Effects of PCB Congeners and PCB Mixtures on Pancreatic Function. The Toxicologist Supplement to Toxicological Sciences — An Official Journal of the Society of Toxicology. 2017; 1503A. Society of Toxicology Poster.

11.   *Hardesty, J.E., Falkner, K.C., Clair, H.B., **Shi, HX**, Wahlang, B., Wilkey, D., Prough, R.A., Merchant, M., Cave, M.C. Hepatic Proteome Alterations Due to PCB Exposure and Diet. The Toxicologist CD Supplement to Toxicological Sciences — An Official Journal of the Society of Toxicology. 2017; 1114A. Society of Toxicology Poster.

PROFESSIONAL MEMBERSHIPS

2016-Present   Society of Toxicology (SOT)
2016-Present   American Association for the Advancement of Science (AAAS)

PUBLICATIONS

1.   **Shi HX,** Hardesty JE, Jin J, Clair HB, Falkner KC, Prough RA, Cave MC. PCB Treatments Differentially Regulate Hepatic Metabolism and Pancreatic Function: Implications for Non-alcoholic Steatohepatitis and Diabetes. (Under review)
2.   **Shi HX**, Hardesty JE, Jin J, Clair HB, Falkner KC, Prough RA, Cave MC. Comparison of Aryl Hydrocarbon Receptor Binding Sensitivity between Human and Mouse after Dioxin-Like PCB Exposure. (In preparation)
3.   **Shi HX**, Hardesty JE, Jin J, Clair HB, Falkner KC, Prough RA, Cave MC. Chronic Polychlorinated Biphenyl (PCB) Exposure Disrupts Hepatic Xenobiotic and Intermediary Metabolism and Increases Hepatic Inflammation/Injury. (In preparation)
4.   Song M, Zhang X, Wei XL, **Shi HX**, Wang YH, Vos MB, Zhou ZX, Yin XM, Prough RA, Cave MC, McClain CJ. Dietary Copper-Fructose Interactions Alter Gut Microbial Activity Concurrent with the Development of Hepatic Steatosis in Male Rats. *American Journal of Physiology Gastrointestinal and Liver Physiology*, 2017, Oct. 12 [PMID: 29025734]
5.   Hardesty JE, Al-Eryani L, Banrida W, Falkner KC, **Shi HX**, Jin J, Brad V, Brian C, Prough RA, Cave MC. Epidermal Growth Factor Receptor Signaling Disruption by Endocrine and Metabolic Disrupting Chemicals. *Toxicological Science*, 2018, Jan. 10 [PMID: 29329451]
6.   Cave MC, Clair HB, Hardesty JE, Falkner KC, Feng W, Clark BJ, Sidey J, **Shi HX**, Aqel BA, McClain CJ, Prough RA. Nuclear receptors and nonalcoholic fatty liver disease. *Biochim Biophys Acta*, 2016,1859(9):1083-1099 [PMID: 26962021]
7.   Li ZM, Wu FZ, Zhang X, Chai Y, Chen DQ, Yang YT, Xu KB, Yin JY, Li R, **Shi HX**, Wang ZG, Li XK, Xiao J, Zhang HY. Valproate Attenuates Endoplasmic Reticulum Stress-Induced Apoptosis in SH-SY5Y Cells via the AKT/GSK3β Signaling Pathway. *International Journal of Molecular Sciences*, 2017, 18, 315 [PMCID: PMC5343851]
8.   **Shi HX**, Lin BB, Huang Y, Wu J, Zhang HY, Lin C, Wang ZG, Zhu JJ, Zhao YZ, Fu XB,Lou ZC, Li XK, Xiao J. Basic Fibroblast Growth Factor Promotes Melanocyte Migration via Activating PI3K/Akt- Rac1-FAK-JNK and ERK Signaling Pathways. *IUBMB Life*, 2016,68(9):735-747 [PMID:27350596]
9.   **Shi HX,** Xie HH, Zhao Y, Lin C, Cui FF, Pan YY, Wang XH, Zhu JJ, Cai PT, Zhang HY, Fu XB, Xiao J, Jiang LP. Myoprotective effects of bFGF on skeletal muscle injury in pressure-related deep tissue injury in rats. *Burns & Trauma*, 2016, 4:26 [PMCID: PMC4987989]
10.   Chen PP, Shen YM, **Shi HX**, Ma XY, Lin BB, Xiao T, Wu FZ, Zhu JJ, Li ZM, Xiao J, Li XK, Zhang HY, Geng FN. Gastroprotective Effects of Kangfuxin-against Ethanol-induced Gastric Ulcer via Attenuating Oxidative Stress and ER Stress in Mice. *Chemico-Biological Interactions*, 2016, 260: 75-83 [PMID:27983966]
11.   Wang ZG, Huang Y, Cheng Y, Tan Y, Wu FZ, Wu JM, **Shi HX**, Zhang HY, Yu XC, Gao HC, Lin L, Cai J, Zhang JS, Li XK, Cai L and Xiao J. Endoplasmic reticulum stress-induced neuronal inflammatory response and apoptosis likely plays a key role in the development of diabetic encephalopathy. *Oncotarget*, 2016, 29;7(48):78455-78472 [PMCID: PMC5346653]
12.   Zhu SP, Wang ZG, Zhao YZ, Wu J, **Shi HX**, Ye LB, Wu FZ, Cheng Y, Zhang HY, He SB, Wei XJ, Fu XB, Li XK, Xu HZ, Xiao J. Gelatin Nanostructured Lipid Carriers Incorporating Nerve Growth Factor Inhibit Endoplasmic Reticulum Stress-Induced

Apoptosis and Improve Recovery in Spinal Cord Injury. *Molecular neurobiology*, 2016, 53(7):4375-4386 [PMID:26232067]

13.   Wu J, Ye JJ, Zhu JJ, Xiao ZC, He CC, **Shi HX**, Wang YD, Lin C, Zhang HY, Zhao YZ, Fu XB, Chen H, Li XK, Lin L, Zheng J, and Xiao J. Heparin-Based Coacervate of FGF2 Improves Dermal Regeneration by Asserting a Synergistic Role with Cell Proliferation and Endogenous Facilitated VEGF for Cutaneous Wound Healing. *Biomacromolecules*, 2016, 17(6):2168-2177 [PMID:27196997]

14.   Zhou YL, Ye LB, Zheng BB, Zhu SP, **Shi HX**, Zhang HY, Wang ZG, Wei XJ, Chen DQ, Li XK, Xu HZ, Xiao J. Phenylbutyrate prevents disruption of blood-spinal cord barrier by inhibiting endoplasmic reticulum stress after spinal cord injury. *American Journal of Translational Research*, 2016, 15;8(4):1864-1875 [PMCID: PMC4859915]

15.   Cui FF, Pan YY, Chang HT, Xie HH, Wang XH, **Shi HX**, Xiao J, Zhang HY and Jiang LP. Pressure combined with ischemia/reperfusion injury induces deep tissue injury via Endoplasmic Reticulum Stress and the Akt /GSK3 pathway in a rat pressure ulcer model. *International Journal of Molecular Sciences*, 2016, 25;17(3):284 [PMCID: PMC4813148]

16.   Zheng BB, Ye LB, Zhou YL, Zhu SP, Wang QQ, **Shi HX**, Chen DQ, Wei XJ, Wang ZG, Li XK, Xiao J, Xu HZ, Zhang HY. Epidermal growth factor attenuates blood-spinal cord barrier disruption via PI3K/Akt/Rac1 pathway after acute spinal cord injury. *Journal of Cellular and Molecular Medicine*, 2016, 20(6):1062-1075 [PMCID: PMC4882989]

17.   **Shi HX**, Cheng Y, Ye JJ, Cai PT, Zhang JJ, Li R, Yang Y, Wang ZG, Zhang HY, Lin C, Lu XH, Jiang LP, Hu AP, Zhu XB, Zeng QQ, Fu XB, Li XK, Xiao J. bFGF Promotes the Migration of Human Dermal Fibroblasts under Diabetic Conditions through Reactive Oxygen Species Production via the PI3K/Akt-Rac1-JNK Pathways. *International journal of biological sciences*, 2015, 11(7):845-859 [PMCID: PMC4466465]

18.   Lin WH, Xiang LJ, **Shi HX**, Zhang J, Jiang LP, Cai PT, Lin ZL, Lin BB, Huang Y, Zhang HL, Fu XB, Guo DJ, Li XK, Wang XJ, Xiao J. Fibroblast Growth Factors Stimulate Hair Growth through β-Catenin and Shh Expression in C57BL/6 Mice. *BioMed research international*, 2015, 2015:730139 [PMCID: PMC4313060]

19.   Zhao HY, Wu J, Zhu JJ, Xiao ZC, He CC, **Shi HX**, Li XK, Yang SL, and Xiao J. Research Advances in Tissue Engineering Materials for Sustained Release of Growth Factors. *BioMed Research International,* 2015, 2015:808202 [PMCID: PMC4548067]

20.   Zhang HY, Wu FZ, Kong XX, Yang J, Chen HJ, Deng LC, Cheng Y, Ye LB, Zhu SP, Zhang X, Wang ZG, **Shi HX**, Fu XB, Li XK, Xu HZ, Li L, Xiao J. Nerve growth factor improves functional recovery by inhibiting endoplasmic reticulum stress-induced neuronal apoptosis in rats with spinal cord injury. Journal of Translational Medicine, 2014,12(1):130-145 [PMCID: PMC4039547]

21.   **Shi HX**, Lin C, Lin BB, Wang ZG, Zhang HY, Wu FZ, Cheng Y, Xiang LJ, Guo DJ, Luo X, Zhang GY, Fu XB, Bellusci S, Li XK, Xiao J. The Anti-scar Effects of Basic Fibroblast Growth Factor on the Wound Repair In Vitro and In Vivo. *PLOS ONE*, 2013, 8(4): e59966 [PMCID: PMC3615060]

22.   Zhang HY, Zhang X, Wang ZG, **Shi HX**, Wu FZ, Lin BB, Xu XL, Wang XJ, Fu XB, Li ZY, Shen CJ, Li XK, Xiao J. Exogenous Basic Fibroblast Growth Factor Inhibits ER Stress–Induced Apoptosis and Improves Recovery from Spinal Cord Injury. *CNS Neuroscience & Therapeutics*, 2013,19(1):20-29 [PMID:23082997]

23.   Qu WL, Xiao J, Zhang HY, Chen Q, Wang ZG, **Shi HX**, Gong L, Chen JQ, Cao RS, Lv JQ. B19, a Novel Monocarbonyl Analogue of Curcumin, Induces Human Ovarian Cancer Cell Apoptosis via Activation of Endoplasmic Reticulum Stress and the Autophagy Signaling Pathway. *International Journal of Biological Sciences,* 2013, 9(8): 766–777 [PMCID: PMC3753441]

24.   Wang ZG, Zhang HY, Xu XL, **Shi HX**, Yu XQ, Wang XJ, Yan YB, Fu XB, Hu HW, Li XK, Xiao J. bFGF inhibits ER stress induced by ischemic oxidative injury via activation of the PI3K/Akt and ERK1/2 pathways. *Toxicology Letters*, 2012, 212(2): 137-146 [PMID:22609091]